



Universität für Bodenkultur Wien

University of Natural Resources and Applied Life Sciences, Vienna

MASTERARBEIT

Titel der Masterarbeit

The role of TMX and TMX4 in the secretion of
vascular endothelial growth factor

angestrebter akademischer Grad

Diplomingenieur

Verfasser:	Kevin Gesson
Matrikelnummer:	0207082
Studienrichtung:	Biotechnologie (H418)
Betreuer:	Privatdozent Dipl.-Ing. Dr.rer.nat.techn. Johannes Grillari

Wien, im Mai 2009

TABLE OF CONTENTS

SUMMARY	page 5
ZUSAMMENFASSUNG	6
1 INTRODUCTION	7
1.1 The secretory pathway	7
1.2 The endoplasmic reticulum (ER)	8
1.3 ER function is vital to many cellular processes	8
1.4 Folding in the ER	9
1.4.1 Ero1, PDI and glutathione in disulfide bond formation	10
1.4.1.1 <i>Ero1 – activity and regulation</i>	10
1.4.1.2 <i>ER redox homeostasis – the role of glutathione</i>	12
1.4.2 The human PDI family	13
1.5 ER chaperones and ER quality control.....	14
1.5.1 The main chaperone families of the ER	14
1.5.2 Quality control in the ER.....	15
1.5.3 The calnexin/calreticulin cycle	16
1.6 Endoplasmic Reticulum-associated Degradation	18
1.7 The unfolded protein response (UPR) and the role of BiP	18
1.7.1 The IRE1 pathway	20
1.7.2 The PERK pathway	20
1.7.3 The ATF6 pathway	20
1.7.4 ER stress-associated apoptosis	21
1.8 ER calcium homeostasis and calcium signaling.....	21
1.9 The roles of the ER in disease	22
1.9.1 ER stress and cancer	22
1.9.2 ER storage diseases	23
1.10 TMX and TMX4 – Trx-related transmembrane proteins	24
1.10.1 TMX (also known as TMX1 or TXNDC)	25
1.10.2 TMX4 (also known as TXNDC13)	26
1.11 PACS-2.....	26
1.12 Vascular endothelial growth factors (VEGFs).....	27
1.12.1 The VEGF family members	28
1.12.2 Regulation of VEGF gene expression	32
1.12.3 VEGF receptors, neuropilins, and VEGF signaling	33
1.13 Hypoxia.....	35

2	Materials & Methods	39
2.1	Chemicals	39
2.2	Melanoma and breast cancer tissue	39
2.3	Cell culture	39
2.3.1	Cell lines	39
2.3.2	Cell culture media	39
2.3.3	Splitting of cells	39
2.3.4	Transfection with Metafectene Pro®	40
2.3.5	Transfection with Lipofectamine™ 2000	40
2.3.6	Transfection constructs and vector systems	41
2.3.7	Transfection with Oligofectamine™	43
2.3.8	Chemical treatment of cells	43
2.3.8.1	<i>Treatment with cobaltous chloride (CoCl₂)</i>	43
2.3.8.2	<i>Treatment with 1,4-dithiothreitol (DTT) and tunicamycin</i>	43
2.4	Protein methodology	44
2.4.1	Cell lysis assay	44
2.4.2	EndoH digest	44
2.4.3	Preparation of tissue lysates	45
2.4.4	VEGF secretion assay	45
2.4.5	SDS Polyacrylamide Gel Electrophoresis (SDS-PAGE)	46
2.4.6	Western blotting	48
2.4.7	Detection	48
2.5	Immunofluorescence	49
2.6	Primary antibodies/antisera	50
2.7	Secondary antibodies	51
2.8	Equipment	51
3	RESULTS	52
3.1	Expression levels of TMX, TMX4, and PACS-2 in melanoma tissue	52
3.2	Subcellular localization of TMX and TMX4 in A375P cells	53
3.3	Effects of overexpression of TMX and TMX4 on the oxidation state of Ero1 α in HEK293 cells	57
3.4	Effects on TMX4 expression in A375P cells	59
3.5	Secretion of VEGF by transfected HeLa cells	63
3.5.1	Overexpression experiments at 1% O ₂	64
3.5.2	Overexpression experiment at 0.1% O ₂	69

3.5.3 Silencing experiment at 0.1% O ₂	71
4 DISCUSSION	73
5 REFERENCES	79
ACKNOWLEDGEMENTS.....	90

SUMMARY

As one of the organelles of a eukaryotic cell, the endoplasmic reticulum (ER) is part of the endomembrane system and accounts for more than 10% of the overall volume of a secretory cell. The ER is endowed with various functions vital to eukaryotic cells; it is not only a key structure for the translation and folding of proteins using a sophisticated quality control system that only allows native proteins to exit the ER, but also mediates the targeting of proteins to the plasma membrane and the secretion of proteins from the cell. Moreover, as the major calcium store of a eukaryotic cell, the ER plays an important role in intracellular calcium signaling.

Oxidative protein folding and the tightly linked quality control for the assessment of the folding status of ER substrates are mediated by a plethora of chaperones, folding enzymes, and oxidoreductases exclusive to this organelle. Among these folding factors, protein disulfide isomerase (PDI) and the ER oxidoreductin 1 (Ero1), which links oxidative protein folding to molecular oxygen, are major players in disulfide bond formation and reshuffling. TMX4, one of the thioredoxin-related transmembrane proteins which are members of the PDI family that otherwise consists only of soluble proteins, has been found to be upregulated in cell lines derived from cancerous skin. Thus, the aims of this thesis were to investigate whether (i) protein levels of TMX and TMX4 are also aberrant in cancerous skin (melanoma), (ii) elevated levels of TMX or TMX4 have any effect on Ero1, and (iii) the secretion of vascular endothelial growth factor (VEGF), a major angiogenic factor, is enhanced, thereby ensuring tumor growth. Moreover, the sub-organelle localization of the two ER-resident proteins, TMX and TMX4, was examined in order to elucidate their biological roles.

To this end, TMX and TMX4 levels in melanoma samples were compared with those in healthy skin, the oxidation state of Ero1 in TMX- and TMX4-transfected HEK293 cells was investigated, the VEGF secretion patterns by TMX- and TMX4-transfected HeLa cells were examined, and finally, subcellular localization of TMX and TMX4 in a human melanoma cell line was studied by immunofluorescence.

The results revealed that TMX4, but not TMX, tended to be upregulated in melanoma, and may change the oxidation state of Ero1. However, overexpression of either TMX or TMX4 altered the secretion of VEGF. Additionally, TMX and TMX4 are localized in distinct domains of the ER.

ZUSAMMENFASSUNG

Eine der Organellen eukaryotischer Zellen ist das endoplasmatische Retikulum (ER). Das ER übt lebensnotwendige Funktionen aus. Es ist nicht nur für die Biosynthese und Faltung von Proteinen verantwortlich, sondern spielt als intrazellulärer Calciumspeicher auch eine wichtige Rolle in der Übertragung von Calciumsignalen. Eine Reihe von Chaperonen, Oxidoreduktasen und anderen Proteinen, die für die oxidative Faltung von Proteinen und deren Qualitätskontrolle zuständig sind, befinden sich ausschließlich im ER. Dabei sind die Faltungsenzyme Proteindisulfidisomerase (PDI) und ER Oxidoreduktin 1 (Ero1) für die Ausbildung von Disulfidbrücken und deren Umordnung essentiell. TMX und TMX4 sind thioredoxin-verwandte membrangebundene Mitglieder der Familie der ansonsten löslichen PDI-Proteine. TMX4 ist in isolierten Hautkrebs-Zelllinien überexprimiert. Daher wurde in dieser Arbeit die Expression von TMX und TMX4 in Hautkrebsgewebe mit jener in gesundem Hautgewebe verglichen. Weiters wurde der Einfluss der TMX- und TMX4-Überexpression in HEK293-Zellen auf Ero1 untersucht, und schließlich, ob diese Überexpression Auswirkungen auf die Sekretion des Vaskulären Endothelialen Wachstumsfaktors (VEGF) von HeLa-Zellen und somit auf das Wachstum von Tumoren hat. Darüberhinaus wurde in einer Melanomzelllinie die Lokalisation von TMX und TMX4 innerhalb des ERs mithilfe von Immunfluoreszenz untersucht, um Rückschlüsse auf mögliche biologische Funktionen ziehen zu können.

Im Vergleich mit gesunder Haut ist die Expression von TMX4, jedoch nicht von TMX, in etwa der Hälfte der untersuchten Hautkrebsgewebeproben erhöht. Weiters wurde ein möglicher Einfluss der Überexpression von TMX4, nicht aber von TMX, auf den Oxidationsgrad von Ero1 beobachtet. Hingegen war das Sekretionsmuster von VEGF durch die Überexpression sowohl von TMX4 als auch von TMX verändert. Darüberhinaus wurden TMX und TMX4 in unterschiedlichen Subdomänen des ER gefunden.

1 INTRODUCTION

1.1 The secretory pathway

In order to be secreted, proteins undergo several sequential steps. In the first step, newly synthesized proteins destined for secretion are targeted to the endoplasmic reticulum (ER), where they undergo N-glycosylation and oxidative protein folding assisted by diverse chaperones and folding enzymes, also called ER-assisted folding (ERAF). Only when the polypeptide chains reach their native conformation, which is controlled by a strict quality control system (ERQC), they are sorted into special domains of the ER, the so-called ER exit sites (ERES). COPII-coated vesicles bud off the ER membrane and transport their folded cargo through the ER-Golgi intermediate compartment (ERGIC) to the *cis*-face of the Golgi complex. Within the Golgi stack, protein cargo is transported forward in anterograde COPII-vesicles, whereas Golgi-resident proteins are retained by retrograde transport in COPI-vesicles. O-glycosylation of proteins is initiated in the ER, and is completed in the *trans*-Golgi. Reaching the *trans*-Golgi network (TGN) proteins are being sorted according to their targeting. In clathrin-coated vesicles, protein cargo can either be transported to lysosomes via endosomes, or to the plasma membrane to be ultimately secreted through a process called exocytosis. In addition, there are two exocytotic mechanisms, one accounting for constitutive secretion, and the other for signal-induced regulated secretion. Figure 1.1 gives an overview of the secretory and endocytic pathways in eukaryotic cells.

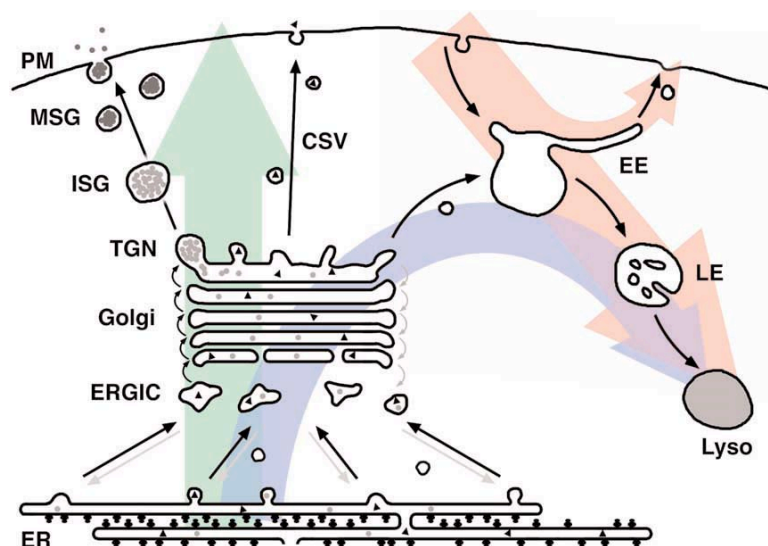


Figure 1.1. Secretory and endocytic pathways of eukaryotic cells. The ER delivers membrane and proteins to the secretory and endocytic compartments of the cell, as well as to the cell surface. ERGIC, ER-Golgi intermediate compartment; TGN, *trans*-Golgi network; ISG, immature secretory granules; MSG, mature secretory granules; CSV, constitutive secretory vesicles; EE, early endosomes; LE, late endosomes; Lyso, lysosomes. (Adapted from Figure 1 by Rutishauser & Spiess, 2002)

1.2 The endoplasmic reticulum (ER)

The endoplasmic reticulum (ER) is an organelle within eukaryotic cells that is surrounded by a single membrane extending throughout the cytoplasm of the cell, thereby constituting 50% of the total membrane, and more than 10% of the overall volume of a secretory cell (Chevet et al., 2001; Verkhratsky & Petersen, 2002). It exists as several morphologically distinguishable forms, which also can be isolated biochemically. The major compartments are the smooth ER, which has no ribosomes attached and the rough ER (rER) that has ribosomes bound to its cytosolic surface rendering it a rough appearance in electron microscopic images. The rER is the domain of the ER where protein folding and degradation take place (Rapoport, 2007); the transitional ER (tER) or ER exit sites (ERES) direct ER-to-Golgi transport (Tang et al., 2005). The mitochondria-associated membrane (MAM), a domain of the ER that is in close contact with mitochondria, serves as a link in calcium signaling and lipid synthesis and transfer (Vance, J.E., 1990; Hayashi & Su, 2007).

1.3 ER function is vital to many cellular processes

The ER is committed to the import, folding, post-translational modification and assembly of all cell surface proteins, of proteins that are secreted, and of proteins that reside in any compartment along the exocytic and endocytic pathways. In eukaryotic cells, the ER is also the major site of membrane lipid synthesis. Via vesicular transport, both membrane lipids and proteins travel to the Golgi apparatus and, eventually, to other destinations in the endomembrane system.

Mitochondria, however, are autonomous organelles, which receive membrane lipids from the ER, not via vesicular transport, but likely via direct membrane contact sites – namely the mitochondria associated membrane (MAM).

The ER is also involved in cellular signaling and interorganellar communication, stress-dependent activation of transcriptional processes, the so-called process of ER-associated degradation (ERAD), and since it functions as a Ca^{2+} store, it plays an important role in Ca^{2+} -mediated signaling as well.

1.4 Folding in the ER

The lumen of the ER, like the lumen of other organelles of the secretory pathway, is extracytosolic and therefore resembles the extracellular space. For the efficient folding and maturation of proteins, the ER provides an optimized environment that differs from other folding compartments (e.g. the cytosol and mitochondria) in its high oxidizing potential, its highly fluctuating Ca^{2+} concentration, the presence of carbohydrates, and a machinery for protein-glycosylation (Stevens & Argon, 1999).

Unlike proteins in the cytosol and mitochondria, which are under permanent surveillance of the chaperones that help their maturation, secretory proteins and proteins of the exocytic and endocytic systems are no longer assisted by chaperones after they have left the ER. As a consequence, the sophisticated and stringent “quality control” mechanisms within the ER that allow only correctly folded proteins to exit the ER are of great importance (reviewed by Ellgard & Helenius, 2003).

During translation, as soon as the signal peptide, a stretch of ~17 – 35 hydrophobic residues at the N-terminus, of the nascent polypeptide chain emerges from the ribosome, it is recognized by SRPs (signal recognition particles) that target the ribosome to the ER membrane. Here, the SRPs bind to the SRP-receptor, a component of the translocon complex through which the nascent polypeptide chains enter the ER.

Upon entry into the ER, it depends on the characteristics of the polypeptide chain whether it becomes a soluble or a membrane-anchored protein. After signal peptide cleavage and complete passage of the C-terminus through the translocon pore, soluble proteins are no longer attached to the membrane. Many other proteins, however, remain anchored in the membrane due to their transmembrane domains, or as a result of the addition of glycerophosphatidylinositol (GPI)-anchors.

It is unique to the ER folding machinery that entering polypeptide chains are N-glycosylated and by default form disulfide bonds. Most proteins that enter the ER are glycosylated, and many are unable to fold without their hydrophilic glycans that prevent aggregation due to hydrophobic interactions. Similarly, the majority of ER residents can only fold correctly in the oxidizing milieu of the ER.

1.4.1 Ero1, PDI and glutathione in disulfide bond formation

As mentioned above, the ER provides a unique oxidizing environment within eukaryotic cells. At first, oxidative protein folding was thought to rely solely on the ratio of oxidized to reduced glutathione (GSSG/GSH) in the ER of about 1:3 (Hwang et al., 1992), in contrast to the cytosol, where it is approximately 1:60. However, for many proteins in order to fold correctly, disulfide bond isomerization, and sometimes, even reduction (Jansens et al., 2002), are required. Considering this, it is evident that a hyper-oxidizing environment in the lumen of the ER can have an inhibitory effect on the folding of proteins with several disulfides, likely leading to aggregation (Molteni et al., 2004). Thus, protein-protein interchange relays are a necessity for coordinated oxidative protein folding. The main pathway through which this transfer of disulfides to folding clients takes place involves PDI (protein disulfide isomerase) and PDI-like proteins (reviewed in van Anken & Braakman, 2005). PDI contains four thioredoxin (trx) domains with the typical CXXC motif, two of which (a and a') confer oxidoreductase activity, with the other two (b and b') mediating binding to client proteins in order to present the protein to the active sites a and a', and can also act in a general chaperone-like function (Wang & Tsou, 1993; Yao et al., 1997; Forster et al., 2006; Wilkinson & Gilbert, 2004). Another protein, the ER oxidoreductin 1 (Ero1)(reviewed in Sevier & Kaiser, 2008), is required for recharging PDI and hence orchestrating PDI-mediated disulfide bond formation and isomerization. Ero1, a glycosylated membrane-associated flavoenzyme localized on the luminal side of the ER is the direct link between molecular oxygen and PDI in the electron flow required for protein folding. Shortly after the characterization of Ero1p in *S. cerevisiae* (Pollard et al., 1998; Frand & Kaiser, 1998), it was discovered that in humans Ero1 exists as two paralogs, Ero1-L α and Ero1-L β (Cabibbo et al., 2000; Pagani et al., 2000). The difference between the two isoforms lies mainly within their distinct tissue distribution and their modes of regulation. Whereas the expression of Ero1-L α increases upon hypoxia, Ero1-L β is induced in the course of the unfolded protein response (UPR, for details see section 1.7).

1.4.1.1 Ero1 – activity and regulation

Four cysteine pairs mediate the activity of Ero1, two of which are catalytic, whereas the other two are regulatory. The two catalytic cysteine pairs, an “active-site” pair and a “shuttle” pair, are used to reoxidize PDI after it had transferred its disulfide bond to a substrate protein. The catalytic cycle of Ero1 is schematically shown in Figure 1.2: (i) reduced PDI is oxidized by the shuttle cysteine pair of Ero1, (ii) the reduced

shuttle cysteines are re-oxidized through an intramolecular dithiol-disulfide exchange with the active site cysteine pair (Sevier & Kaiser, 2006), (iii) and finally, to restore the active-site disulfide, the electrons are transferred to the flavin cofactor (FAD, flavine adenine dinucleotide) and molecular oxygen. Ero1 can now “recharge” another PDI molecule. Overall, per substrate disulfide, one molecule of H₂O₂ is produced (Gross et al, 2006).

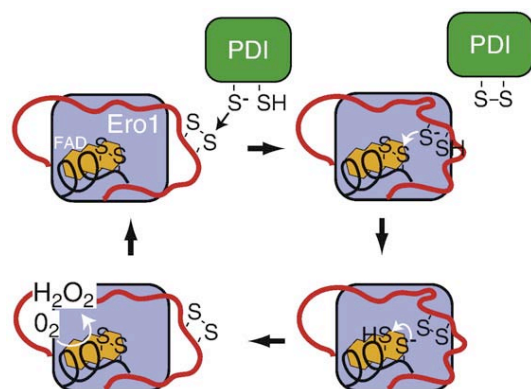


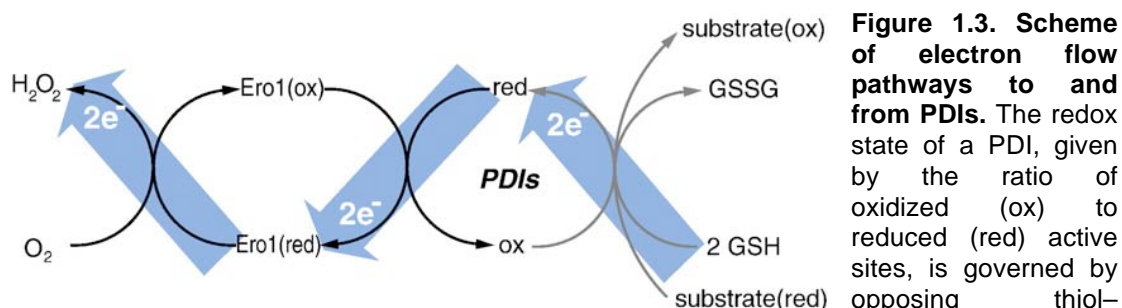
Figure 1.2. Catalytic mechanism of Ero1. The shuttling cysteines are located on a flexible loop (red). The active site cysteines (on black helix) lie within the core of Ero1, next to the FAD cofactor (orange). Thin arrows point out the electron flow. (Adapted from Figure 2 in the review by Sevier & Kaiser, 2008)

The redox state of the ER, and therefore the resulting redox state of two non-essential cysteine pairs regulates the activity of Ero1. If oxidizing conditions in the ER prevail, the flexibility of the loop containing the shuttle cysteines is decreased, thereby limiting the ability of Ero1 to re-oxidize PDI. This regulatory mechanism, rendering Ero1 able to sense the ER oxidation state, has been suggested to compensate for the fluctuating redox environment of the ER (reviewed by Sevier & Kaiser, 2008). The above described redox regulation of Ero1 has only been demonstrated for *S. cerevisiae* Ero1 to date. However, due to the existence of cysteines in addition to cysteines in the catalytic site of all Ero1 homologs, a capacity for Ero1 regulation is likely to exist in various organisms including man.

As addressed above, functional folding of proteins in the ER does not only rely on the formation of disulfides, but also on the ability to reduce substrate proteins to such an effect as to isomerize disulfides, and equally important, to reduce terminally misfolded proteins so that they can exit the ER through the retrotranslocon via the ERAD pathway (Tortorella et al., 1998; Fagioli et al., 2001). Compromised Ero1 function would increase the fraction of reduced PDI and its ability to reshuffle non-native disulfides, which could possibly counteract an accumulation of misoxidized proteins by catalyzing their unfolding and subsequent degradation (Tsai et al., 2001). Thus, PDI could then act as an oxidoreductase capable of oxidizing and reducing substrate proteins through the regulation of Ero1. Moreover, Ero1-mediated oxidative stress resulting from e.g., increased secretory loads of a particular cell type, can be alleviated via the PERK-dependent UPR pathway (described in detail in section 1.13).

There are several roles for Ero1 implicated in diseases, suggesting that correct regulation of Ero1 is crucial for a cell to perform its purpose. For example, it has been shown that the enhanced Ero1 activity under hypoxia is able to increase secretion of the vascular endothelial growth factor (VEGF), essential to tumor development and growth (May et al., 2005). Additionally, in diabetic rats, Ero1 was found to exist as a more oxidized form, possibly reflecting an inactivation of Ero1 by oxidation of the regulatory cysteines (Nardai et al., 2005). Taken together, it is evident that both, hyperactivation and decreased activity of Ero1, lead to conditions favoring aberrant ER protein folding and degradation resulting in disease (see review by Sevier & Kaiser, 2008 and references therein).

Figure 1.3 summarizes the mechanism underlying the electron flow mediated by the interplay of PDI and Ero1.



disulfide exchange reactions. While reduced PDIs can be oxidized by oxidized Ero1 that ultimately transfers the electrons ($2e^-$) onto molecular oxygen (O_2) (black arrows), oxidized PDIs can react with GSH or reduced substrates (gray arrows). The electron fluxes associated with the formation of GSSG and oxidized substrates (big gray arrows) lead to the stoichiometric generation of hydrogen peroxide (H_2O_2). For simplicity, reduction of substrates by (reduced) PDIs is omitted from the scheme, and only the net flow of electrons from nascent polypeptide substrates onto PDIs is depicted. (Adapted from Figure 3 in Appenzeller-Herzog & Ellgaard, 2008)

1.4.1.2 ER redox homeostasis – the role of glutathione

The role of glutathione for the efficient folding of proteins in the ER appears to be ambivalent. Until recently, glutathione was regarded as an antagonist of the Ero1-PDI oxidation pathway, since reduced glutathione limits the Ero1-dependent oxidation (Molteni et al., 2004; Cuozzo & Kaiser, 1999). Interestingly though, it was demonstrated that lowered glutathione (GSH) levels retained a hyperactive mutant of Ero1 in the oxidized inactive state (Sevier et al., 2007), suggesting a role for glutathione in the reduction and the resulting activation of Ero1 under normal conditions. It remains unclear, however, through which direct reductant glutathione regulates Ero1, since glutathione itself is a poor substrate and activator of purified Ero1 *in vitro* (Sevier et al., 2007; Tu et al., 2000; Sevier & Kaiser, 2006).

Moreover, elevated Ero1 activity increases the formation of GSSG, arguably an

indicator for glutathione-mediated reduction of (misoxidized) substrate proteins and/or PDI (Chakravarthi & Bulleid, 2004; Jessop et al., 2004), but also influences glutathione synthesis (Molteni et al., 2004), which would allow ROS depletion by an increased level of GSH. Otherwise, Ero1 would be in the incongruous role of generating ROS and depleting a scavenger of ROS at the same time. Clearly, the complex mechanisms of Ero1 regulation need further investigation, possibly aided by computational modeling, with emphasis on the mammalian homologs.

1.4.2 The human PDI family

The classification of proteins as members of the human PDI-family is based on sequence and structural similarity as well as ER localization, rather than on functional similarities. All of the family members are thiol-disulfide oxidoreductases, containing at least one thioredoxin (trx)-like domain with the characteristic CXXC active-site motif. Thus far, the PDI-family consists of 19 members (reviewed by Appenzeller-Herzog & Ellgaard, 2008; Mattanen et al., 2006). Their designated functions, besides promoting oxidative protein folding, include roles in ER trafficking, calcium homeostasis, ERAD, virus entry, and antigen presentation. The multitude of functions is performed by catalytic (a-type) and/or non-catalytic (b-type) trx-like domains. Mostly, human PDIs are soluble proteins in the ER; however, four exist as transmembrane proteins anchored in the ER membrane (the thioredoxin-related transmembrane proteins TMX and TMX 2-4). As described above, section 1.4.1, the founding member of the PDI-family, PDI itself, is capable of catalyzing protein folding by oxidation, isomerization and reduction of cysteine pairs in substrate proteins, as well as generally acting as a chaperone. The closest homolog of PDI, ERp57, performs its thiol-disulfide interchange reactions primarily in association with calnexin (CNX) and calreticulin (CRT), but also plays a role in ER calcium homeostasis, along with ERp44 (see section 1.8). Other members of the PDI-family with varying functions include ERp29, ERp46 (also known as EndoPDI), ERp72 and the TMXs. Characterized as an escort protein rather than being part of the protein folding process, ERp29, is required for the efficient secretion of thyroglobulin, a 660 kDa precursor for thyroid hormone synthesis (Baryshev et al., 2006; Herrmann et al., 1999). Another PDI-family member, ERp46, which is implicated in the secretion of survival factors by endothelial cells, where it is highly expressed, is upregulated in response to hypoxia (Sullivan et al., 2003). ERp72 has been reported to be part of a large complex together with PDI and other members of the PDI-family, and also to be a limiting factor in the retrotranslocation of proteins to the cytosol (see review by

Appenzeller-Herzog & Ellgaard, 2008, and references therein). Besides the protective role of TMX, which depends on the intact CPAC active site, upon brefeldin A-induced apoptosis (Matsuo et al., 2001), little is known about TMX and its homologs, which will be addressed in section 1.10.

1.5 ER chaperones and ER quality control

Within the ER, various folding enzymes, molecular chaperones, and folding sensor molecules assist protein folding and are part of the ER quality control system (see review by Ellgaard & Helenius, 2003, and references therein).

1.5.1 The main chaperone families of the ER

Besides chaperones and folding enzymes that are exclusively present in the ER such as CNX, CRT, and the family of thiol-disulfide oxidoreductases, the ER also contains chaperones belonging to various classical chaperone families i.e., the heat shock (stress) proteins (Hsps). Abundant in the ER are family members of the Hsp40, Hsp70 and Hsp90 families, but not members of the Hsp104 and Hsp60/Hsp10 proteins.

Glucose regulated protein (GRP) 78, which is also known as Immunoglobulin Binding Protein (BiP), is the main member of the Hsp70 family, and is endowed with several functions in the ERQC. On the one hand, it binds to various nascent and newly synthesized proteins and assists their proper folding; on the other hand, it is also involved in the processes of the unfolded protein response (UPR) and ER-associated degradation (ERAD), which will be addressed in more detail in section 1.7 and 1.6, respectively. Binding to substrate proteins is achieved through its C-terminal domain with affinity to hydrophobic patches in an ATP-dependent manner. Subsequent release of folded proteins is regulated by the N-terminal ATPase domain of the BiP protein. The second member of the Hsp70 proteins is GRP170, the function of which is relatively unexplored.

Five Hsp40 family members, ERdj1-5, have been described so far. With their N-terminal J-domain, the ERdjs, especially ERdj5, are capable of binding to and stimulating the generally low ATPase activity of BiP *in vivo* (Cunnea et al., 2003; Hosoda et al., 2003).

Grp94, the only known member of the Hsp90 family to date, appears not to be essential for cell viability, despite being abundant in the ER. Unlike BiP or calnexin, it binds only to a limited number of substrate proteins that are in a relatively advanced state of folding. Furthermore, each of the Grp94-substrates has been shown to

interact with BiP or calnexin as well. The current knowledge on Grp94 is summarized in Argon & Simen (1999) and was recently complemented by Frey et al. (2007).

The two members of a major folding pathway in the ER, CNX and CRT, are addressed in section 1.5.3.

1.5.2 Quality control in the ER

Many quality control proteins interact with nascent polypeptide chains and remain bound to the incompletely folded protein until it acquires its native conformation, i.e. the most favorable energetic state. In order to prevent incompletely folded or misfolded proteins from leaving the ER, exit is stringently regulated such as to allow only correctly folded proteins to be transported further. Thus, the quality control in the ER ensures that potentially malfunctioning proteins, which could damage the cell or the organism as a whole, are retained and eventually degraded. ER quality control (ERQC) is performed at several levels by a plethora of proteins, whose task is to either assist folding, to assess the folding status, to retain incompletely folded proteins within the ER, or to facilitate the transport of newly synthesized proteins along the secretory pathway. Whereas the so-called primary quality control applies to all proteins in the same fashion, the secondary quality control is more specialized addressing the individual characteristics of selected categories of proteins. Primary quality control relies largely on the association with chaperones and folding enzymes abundant in the ER such as the Ca^{2+} -dependent lectins CNX and CRT, BiP/GRP78, GRP94, the ER-to-Golgi transporter ERGIC-53, and the thiol-disulfide oxidoreductases PDI, ERp57 and ERp72 (Ellgaard et al., 1999). They monitor non-native structures e.g., exposure of hydrophobic patches, tendency to aggregate, presence of immature glycans, or reactive thiols, within proteins. Upon recognition, incompletely folded proteins and unassembled oligomers are bound by one or more of these folding factors, and are thereby prevented from aggregating, and also selectively retained in the ER until the protein achieves its native conformation, or, if terminally misfolded, are eventually degraded via ERAD. The chaperones and folding enzymes themselves are localized in the ER due to the possession of retention and retrieval signals i.e., KDEL and KKXX motifs. In order to be secreted, after passing the checkpoints of the primary QC system, many proteins undergo protein-specific quality control beyond the criteria of primary QC, also called the secondary QC system (reviewed by Ellgaard et al., 1999 and Ellgaard & Helenius, 2003). Frequently, secondary ERQC processes are involved in the regulation of ER retention and export, which often are cell-type specific. The various selective

mechanisms, resulting from specific substrate recognition by the secondary QC proteins, regulate the export of individual proteins or protein families. According to their function, the secondary QC proteins can be classified in three distinct groups (Herrmann et al., 1999), so-called 'outfitters' or proteins that are required to fold and assemble specific proteins, 'escorts' that accompany correctly folded proteins on their way out of the ER, and 'guides' providing signals for intracellular transport. In the following, exemplary members of the respective groups are described briefly, to provide an overview of the tasks performed. A member of the Peptidyl-prolyl isomerase family, Nina A, one of the specialized chaperones and enzymes comprising the group of 'outfitters', ensures secretion competence of specific rhodopsins in *Drosophila melanogaster* (Stamnes et al., 1991). Receptor-associated protein (RAP), a well-known 'escort', protects low density lipoprotein-receptor (LDLR) from premature ligand-binding by binding and escorting the potential receptor to the Golgi apparatus (Bu, 2001). The lectin, ER-Golgi intermediate compartment (ERGIC)-53, which cycles between the ER and the Golgi complex, apparently functions as a cargo receptor for certain proteins that carry high-mannose N-linked glycans (Appenzeller et al., 1999). For other proteins in the secondary ERQC it is not quite sure yet to which of the three groups they belong. For instance, B-cell receptor-associated protein (Bap) 31, ensures ER secretion competence of transmembrane substrate proteins prone to ERAD, likely through a sorting function (Annaert et al., 1997; Wakana et al., 2008), but also is involved in the fragmentation of mitochondria upon induction of apoptosis (Simmen et al., 2005 and references therein).

1.5.3 The calnexin/calreticulin cycle

One of the best-studied mechanisms of the primary ERQC is the CNX/CRT cycle (see Figure 1.4), which entails specific mechanisms reserved to N-glycosylated proteins destined for secretion, but is capable of chaperoning non-glycosylated substrates as well (Ireland et al., 2008). Whereas CNX is bound to the ER membrane, CRT exists as a soluble protein within the ER lumen. The CNX/CRT cycle/chaperoning mechanism is a system of trimming and readdition of glucose residues on the previously attached preformed oligosaccharide (Glc3Man9GlcNAc2), in which UDP-glucose glycoprotein glucosyltransferase (UGGT) acts as a folding sensor that is capable of tagging yet incorrectly folded glycoproteins to reenter the CNX/CRT folding cycle. Oxidative folding itself is promoted via interactions of CNX/CRT with the thiol oxidoreductase ERp57 (Ellgaard & Helenius, 2001; Kozlov et al., 2006; Frickel et al., 2002; Russell et al., 2004). Glucosidase II trims off the third

glucose residue, thereby releasing the protein from CNX/CRT. Thereafter, if correctly folded, the protein may exit the ER through ER exit sites (ERES), reenters the cycle promoted by UGGT, or is targeted for degradation through removal of the terminal mannose moieties by ER α 1,2-mannosidase I enabling recognition by the ER degradation-enhancing 1,2-mannosidase-like proteins (EDEM1-3). For a detailed description of the role and mechanisms of the N-glycan processing in the ER quality control, see the review of Ruddock & Molinari (2006).

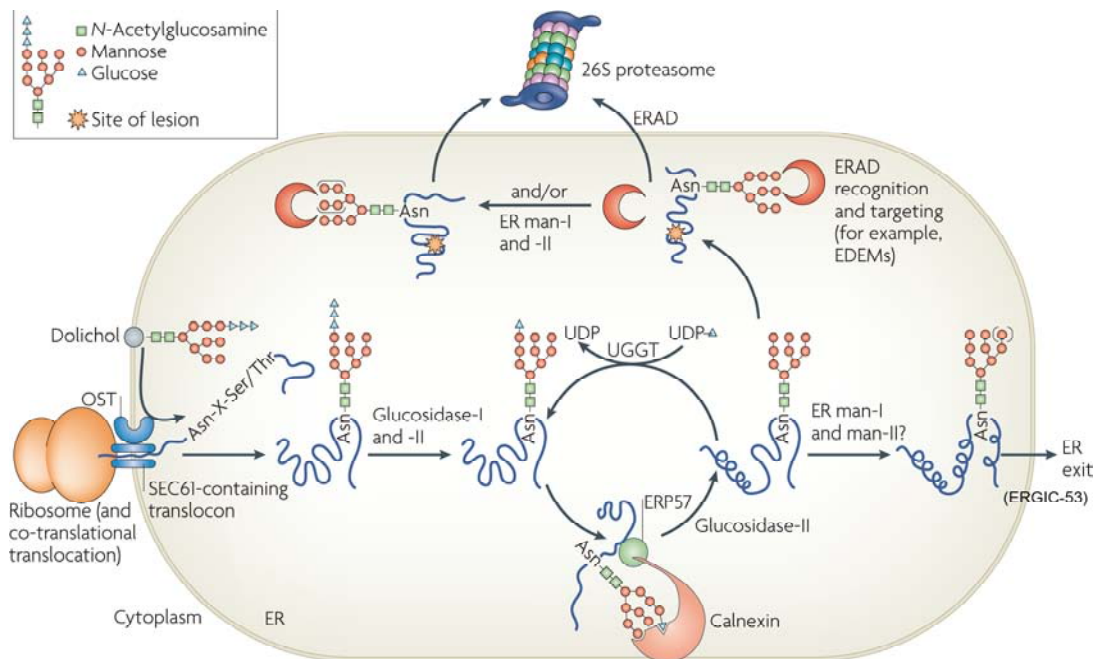


Figure 1.4. CNX/CRT cycle in mammalian cells. Proteins that enter the endoplasmic reticulum (ER) are often modified by the addition of a GlcNAc₂-Man₉-Glc₃ glycan to the side-chain nitrogen of Asn residues in the consensus Asn-X-Ser/Thr motif. First, the translocon-associated oligosaccharyl transferase (OST) complex co-translationally transfers GlcNAc₂-Man₉-Glc₃ glycans from dolichol to substrate proteins. Next, glucosidase-I and glucosidase-II sequentially remove two terminal glucoses, generating monoglucosylated substrates that are recognized by calnexin and calreticulin through their carbohydrate-binding globular domains (calreticulin is a soluble protein and is not shown). The interaction with calnexin and calreticulin facilitates folding. ERP57, a protein disulfide isomerase homologue that is associated with the arm domain of calnexin and calreticulin, catalyzes disulfide bond formation. Following release from the calnexin–calreticulin cycle, the final glucose is trimmed by glucosidase-II. If glycoproteins have adopted their native conformations, they can be demannosylated (denoted by the use of parentheses around the mannoses) by ER mannosidases I and II (ER man-I and man-II) and exit the ER through coatamer protein complex-II vesicles. However, the folding of some glycoproteins requires multiple rounds of association with calnexin–calreticulin. Such proteins are reglucosylated by UDP-glucose:glycoprotein glucosyltransferase (UGGT), which recognizes non-native states and transfers a glucose from UDP-glucose to the N-linked GlcNAc₂-Man₉ glycan. Remonoglucosylation promotes re-entry into the folding cycle. Terminally misfolded glycoproteins might also be targeted for ER-associated degradation (ERAD) by calnexin and calreticulin or by other ERAD-requiring components. EDEM, ER degradation enhancing α -mannosidase-like lectins; Glc, glucose; GlcNAc, N-acetylglucosamine; Man, mannose. (Adapted from Figure 2 in Vembar & Brodsky, 2008)

1.6 Endoplasmic Reticulum-associated Degradation

With few exceptions, it is generally unresolved how ERAD substrates are distinguished from proteins that are already properly folded or in the course of being folded correctly. Approximately 30% of newly synthesized proteins are degraded rapidly (Schubert et al., 2000). However, increasing evidence points to 'false' recognition and subsequent degradation of a good portion of 'wild-type' proteins (Varga et al., 2004). Among the potential ERAD substrates are soluble and integral membrane proteins, misfolded and incorrect post-translationally modified polypeptides, and unassembled subunits of multiprotein complexes.

The ERAD pathway itself includes the recognition of potential substrates, their targeting to the ER membrane, unfolding of the proteins, retrotranslocation out of the ER, polyubiquitination, and finally, degradation of aberrant proteins by the 26S proteasome (reviewed in Vembar & Brodsky, 2008). Most of the major chaperones in the ER are involved in the recognition of ERAD substrates, which are then possibly targeted for retrotranslocation by EDEM1-3. Retrotranslocation in turn relies either on the Sec61 complex, which therefore would be given a double role as translocon and retrotranslocon, or a family of proteins called Derlin1-3, which have been shown to interact with the EDEMs. Among others, Bap31 is a potential regulator of retrotranslocation (also see section 1.5.2). Polyubiquitination starts already during retrotranslocation, and depends on ubiquitin-activating enzymes (E1), ubiquitin-conjugating enzymes (E2) and ubiquitin-protein ligases (E3). Post-translocational proteasomal targeting is aided by the cell-division cycle-48 (Cdc48) complex; however, it remains unclear to what extent Cdc48 is needed. Finally, ERAD substrates are de-ubiquitinated, and broken into peptide fragments by the 26S proteasome (see Figure 1.4). In addition, there is a backup mechanism if efficient ERAD is compromised. ER-stress-induced autophagy, i.e. engulfment, of in particular protein aggregates in a double-membrane structure (autophagosomes) and their delivery to lysosomes or vacuoles for degradation, can complement ERAD when its capacity to degrade proteins is insufficient.

1.7 The unfolded protein response (UPR) and the role of BiP

The UPR is an interconnected network of three distinct pathways, which are initialized to alleviate ER stress resulting from altered ER luminal conditions, such as perturbations in the ER redox state, or luminal calcium levels, but also when the chaperone capacity within the ER is overwhelmed (reviewed by Lai et al., 2007). To counteract these conditions, at first, protein synthesis is transiently inhibited, followed

by induced transcription of chaperone genes, and induction and activation of ERAD (McCullough et al., 2001; Oyadomari et al., 2006). In the case the UPR is deranged or unable to confront the stress conditions, apoptotic cell death is induced. Therefore, UPR signaling is in charge of initializing responses to protect the cell, but also involved in the mechanisms of apoptosis induction, which are medically relevant in pathologies inflicted by accumulation of aggregated proteins leading to chronic ER stress, such as neurodegenerative diseases and diabetes. In addition, the signaling pathways of ER stress are required for the differentiation and/or normal function of secretory cells (reviewed in Wu & Kaufman, 2006).

The three main signaling systems comprising the UPR are induced by three stress sensors localized in the ER membrane, namely IRE1 (inositol requiring), PERK (PKR-like ER kinase), and ATF6 (activating transcription factor 6) (see Figure 1.5 for an overview).

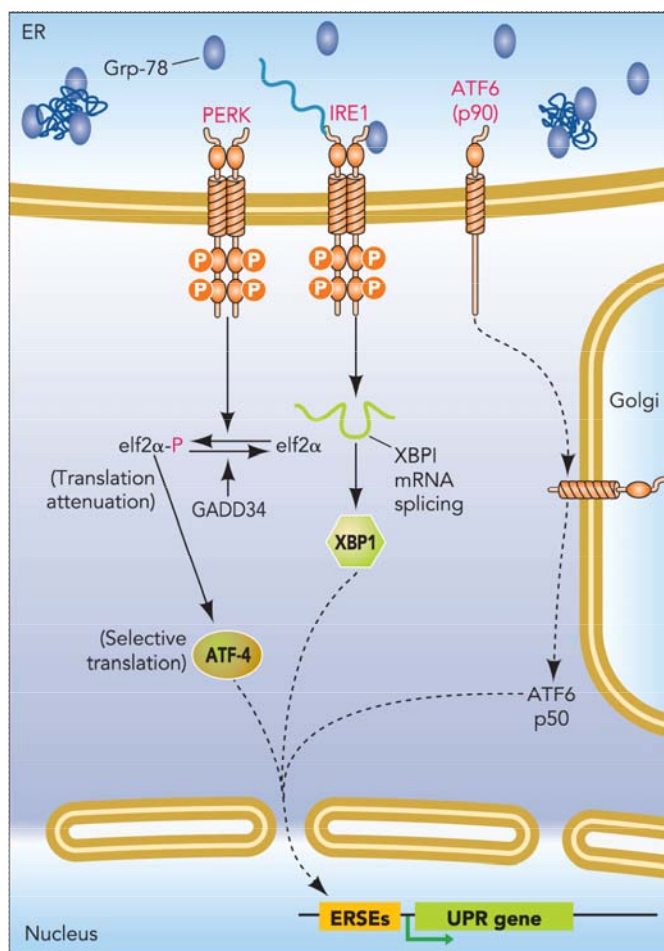


Figure 1.5. The three UPR signaling pathways in mammalian cells.

The PERK kinase is activated by dimerization and phosphorylation. Once activated, it phosphorylates eIF2 α , resulting in translation attenuation. Phosphorylated eIF2 α selectively enhances translation of the ATF4 transcription factor that induces expression of UPR target genes. Activation of IRE1 by dimerization and phosphorylation causes IRE1-mediated splicing of XBP1 mRNA. Translation of spliced XBP1 mRNA produces a transcription factor that upregulates target genes via the ERSE promoter. ATF6 activation involves regulated intramembrane proteolysis. The protein translocates from the ER to the Golgi where it is proteolytically processed to release a 50-kDa transcription factor that translocates to the nucleus and binds the ERSEs of UPR target genes. All three ER-resident transmembrane proteins are thought to sense ER stress through Grp78 binding/release via

their respective luminal domains, although structural studies have also suggested that IRE1 may interact with unfolded proteins directly. The GADD34 protein, a protein phosphatase upregulated by the PERK pathway, dephosphorylates eIF2 α to restore global protein synthesis. (Adapted from Figure 1 in Lai et al., 2007)

1.7.1 The IRE1 pathway

In mammalian cells, there are two IRE1 genes, encoding IRE1 α and IRE1 β . These type I transmembrane proteins with serine/threonine kinase activity catalyze the splicing of the mRNA of X-box-binding protein 1 (XBP1) (Calfon et al., 2002), which, once translated, translocates to the nucleus where it binds to the ER stress-response element (ERSE) in the promoter of target genes inducing their transcription (Lee et al., 2003; Yoshida et al., 1998). Additionally, IRE1 has been reported to mediate the cleavage of other mRNAs (Hollien & Weissman, 2006), and also the cleavage of the 28S ribosomal subunit (Iwawaki et al., 2001), thereby attenuating translation. Under normal conditions BiP is bound to the ER luminal domain of IRE1, locking IRE1 in an inactive, monomeric state. Upon ER stress, BiP dissociates from IRE1 to bind substrate proteins and assist their folding, thereby allowing IRE1 to dimerize and become activated (Bertolotti et al., 2000; Liu et al., 2000).

1.7.2 The PERK pathway

The initial response to ER stress, the transient global attenuation of protein translation, is performed by the PERK signaling pathway via phosphorylation of eukaryotic initiation factor 2 α (eIF2 α) (described in detail in section 1.13). Like IRE1, PERK is a type I transmembrane Ser/Thr kinase in the ER that is capable of sensing ER stress through its luminal domain in a BiP-dependent fashion (Shi et al., 1998; Bertolotti et al., 2000). The same mechanism of BiP dissociation, as described in “The IRE1 pathway”, is assumed to regulate PERK activity. Phosphorylation of eIF2 α leads to initiation of the ATF4 mRNA, which in turn upregulates ER stress target genes (Harding et al., 2000; Lu et al., 2004). Recovery from translation attenuation is also induced by ATF4 through upregulation of the stress-induced phosphatase named “growth arrest and DNA damage-inducible gene 34” (GADD34), which dephosphorylates eIF2 α , enabling return to normal protein translation (Novoa et al., 2001; Ron, 2002). According to several publications, the PERK pathway is essential for normal physiological control of translation, and required for normal development of several tissues, as well (see review by Lai et al., 2007 and references therein).

1.7.3 The ATF6 pathway

The mammalian isoforms of ATF6 (ATF6 α and ATF6 β) transmit the UPR signal through a mechanism different from IRE1 and PERK. It involves a process termed regulated intramembrane proteolysis (RIP), in which upon activation by dissociation

of BiP from ATF6 (thereby revealing two Golgi localization signals), the 90-kDa ATF6 translocates to the Golgi complex. There, ATF6 is proteolytically processed by Golgi resident proteases, releasing a 50-kDa cytosolic basic leucine zipper (bZIP) transcription factor (Chen et al., 2002; Shen et al., 2002). The transcription factor then translocates to the nucleus, where it upregulates ER stress genes. Through the ATF6 α pathway BiP/GRP78, Grp94, and PDI are targeted for enhancement of transcription (Okada et al., 2002). In addition to BiP dissociation, also the redox state of the ATF6 luminal domain has regulatory functions. In the course of ER stress, disulfide bonds in this domain, which are proposed to keep ATF6 in an inactive state, are reduced thereby elevating the ability of ATF6 to exit the ER (Nadanaka et al., 2007).

1.7.4 ER stress-associated apoptosis

If attempts to overcome ER stress fail, all three UPR signaling pathways are capable of inducing apoptosis through various mediators (see review by Lai et al., 2007 and references therein). One of these mediators is CHOP (C/EBP homologous protein transcription factor), a bZIP-containing transcription factor identified as a member of the CCAAT/enhancer binding protein (C/EBP) family, also known as GADD153. CHOP is one of the most highly upregulated genes under prolonged ER stress. Although in principal all three pathways enable its transcriptional induction, the PERK pathway has been reported to be essential. CHOP in turn regulates the overexpression of e.g., GADD34 and Ero1 α , thereby allowing recovery of protein synthesis and folding, and thus further promoting ER stress. Another pathway of UPR-induced apoptosis targets c-Jun NH₂-terminal kinase via the adaptor protein TNF receptor-associated factor 2 (TRAF2) and apoptosis signal-regulating kinase 1 (ASK1).

In addition, prolonged ER stress induces mitochondria-mediated apoptosis by influencing the character and balance of pro- and anti-apoptotic Bcl-2 family members acting through the caspase system (reviewed in Jeong & Seol, 2008).

1.8 ER calcium homeostasis and calcium signaling

One of the diverse functions of the ER is the storage of Ca²⁺. Consequently, in response to a variety of cellular signals (Giacomello et al., 2007), this intraorganellar Ca²⁺ pool can be used for different signaling purposes by releasing Ca²⁺ into the cytosol or to mitochondria via the MAM. The activated signal transduction cascades

regulate multiple processes, such as membrane permeability, glycogen metabolism, muscle contraction, ATP production via the tricarboxylic acid (TCA) cycle, and particularly important, induction of mitochondria-mediated apoptosis (Brostrom & Brostrom, 2003; Jeong & Seol, 2008). Calcium is actively transported from the cytosol into the ER lumen by sarcoplasmic/endoplasmic reticulum Ca^{2+} ATPase (SERCA) pumps, and can be released through inositol 1,4,5-triphosphate (IP3) receptors. In the ER lumen most of the calcium is bound to the protein matrix, i.e. the calcium-binding proteins CNX, CRT, BiP, and others, which all bind calcium, although unlike dedicated calcium binders, the calsequestrins, which are exclusive to muscle tissue. The uptake of calcium via SERCA pumps is regulated by calnexin in collaboration with ERp57, whereas release of calcium into the cytosol is controlled by ERp44, which is capable of restricting calcium efflux from type-1 and type-3 IP3 receptors (IP3R1 and IP3R3, respectively). Therefore, calcium homeostasis in the ER is tied to the luminal redox environment. Additionally, a calcium-dependent IP3R3-stabilizing mechanism, comprised of BiP and Sigma-1 receptor, prevents the degradation-prone IP3R3 from ubiquitination. Direct release of calcium to the mitochondria via the MAM is achieved through bridging IP3R3 in the ER membrane and the voltage-dependent anion channel (VDAC) in the outer mitochondrial membrane (OMM) with Grp75, thereby shortening the distance between the MAM and the mitochondria. A calcium uniporter in the inner mitochondrial membrane transports calcium into the mitochondrial lumen. For an excellent review on this topic, see Hayashi et al., 2009. The presence of calcium-binding chaperones (CNX, CRT, and BiP) at the MAM appears to provide a rapidly releasable calcium store (Hayashi & Su, 2007). Finally, ER stress-induced depletion of ER calcium stores and subsequent increase of cytosolic calcium levels lead to mitochondria-mediated apoptosis (Lai et al., 2007; Jeong & Seol, 2008).

1.9 The roles of the ER in disease

1.9.1 ER stress and cancer

Diverse functions of the ER have been implicated in cancer development (Li & Lee, 2006; Lee & Hendershot, 2006; Boelens et al., 2007; Ni & Lee, 2007). The rapid growth of tumors often outpaces the angiogenesis required for sufficient blood supply, and therefore leads to hypoxic conditions within the tumor mass (Brahimi-Horn et al., 2007). Thus, due to the need of oxygen in order for oxidative protein folding to take place (see section 1.4.1), ER stress, with the corresponding attempts of the cell to adapt, is the result. However, activation of HIF-1 α , and subsequent

upregulation of the redox-sensitive oxidoreductases PDI and Ero1 α , may also occur in response to the altered ER redox conditions (Liu et al., 2004). Elevated levels of oxidoreductases in the ER promote the secretion of VEGF in order to improve the blood supply of hypoxic tumors through neoangiogenesis (May et al., 2005; Gess et al., 2003). Hence, tumor growth is also promoted by the UPR, which not only counteracts tumor cell apoptosis, but also enables tumor angiogenesis (through the enhanced production of VEGF) by increasing levels of the chaperones GRP94, ORP150, calreticulin and BiP/GRP78 (Li & Lee, 2006; Ni & Lee, 2007; Ozawa et al., 2001). Therefore, clinical trials for the treatment of cancer with versipelostatin, a downregulator of Bip/GRP78 expression, are currently underway, targeting the induction of ER chaperones (Park et al., 2004; Shin-Ya, 2005). Moreover, tumor invasiveness has been linked to the levels of ER chaperones, e.g., BiP/GRP78 and PDI, which if expressed at high levels promote tumor metastasis, and correlate with the invasiveness of glioma, respectively (Chiu et al., 2008; Zheng et al., 2008; Goplen et al., 2006). Additionally, the PERK pathway, a component of UPR signaling, causes degradation of a crucial tumor suppressor, p53, and of cyclin D1, which is essential for cell division, and thus leads to formation of smaller and less angiogenic tumors (Raven & Koromilas, 2008; Baltzis et al., 2007; Blais et al., 2006). Calcium signaling via the MAM, and its association with induction of apoptosis, plays an important role in carcinogenesis as well. For example, upregulation of the bridging factor between the IP3R on the ER and the VDAC on mitochondria, GRP75, results in inactivation of p53 (Wadhwa et al., 2006; Kaul et al., 2005). Therefore, the possibility of tumor promoting or counteracting effects of other proteins that are involved in the calcium-signaling pathway at the MAM, such as calnexin, and the PDI-family members ERp44 and ERp57, seems likely, but remains to be investigated further.

1.9.2 ER storage diseases

ER storage diseases (ERSD) arise from mutant proteins that fail to pass the ERQC. Diseases then are caused by the mere lack of the protein and/or result from possible toxic effects on the cell of the misfolded protein or aggregates thereof. Moreover, persistent activation of signaling pathways in response to ER stress ultimately have detrimental effects. ERSDs provide insights into the reactions of cells to a variety of perturbations, therefore elucidating the links between ER stress and cell degeneration.

In ERSDs, three pathogenetic groups can be distinguished, resulting from (i) the mere lack of the protein due to retention in the ER, (ii) toxic proteins or protein aggregates, or (iii) a defective transport machinery. Typical examples for (i) are cystic fibrosis (OMIM entries 219700, 602421), where a mutation (F Δ 508) in the cystic fibrosis transmembrane conductance regulator (CFTR) leads to retention in the ER, and eventually to its degradation, and hypothyroidism (OMIM entry 188450), due to the absence of thyroglobuline, a precursor of thyroid hormone, and hence circulating thyroid hormone. Deficiencies in α 1-antitrypsin (or α 1-protease inhibitor; A1Pi; OMIM entry 107400) result in conditions exemplary for (i) and (ii). On the one hand, patients homozygous for a null mutation cannot produce A1Pi, putting them at risk for bronchiectasis and pulmonary emphysema due to the unopposed proteolytic activity of neutrophil elastase in the lung, which leads to chronic tissue destruction. On the other hand, a subset of homozygotic patients (~15%) develops liver cirrhosis and hepatoma (Eriksson et al., 1986). Experimental evidence suggests that ERAD of a particular mutant of A1Pi is specifically delayed (Wu et al., 1994). Furthermore, an example for (iii) is a mutation in ERGIC-53, leading to a significant reduction of the ER exit of a small number of proteins, in particular coagulation factors V and VIII, which results in congenital bleeding disorder (Nichols et al., 1998).

The list of ER stress-linked diseases is long, and includes among others for example Alzheimer's disease, Parkinson's disease, stroke, atherosclerosis, and diabetes (For excellent reviews on this topic, see Rutishauser & Spiess, 2002; Kim et al., 2008).

1.10 TMX and TMX4 – Trx-related transmembrane proteins

TMX/TMX1 and TMX4 (also known as TXNDCs, thioredoxin domain containing proteins) are both members of the human PDI-family (see section 1.4.2), which all contain thioredoxin (trx)-like domains. Thioredoxin (Trx) is a small multifunctional protein, characterized by an active site motif (Cys-Gly-Pro-Cys) conserved from prokaryotes to higher eukaryotes. Trx, in cooperation with thioredoxin reductase and NADPH, performs its function via reversible reduction and oxidation of the thiol-groups on these two cysteines (Holmgren A., 1985 and 1989; Tagaya et al. 1989). It plays a key role in the control of cellular redox balance and has functions in various thiol-dependent biological processes, such as gene expression, signal transduction, cytoprotective action, and proliferation (H. Nakamura et al., 1997).

1.10.1 TMX (also known as TMX1 or TXNDC)

TMX was identified as the product of a TGF- β -responsive gene (Matsuo et al., 2001). The gene encodes 280 amino acid residues, expressed as a protein of approximately 30 kDa. TMX is endowed with an N-terminal cleavable signal peptide, an adjacent thioredoxin (trx)-like domain (Cys-Xxx-Xxx-Cys) with an atypical active site-sequence, Cys-Pro-Ala-Cys, a transmembrane domain, an acidic cluster, and a non-classical ER targeting signal, i.e., an RQR-motif at the C-terminus (Roth et al., unpublished). Besides these findings no further functions for the cytosolic domain have been revealed to date. The N-terminus protrudes into the ER lumen, while the C-terminus forms a cytosolic tail (Matsuo et al., 2004) (see Figure 1.6).

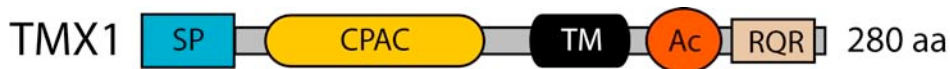


Figure 1.6. Schematic outline of the human TMX1 protein. The 30 kDa protein consists of an N-terminal signal peptide targeting it to the ER, a trx-like (CPAC) domain, a transmembrane domain, and one acidic cluster and a non-classical ER-retention signal (RQR) at the C-terminus. The trx-like domain with the active site protrudes into the ER lumen, while the C-terminus forms a cytosolic tail.

It has been shown that Myc-tagged TMX colocalizes with the transmembrane lectin chaperone CNX in the ER. Mislocalization due to the Myc-epitope cannot be ruled out, however.

Regarding a possible biological function of TMX, significant resistance to ER stress resulting in apoptosis induced by treatment with brefeldin A, an inhibitor of ER-to-Golgi transport, has been reported. Moreover, a trx-like reducing activity of TMX has been observed *in vitro* (Matsuo et al., 2001), by reducing interchain disulfide bridges and subsequent cleavage of insulin. Also, the ability to interchange disulfide bonds and therefore reconstitute the activity of scrambled RNase has been observed (Matsuo et al. 2004).

An ortholog of TMX in *C. elegans* (DPY-11) is required for body and sensory organ morphogenesis. Furthermore, there is a possible role for proteins like TMX in the ER-associated degradation of proteins. As mentioned in section 1.6, in order to retranslocate terminally misfolded proteins from the ER back to the cytosol through the translocon complex and to degrade them by the ubiquitin-proteasome complex, polypeptides have to be unfolded by reduction of inter- and intramolecular disulfide bonds (Tsai et al., 2002 and Plemper et al., 1999). While much is known about molecular chaperones promoting protein folding, little is known about the manipulation of disulfide bonds catalyzed by oxidoreductases in the ER. ER-resident oxidoreductases can be implicated in unfolding of proteins destined for degradation

by ERAD, although none has yet been found to catalyze disulfide reduction in the oxidizing environment of the ER (Matsuo et al. 2004).

Most recent, yet unpublished, results by Simmen et al. indicate that TMX, like Ero1 α , is targeted to the MAM, a site where mitochondria are in close proximity to the ER. In order for the successful folding of secretory proteins, the maintenance of normal mitochondrial metabolism is required (Kuznetsov et al., 1996 and Osibow et al., 2006). Since the disruption of the MAM induces the unfolded protein response (UPR), normal MAM function is required for oxidative protein folding as well (Simmen et al., 2005).

1.10.2 TMX4 (also known as TXNDC13)

Currently, little is known about TMX4. It is an ER-localized protein of approximately 46 kDa. The overall structure of TMX4, depicted in Figure 1.7, is very similar to that of TMX, with the exception that TMX4 has two acidic clusters in its C-terminal cytosolic tail and an N-glycosylation site at Asn46 (Roth et al., unpublished). Unlike TMX and calnexin, despite harboring similar acidic clusters, TMX4 is not targeted to the MAM, and generally shows differing suborganellar localization as analysed with discontinuous 5–25% OptiPrep gradients (Simmen, personal communication).



Figure 1.7. Schematic outline of the human TMX4 protein. The 46 kDa protein consists of an N-terminal signal peptide targeting it to the ER, a trx-like (CPSC) domain, a transmembrane domain, and two acidic clusters and a non-classical ER-retention signal (RQR) at the C-terminus. The trx-like domain with the potential active site protrudes into the ER lumen, while the C-terminus forms a cytosolic tail.

1.11 PACS-2

Currently, there are two known homologs of the phosphofurin acidic cluster sorting protein, (PACS)-1 and PACS-2. Their function has been characterized as adaptor proteins that recognize C-terminal acidic clusters. By simultaneously binding these acidic cluster in a phosphorylation-dependent manner, and vesicle-specific coat proteins such as adaptor protein complex (AP)-1, AP-3 and coat protein (COP) I, the PACS proteins direct trafficking of their cargo. It has been demonstrated that the subcellular localization of polycystin-2, a Ca²⁺ permeable nonselective cation channel of the transient receptor potential (TRP) channel family, is orchestrated by PACS-1 and PACS-2. Thus, the presence of acidic clusters within many ion channels

suggests a potential role for PACS proteins in the sorting of ion channels to cellular compartments (Kottgen et al., 2005; Crump et al., 2001; Scott et al., 2006).

Additionally, PACS-2 has been reported to have important roles in the subcellular localization of the ER chaperone calnexin (Myhill et al., 2008) and the sorting of internalized cation-independent mannose-6-phosphate receptor (CI-MPR); it also interacts with HIV-1 negative factor (Nef), a regulator of viral replication and pathogenesis, thereby assisting the assembly of a multikinase cascade that triggers MHC-1 downregulation (Atkins et al., 2008).

Moreover, PACS-2 integrates ER–mitochondria communication, ER homeostasis, and apoptosis, by regulating the integrity and molecular composition of the MAM (Simmen et al., 2005).

1.12 Vascular endothelial growth factors (VEGFs)

Originally, vascular endothelial growth factor (VEGF) was discovered as vascular permeability factor (VPF) by (Senger et al., 1983). Only shortly after, it was revealed that VPF and VEGF are the same protein, and VEGF was characterized as a heparin-binding protein acting as a mitogen specific for endothelial cells (Leung et al., 1989; Keck et al., 1989).

Due to the multitude of its potent functions, VEGF has been found to be critical to human cancer angiogenesis, which is essential for tumor development and progression. Among the reported effects are the stimulation of endothelial cell survival, mitogenesis, migration, differentiation, and self-assembly, as well as enhancement of vascular permeability, lymphangiogenesis, immunosuppression, stimulation and recruitment of bone-marrow-derived endothelial and hematopoietic precursor cells in angiogenesis, and regulation of hematopoietic stem cell survival (reviewed by Xie et al., 2004). It has to be mentioned that neovascularization and vessel maturation are processes of high complexity and coordination, where sequential activation of different receptors by numerous ligands is required. However, the VEGF signaling system often is the rate-limiting step in physiological angiogenesis. Thus, VEGF and its receptors are rapidly emerging targets in cancer therapy. Especially the combination of anti-VEGF treatments with chemotherapy and radiation therapy is a potent instrument in the treatment of cancer.

Containing the eight characteristic and highly conserved cysteines, which form dimers linked by a disulfide bond (cystines), VEGFs belong to the VEGF/PDGF (platelet-derived growth factor) group of the cystine-knot superfamily of hormones

and extracellular signaling molecules, and are evolutionarily related to the glycoprotein hormone and mucin-like protein families and, more distantly, the transforming growth factor- β (TGF- β) family. Since no member of the cystine-knot superfamily is present in unicellular eukaryotes such as yeasts, it can be assumed that these proteins evolved as hormones and extracellular signaling molecules exclusively in multicellular organisms with tissue-level organization. The presence of VEGF-like molecules in invertebrates suggests that they appeared relatively early in the evolution of multicellular animal life.

1.12.1 The VEGF family members

Currently there are 6 known VEGF genes mentioned in the literature, VEGF or VEGF-A located on chromosome 6p12-21, VEGF-B (11q13), VEGF-C (4q34), VEGF-D (Xp22.31), VEGF-E (*Parapox*, *Orf* virus), and the placenta growth factor (PLGF) (14q24-q31). Characteristic for the human VEGF genes is that all of them, with the exception of VEGF-A having eight exons, are organized in seven exons. VEGF gene products are all proteins targeted for secretion (reviewed in Holmes & Zachary, 2005).

At least six different transcripts arise from the human VEGF-A gene through alternative splicing. These transcripts code for the following isoforms: VEGF-A₁₂₁, VEGF-A₁₄₅, VEGF-A₁₆₅, VEGF-A_{165b}, VEGF-A₁₈₃, VEGF-A₁₈₉ and VEGF-A₂₀₆ (the numbers indicate the length in amino acids, not counting the signal sequence). Whereas exons 1-5 and 8 are common to all transcripts, diversity is produced by alternative splicing of exons 6 and 7. Since exons 6 and 7 harbor the heparin-binding domain and the neuropilin1 (NRP1)/heparin-binding domain, respectively, the different isoforms of VEGF-A exhibit variable affinities for heparin and heparin sulfate, and differ in their ability to bind to neuropilins (NRP1 and NRP2). The different human VEGF genes and their structural characteristics are summarized along with related genes in *Drosophila* in Figure 1.8. As indicated, exon 1 and a small portion of exon 2 comprise the hydrophobic signal peptide necessary for secretion of VEGF-A. Exons 3 and 4 encode the VEGF/PDGF homology domain (VHD). Most cell types express multiple variants of VEGF-A, albeit VEGF-A₁₂₁ and VEGF-A₁₆₅ are the two major VEGF-A isoforms in mammals. Due to the lack of exons 6 and 7, which are needed in order to bind heparin, VEGF-A₁₂₁ is not able to interact with the polysaccharide and is generally less potent than VEGF-A₁₆₅. All the other isoforms, however, are assumed to possess this binding capability. In contrast

to VEGF-A₁₄₅ (containing exon 8, but lacking exon 7), which only binds to neuropilin 2 (NRP2), VEGF-A₁₆₅ (containing exons 7 and 8) binds to NRP1 and NRP2. VEGF-A_{165b}, a recently discovered splice variant that is proposedly inhibitory to VEGF activity, misses exon 6 and contains a novel C-terminal sequence transcribed from an alternative exon 8. Typically, human VEGF-A₁₆₅ is expressed as a homodimer of 46 kDa with glycosylation sites at Asn76. Although all the VEGFs are secreted proteins, in contrast to VEGF-A₁₂₁ and VEGF-A₁₆₅, which are both secreted as covalently linked homodimers, the bioavailability of the larger isoforms, VEGF-A₁₈₉ and VEGF-A₂₀₆, is assumed to be regulated by plasmin-mediated cleavage that releases more diffusible, biologically active species (VEGF-A₁₁₀) from the extracellular matrix (ECM) (see Figure 1.9). Table 1.1 gives an overview of the isoforms of human VEGF-A.

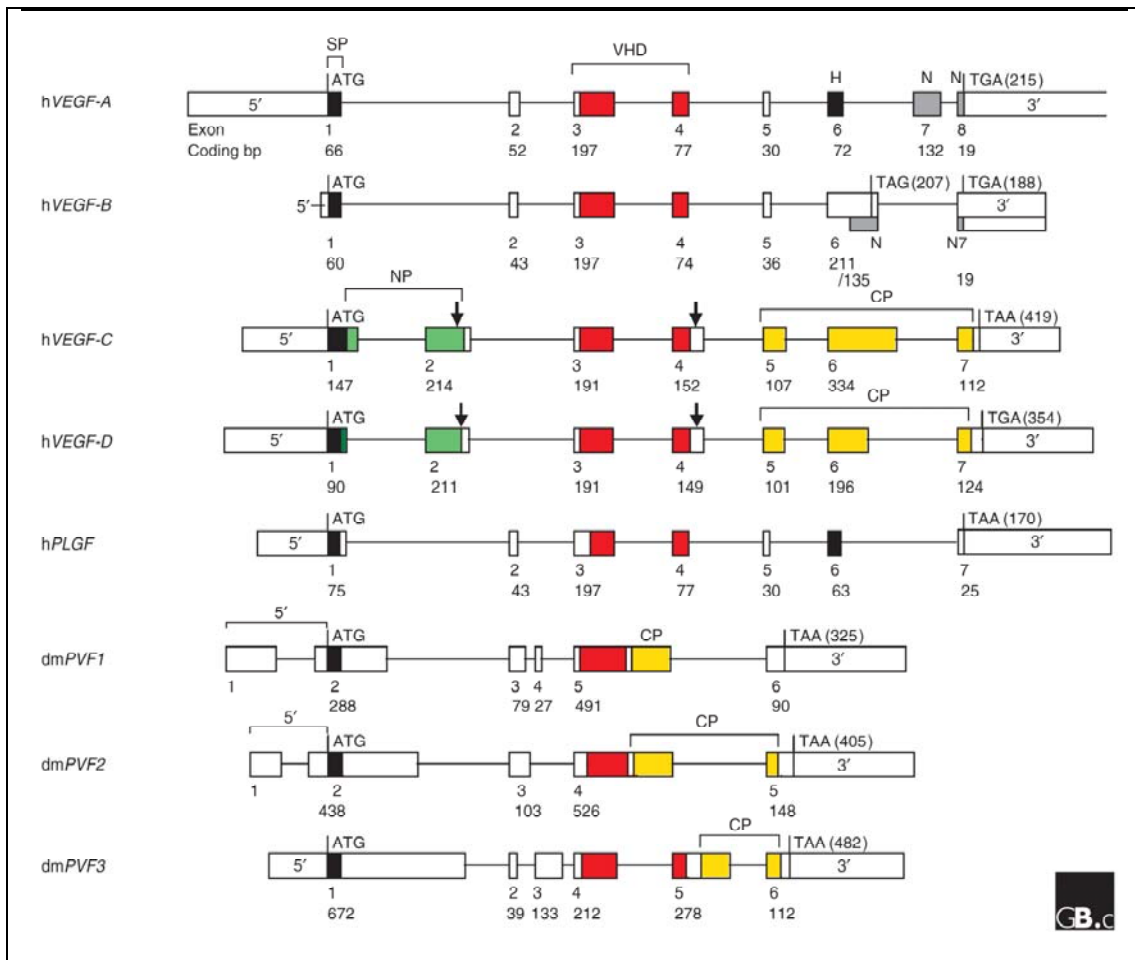


Figure 1.8. Gene organization and encoded functional domains of the human VEGF genes and related genes from *Drosophila*. Exons, represented by boxes, are numbered, and the length of coding sequence in each is marked below in base-pairs. Start (ATG) and stop (TAA, TAG, TGA) codons are shown, and the length (in amino-acid residues) of each encoded unprocessed polypeptide including the signal peptide is indicated in parentheses. Exons are drawn to scale, except for the last exon of *hVEGF-A*, which is longer than 1 kilobase (kb). Introns, represented by horizontal lines, are not drawn to scale. Alternative exons and splicing patterns are not shown, with the exception of *hVEGF-B*, in which the isoforms result from alternative splicing of exon 6. Arrows represent proteolytic cleavage

sites. Abbreviations: 3', 3' untranslated region (UTR); 5', 5' UTR; CP, region encoding the carboxy-terminal propeptide domain; H, encodes the heparin-binding domain; N, encodes the NRP1/heparin-binding domain; NP, encodes the amino-terminal propeptide domain; SP, signal peptide; VHD, encodes the VEGF/PDGF homology domain; PVF, PDGF/VEGF-like factors. (Adapted from Figure 2 in Holmes & Zachary, 2005).

Table 1.1. Overview of the isoforms of human VEGF-A (Holmes & Zachary, 2005)

Isoforms of human VEGF-A			
Isoform	Nr. of amino acids	Exons translated	Features
VEGF-A ₁₂₁	121	1-5, 8	Secreted
VEGF-A ₁₄₅	145	1-6, 8	Binds NRP2 but not NRP1; secreted
VEGF-A ₁₆₅	165	1-5, 7, 8	The most abundant and biologically active isoform; secreted; binds NRP1 and NRP2
VEGF-A _{165b}	165	1-5, 7, alternative exon 8	Secreted; endogenous inhibitory form of VEGF-A ₁₆₅
VEGF-A ₁₈₃	183	1-5, short exon 6, 7, 8	Sequestered to ECM but released by cleavage
VEGF-A ₁₈₉	189	1-8	Sequestered to ECM but released by cleavage
VEGF-A ₂₀₆	206	1-8 plus additional exon 6-encoded sequence	Sequestered to ECM but released by cleavage

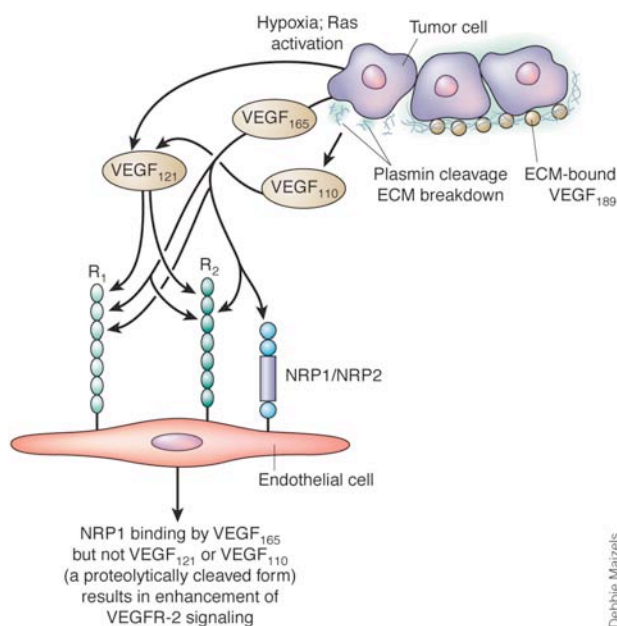


Figure 1.9. The VEGF isoforms and their interaction with VEGF receptors. In response to stimuli, the diffusible VEGF isoforms, VEGF₁₂₁ and VEGF₁₆₅, are released by a variety of normal and transformed cells (tumor cells shown) and may bind to VEGFR-1 (R₁) and VEGFR-2 (R₂). VEGF₁₆₅, but not VEGF₁₂₁, also interacts with NRP1 and NRP2. This binding results in enhanced VEGFR-2-dependent signaling in endothelial cells (EC). Following plasmin generation and extracellular matrix (ECM) breakdown, VEGF₁₈₉ is cleaved at the COOH-terminus and the resulting 110-amino acid NH₂-terminal fragment is diffusible and bioactive. (Adapted from Figure 1 by Ferrara et al., 2003)

Debbie Maizels

VEGF-B only has two splice variants, a transcript encoding for the 167-amino-acid form containing an alternative exon 6 (exon 6b; generated by a frameshift due to the use of an alternative splice acceptor site) with an NRP1/heparin-binding domain similar to that encoded by exons 7 and 8 in VEGF-A₁₆₅, and a transcript which contains the entire exon 6, encoding for a freely secreted, soluble 186-amino-acid form. VEGF-B is structurally closely related to VEGF-A, and both of its isoforms are able to form heterodimers with VEGF-A.

VEGF-C, originally cloned from human prostate carcinoma cells, and VEGF-D (also known as c-fos-induced growth factor) are very similar regarding both structure and function. They share 61% sequence identity and the proteolytical processing is alike. Also common to VEGF-C and VEGF-D is that they appear to be unable to bind NRPs, resulting from the lack of the NRP/heparin-binding domain. Synthesized as a preproprotein, VEGF-C exists as several forms generated by stepwise proteolytic processing, in the course of which binding and activity for its receptors increase sequentially. The mature form of VEGF-C, consisting of the VEGF homology domain, shares 30% identity with VEGF-A₁₆₅. The regulation of the biological activity and the receptor specificity of VEGF-D appear to be dependent on the proteolytic processing, similarly to VEGF-C, which is possibly cleaved by plasmin during or after secretion, thereby releasing the VHD to produce a mature form of about 21 kDa able to bind VEGFR-2 with high affinity as homodimers.

VEGF-Es are VEGF-like molecules that were discovered in the genome of *Parapoxvirus* (orf virus). Forming two distinguishable groups, VEGF-E_(NZ2) and VEGF-E_(D1701) are most closely related to VEGF-A and PLGF, whereas VEGF-E_(NZ7) is related more closely to VEGF-C and VEGF-D.

Four isoforms of human placental growth factor (PLGF) are known so far, PLGF-1 to PLGF-4. PLGF-1 and PLGF-2 are thought to be the major isoforms encoding 131 and 152 amino acids (not counting the signal peptide), respectively. The difference between PLGF-1 and PLGF-2 is that the former lacks the heparin-binding domain encoded by exon 6 rendering it unable to bind heparin. PLGF-3 is also unable to bind heparin due to the lack of exon 6, but contains a 216-nucleotide insertion between exons 4 and 5. PLGF-4 consists of the same sequence as PLGF-3 but additionally contains the heparin-binding domain in exon 6. It is assumed that PLGF-3 and PLGF-4 (consisting of 203 and 224 amino acids plus signal peptide, respectively) have functions similar to those of the larger 189 and 206 amino acid isoforms of VEGF-A.

1.12.2 Regulation of VEGF gene expression

The expression of VEGF is regulated by numerous pathways at several levels, possibly due to its crucial role in, e.g. angiogenesis, mitogenesis, and as a stimulator of cell survival. Arising from its functional potency, perturbations in the expression and signaling of VEGF and its receptors unequivocally confer an immense survival and growth advantage to the affected cells resulting in exuberant tumor angiogenesis and its consequent malignancy. Constitutive, as well as inducible, expression of VEGF has been found to be regulated at the levels of gene transcription and translation, and at the posttranslational level. With the aid of computer-based sequence analysis of the VEGF promoter, gene transcription has become the best-studied regulatory mechanism for VEGF expression. The numerous transcription factors involved indicate the sophistication of VEGF transcriptional regulation. The key proteins that bind to the 5'-UTR of the VEGF gene thereby regulating its transcription are e.g., activator protein-1 (AP-1), signal transducer and activator of transcription-3 (Stat3), specific protein-1 (Sp1), and hypoxia-inducible factor-1 (HIF-1), which will be described in detail in section 1.13. At the posttranscriptional level the expression of VEGF is controlled and therefore enhanced through stabilization of VEGF mRNA. Under hypoxic conditions, i.e. decreased oxygen tension, a protein called HuR (Human antigen R), which itself is being controlled via stress-activated pathways, binds to AU-rich elements in the 5'-UTR and 3'-UTR of VEGF mRNA to such an effect as to stabilize the mRNA by increasing its half-life. Furthermore the 5'-UTR of VEGF mRNA contains two functional internal ribosome entry sites (IRES) making it independent of the usual cap-dependent mechanism of protein translation. In addition, several other factors seem to play roles in the molecular regulation of VEGF expression e.g., overexpression of eukaryotic initiation factor 4E (eIF4E), as observed in various cancers, has been reported to increase VEGF secretion up to 130-fold. Also, hypoxia-mediated overexpression of the 150 kDa oxygen-regulated protein (ORP150), a molecular chaperone in the ER responsible for folding and trafficking of newly synthesized proteins to the Golgi apparatus for subsequent secretion, appears to be essential for enhanced secretion of VEGF as indicated by overexpression- and silencing-experiments of ORP150.

VEGF-mediated tumor angiogenic switch-on, essential for sustained growth and metastasis of tumors, is assumed to be a synergistic effect of constitutive VEGF expression, serving as an initiation signal, and an inducible expression of VEGF. Constitutive expression of VEGF can be generally related to genetic alterations necessary for the formation of tumors and depends on loss of function of tumor

suppressor genes (VHL, von Hippel-Lindau factor; TP53, encoding for p53; p73, capable of activating p53-responsive promoters; PTEN, phosphatase and tensin homolog, an inhibitor of PI3K/Akt signaling; p16, an inhibitor of cyclin-dependent kinase 2A) and/or gain of function of oncogenes, such as *Ras* (an activating factor of MAPK and PI3K/Akt signaling), *Src* kinase, HER2 (human epidermal growth factor receptor 2) and others. Inducible VEGF expression, however, emerges from tumor microenvironmental factors, such as overproduction of growth factors and cytokines, oxidative stress, acidosis, and hypoxia. Oxidative stress is caused by imbalances in the cellular products, reactive nitrogen (NO) and oxygen species (ROS: superoxide O_2^- , hydroxyl radical OH^\bullet , H_2O_2). While ROS are continuously generated as products of cellular mitochondrial metabolism, the low pH and the elevated levels of NO within cells are tied to hypoxic conditions and therefore hypoxia can be defined as the major factor influencing inducible VEGF expression. For further detail see section 1.13.

1.12.3 VEGF receptors, neuropilins, and VEGF signaling

Two classes of high-affinity receptors for VEGF have been reported so far. The first class is formed by VEGFR-1, VEGFR-2 and VEGFR-3, all of which are members of the receptor tyrosine kinase family and are expressed as cell surface proteins. Their structure is determined by seven extracellular immunoglobulin homology domains and two intracellular tyrosine kinase domains separated by a kinase insert. The precise function of VEGFR-1 is still not fully clarified. It is assumed that its particular functions and signaling properties depend on the developmental stage of the animal and cell type. The primary function of VEGFR-1 and its soluble form generated by alternative splicing, which has an inhibitory effect on VEGF activity, is still a matter of an ongoing debate. It has been proposed that instead of being a receptor transmitting a mitogenic signal, VEGFR-1 competes with VEGFR-2 in binding VEGF and thereby inhibits the activation of downstream signaling through VEGFR-2. This could also be an explanation for the potentiating effect of VEGF binding to NRP-1, which raises the level of VEGF available for binding to VEGFR-2. VEGFR-2 itself is well established as the main mediator of the mitogenic, angiogenic and permeability-increasing effects of VEGF. VEGFR-3 plays a role in the binding of VEGF-C and -D.

The receptor-ligand interactions and the cells expressing the respective VEGFR isoforms are summarized in Figure 1.10 and Table 1.2.

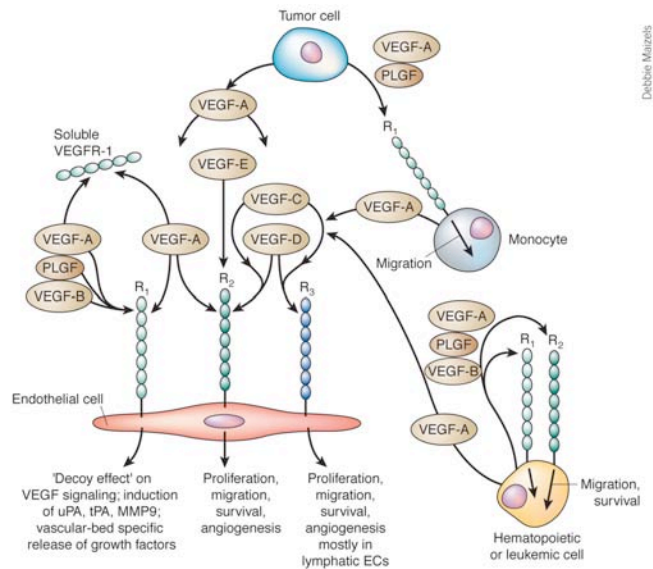


Figure 1.10. Role of the VEGF receptor tyrosine kinases in different cell types. VEGFR-1 and VEGFR-2 are expressed on the cell surface of most blood vessel ECs. However, VEGFR-3 is largely restricted to lymphatic EC. VEGF-A binds both VEGFR-1 and VEGFR-2. In contrast, PLGF and VEGF-B interact only with VEGFR-1. The orf-virus-derived VEGF-E is a selective VEGFR-2 agonist. VEGF-C and VEGF-D bind to VEGFR-2 and VEGFR-3. There is ample evidence that VEGFR-2 is the major mediator of EC mitogenesis and survival, as well as angiogenesis and microvascular permeability. In contrast, VEGFR-1 does not mediate an effective mitogenic signal in EC and it may, especially during early embryonic development, perform an inhibitory role by sequestering VEGF and preventing its interaction with VEGFR-2. Such a “decoy” role might be also performed by the alternatively spliced soluble VEGFR-1. However, VEGFR-1 has an established signaling role in mediating monocyte chemotaxis. Also, in hematopoietic stem cells (HSC) or leukemic cells, both VEGFR-1 and VEGFR-2 may mediate a chemotactic and survival signal. R₁, VEGFR-1; R₂, VEGFR-2; R₃, VEGFR-3. (adapted from Figure 2 by Ferrara et al., 2003)

Table 1.2. Overview of the localization of expression and interactions of the human VEGF receptors

Receptor	Ligands	Expression of Receptor
VEGFR-1	VEGF-A, VEGF-B, PLGF-1 and PLGF-2	Selectively, though not exclusively, expressed on vascular endothelium
VEGFR-2	VEGF-A, -C, -D and -E	Selectively, though not exclusively, expressed on vascular endothelium; also present on lymphatic endothelium
VEGFR-3	VEGF-C and VEGF-D	Mainly expressed on lymphatic endothelium, but also on vascular endothelium

Neuropilin-1 and -2 (NRP-1 and -2) constitute the second class of VEGF receptors. They are nontyrosine kinase receptors able to bind VEGF-A, -B and -E and PLGF-2 with high affinity. Their short cytoplasmic tails exhibit no known signaling function and therefore might not be functional receptors on their own. However, they have been described as co-receptors of the different VEGFRs. For example, it has been reported that NRP-1, acting as a co-receptor for binding VEGF-A₁₆₅, increases the affinity of VEGF-A₁₆₅ to VEGFR-2 by approximately 10-fold. As a result, VEGF-A₁₆₅ is

the most potent signal transducer among the VEGF isoforms. Cells expressing exclusively NRP-1, but no other VEGFR, do not respond to VEGF-A₁₆₅. Generally NRP-1 is co-expressed with VEGFR-1 and VEGFR-2 on the vascular endothelium, neurons, and certain tumor cells. Furthermore, NRP-2 is co-expressed with VEGFR-3 in the endothelium of the lymphatic vasculature, and has been found to bind VEGF-C (reviewed in Ferrara et al., 2003).

As soon as VEGF binds to its receptors, it initiates a signaling cascade starting with receptor dimerization, leading to autophosphorylation by the tyrosine kinase domain to become active receptors. Subsequently, numerous downstream proteins and their respective pathways are activated, among which are mitogen-activated protein kinase (MAPK), phospholipase C- γ /protein kinase C (PKC), phosphatidylinositol-3 kinase (PI3K), the *Ras* pathway members, and others, to achieve various effects, such as an increase in vascular permeability, inhibition of apoptosis, cell proliferation, and migration.

1.13 Hypoxia

It is a hallmark of solid tumors to contain regions of low oxygenation, which itself is an indicator of poor patient prognosis also regarding the prevalence of metastasis. Whereas the oxygen concentration in normal tissue lies within the range of ~3-9% O₂ (average around 7% O₂), in solid tumors it varies from complete anoxia to ~4% O₂ with an assumed average of approximately 1.5% O₂ (reviewed by van den Beucken et al., 2006). In order for cells, i.e. tumor cells, to avoid undergoing apoptosis and to maintain functional cell metabolism under hypoxic conditions, they have to adapt by exhibiting an altered gene expression pattern. Critical to these cellular responses is the role of the hypoxia-inducible factor 1 (HIF-1). HIF-1, member of the basic helix-loop-helix (bHLH) family of transcription factors, is a heterodimer of HIF-1 α (120 kDa) and HIF-1 β (~90 kDa). It activates a transcriptional program that stimulates genes involved in angiogenesis (e.g., VEGF), cell metabolism, apoptosis resistance, and cell invasion. Generally, if undersupplied with oxygen, cells try to save energy by suppressing the highly energy-consuming protein synthesis. To this end cells use two distinct pathways. As soon as 30 min after exposure to severe as well as more moderate hypoxia (<0.05% and ~1% O₂, respectively) translation initiation is transiently inhibited utilizing an unfolded protein response (UPR) pathway by phosphorylating the eukaryotic initiation factor 2 α (eIF2 α) in a PERK-dependent fashion thereby blocking the formation of the ternary complex and impeding the

recruitment of ribosomes onto mRNA transcripts. The second step occurs after prolonged hypoxic conditions (~16 h) mainly by the disruption of the cap binding complex eIF4F (consisting of the cap binding protein eIF4E, the scaffolding protein eIF4G and an ATP-dependent helicase eIF4A) by inhibiting the activation of mTOR (mammalian target of rapamycin), which is now unable to inactivate eIF4E binding proteins by phosphorylating them. However, not all proteins are affected to the same extent by this translation inhibition. There are several instruments for bypassing these regulatory mechanisms of protein synthesis readily available under hypoxic conditions, which are all based on specific sequences in the 5'- and 3'-UTRs of the affected mRNAs. The pathways enabling efficient protein synthesis despite its global impairment can be divided in HIF-1-dependent and HIF-1-independent systems. One of the latter is the PERK-eIF2 α -ATF4 pathway, a UPR pathway. Paradoxically, PERK-eIF2 α also facilitates the expression of ATF4, a member of the activating transcription factor (ATF)/cAMP responsive element binding protein (CREB) family. Because the availability of ternary complexes upon eIF2 α phosphorylation is low, instead of upstream ORFs (uORFs) used under normal circumstances and not encoding a functional protein, the ATF4 ORF is used resulting in ATF4 translation (reviewed in Fels & Koumenis, 2006). As this is just an example for the mechanism of selective translation, it remains unclear how many genes contain translation inhibitory uORFs. Additional HIF-1-independent positive regulators of transcription are the already mentioned IRES. Their mRNA secondary structure enables direct ribosome binding without the need for cap-structures on mRNAs. Prominent examples of mRNAs containing IRES activity are those of VEGF, BiP/Grp78, and HIF-1 α itself. The third known HIF-1-independent mechanism to bypass translation inhibition is based on the existence of 5' terminal oligopyrimidine tract (TOP) sequences. The translation of mRNAs containing such a sequence is greatly increased via an mTOR-S6K pathway (Ruvinsky & Meyuhas, 2006). Interestingly, again the 5'-UTR of HIF-1 α has been reported to contain such 5'TOP sequences. Nevertheless, despite this variety of HIF-1-independent mechanisms, upregulation of gene expression by hypoxia is thought to be mediated mainly by HIF-1 (reviewed, e.g., by Greijer et al, 2005). However, it should be mentioned that HIF-1 also causes downregulation of certain genes. The hypoxia inducible factor 1 complex comprises two subunits, HIF-1 α and HIF-1 β . Whereas HIF-1 β , also known as aryl hydrocarbon receptor nuclear translocator (ARNT), is constitutively expressed, the expression of HIF-1 α is tightly regulated by an oxygen-sensing system. Although there are pathways through which HIF-1 α translation can be induced, its regulation by hypoxia

takes place primarily at the protein level. Under normoxic conditions, HIF-1 α is subject to ubiquitination and proteasomal degradation, a process inhibited under hypoxic conditions, in turn leading to the formation of the heterodimeric active transcription factor (Semenza, 2001). So far, at least 45 human genes have been identified as HIF-1 regulated (reviewed by Greijer et al., 2005), through which the whole metabolism of cancer cells is determined (Semenza, 2009).

Given aerobic conditions, one of the members of the prolyl hydroxylase enzyme family (PHD1-3) hydroxylates two proline residues in the oxygen dependent degradation domain (ODD) of HIF-1 α . In order for this reaction to take place, of course, dioxygen is needed, but also α -ketoglutarate from the TCA-cycle. Most recent findings (Pollard & Ratcliffe, 2009) point to a role of IDH1 (cytoplasmic localized isocitrate dehydrogenase) in the hydroxylation pathway of HIF-1 α . A mutated form of IDH1 that inefficiently catalyzes the formation of α -ketoglutarate has been found in tumor cells, thus promoting HIF-1 activity. Another protein, the von Hippel-Lindau factor (pVHL), specifically recognizes the hydroxylated form of HIF-1 α , and together with cofactors targets it for ubiquitination and subsequent degradation by the 26S proteasome. Moreover, normoxic conditions also cause hydroxylation of HIF-1 α at a second site, thereby inhibiting the binding of the co-activators CBP (CREB binding protein) and p300 (E1A binding protein p300) needed for transcription (Semenza, 2009). However, if oxygen levels are low, HIF-1 α and HIF-1 β form a heterodimer that binds to a DNA element referred to as the hypoxia responsive element (HRE) in 5'-UTRs of genes. The general sequence of the HRE, 5'-(A/G)CGTG-3', is subject to mutations, resulting in different binding affinities of HIF-1 (Kaluz et al., 2008) These mechanisms are summarized in Figure 1.11.

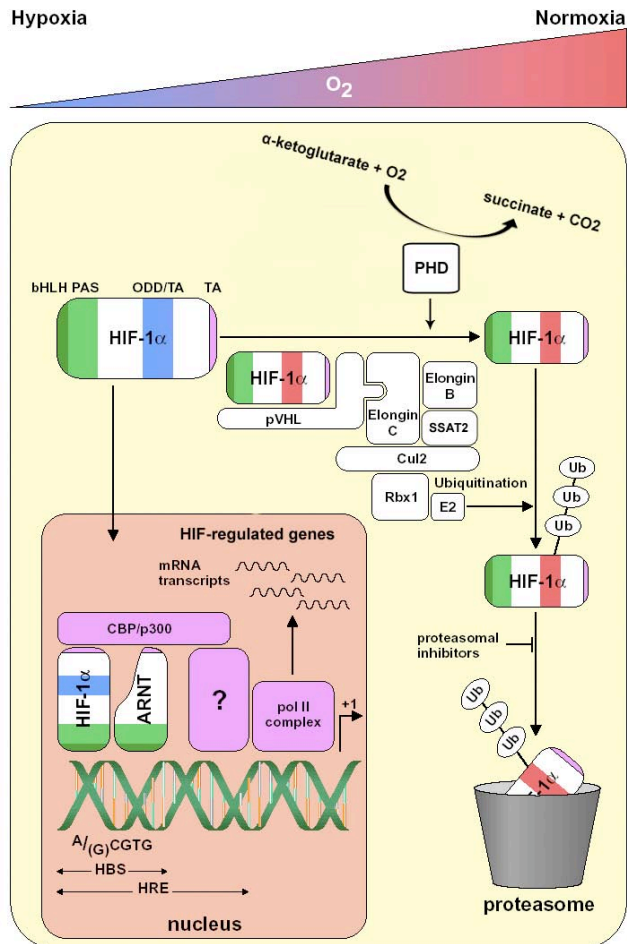


Figure 1.11. Schematic model of the regulation of HIF-1. Under hypoxic conditions, the ODD/TA domain of HIF-1 α (blue) is stable and allows nuclear translocation and gene regulation. Under normoxic conditions, the ODD/TA domain (red) gets hydroxylated by PHD and targets HIF-1 α for proteolytic degradation via ubiquitination by a complex containing pVHL. ARNT, aryl hydrocarbon receptor nuclear translocator (HIF-1 β); bHLH, basic-helix-loop-helix; CBP, CREB binding protein (CBP and p300 are two related transcriptional coactivators with histone acetyltransferase activity); SSAT2, Spermidine/Spermine N1-Acetyltransferase 2; Cul2, cullin 2; E2, unknown ubiquitin-conjugating enzyme; HBS, HIF-1 binding site; HRE, hypoxia-response element; ODD, oxygen-dependent degradation domain; PAS, Per-AhR/ARNT-Sim domain; pol II, RNA polymerase II; pVHL, von-Hippel-Lindau tumour suppressor protein;

Rbx1, a RING-H2 finger protein; TA, transactivation domain; Ub, ubiquitin; +1 indicates the transcriptional start site. Additional hydroxylation of HIF-1 α by FIH-1 (factor inhibiting HIF-1) and therefore blockage of the binding site of CBP/p300 is not shown. For a detailed explanation, see Semenza, 2009.

2 Materials & Methods

2.1 Chemicals

Chemicals used for buffers, solutions, and media were obtained from GE Healthcare, Sigma Aldrich, Fisher Scientific, or Invitrogen, if not stated otherwise.

2.2 Melanoma and breast cancer tissue

All samples were obtained from the Cross Cancer Institute, 11560 University Avenue Edmonton, Alberta T6G 1Z2.

2.3 Cell culture

2.3.1 Cell lines

HeLa: Human cervix epitheloid carcinoma / Human epithelial carcinoma cell line derived from cervical cancer.

HEK293: Human embryonic kidney cell line.

A375P: Human melanoma cell line, low metastatic properties.

A375M: Human melanoma cell line, medium metastatic properties.

2.3.2 Cell culture media

For the cultivation of HeLa and HEK293 cells, DMEM (Invitrogen) supplemented with 10% FBS (Invitrogen) was used. For the melanoma cell lines, A375P and A375M, RPMI 1640 (Invitrogen) supplemented with 10% FBS (Invitrogen) was used. Transfections were carried out in Opti-MEM® (Invitrogen). For secretion assays DMEM or RPMI 1640 without FBS were used.

DMEM: Invitrogen, Cat. No. 11995-065

RPMI 1640: Invitrogen, Cat. No. 11875-093

FBS: Invitrogen, Cat.No. 12483-020

2.3.3 Splitting of cells

All cell lines were incubated at 37°C and 5% CO₂. Morphology and growth were monitored under the microscope.

After assuring a confluent state, the cell culture medium was aspirated and 2ml of 0.25% trypsin were added and aspirated again immediately. Another 2ml of trypsin

were added of which ~1ml was aspirated at once. For 5-10 min (depending on the cell type), the cells were put back into the incubator (37°C, 5% CO₂). After this incubation time, cells were checked for loss of adhesion. The cells were then carefully washed off with 9ml of cell culture medium containing 10% FBS and resuspended. For propagation of the cells, aliquots of the cell suspension were transferred to a new cell culture flask containing fresh cell culture medium. If a certain cell number was required, 10 µl of the cell suspension were transferred to a hemacytometer and the cells were counted under the microscope. Depending on the cell number, the required volume of the cell suspension was mixed with the required volume of fresh medium.

2.3.4 Transfection with Metafectene Pro®

According to the manufacturer's protocol, 9×10^5 cells per well were seeded into a 6-well cell culture plate and put back into the incubator (37°C, 5% CO₂) for 4-6 h. Per well, 2 µg of plasmid DNA were diluted in 100 µl PBS++, and 7 µl of Metafectene Pro® were diluted in 100 µl PBS++ as well. The solutions were mixed by carefully pipetting them once. In the next step the two solutions were combined and mixed by gently shaking them once. The transfection mix then was put aside to let it incubate for 15 to 20 min at room temperature. 200 µl of the transfection mix were added dropwise to the wells and the plates were put back into the incubator (37°C, 5% CO₂). After 3 to 6 h the medium in the wells containing the transfection mix was removed because of the toxicity of the transfectant.

1x PBS:

137 mM NaCl

2.7 mM KCl

10 mM Na₂HPO₄

1.76 mM KH₂PO₄

pH 7.4

PBS++:

1x PBS

0.5 mM MgCl₂

1 mM CaCl₂

2.3.5 Transfection with Lipofectamine™ 2000

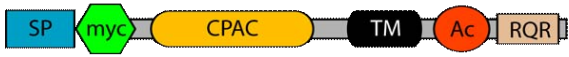
According to the manufacturer's protocol, 9×10^5 cells per well were seeded into a 6-well cell culture plate and put back into the incubator (37°C, 5% CO₂) for 18 to 24 h. Per well, 2 µg of plasmid DNA were diluted in 250 µl Opti-MEM®, and 4 µl of Lipofectamine™ 2000 were diluted in 250 µl Opti-MEM® as well. After 5 min of incubation at room temperature, the two solutions were combined and carefully

mixed. This transfectant mixture was put aside for a 30-incubation. The medium of the 6-well plates was aspirated, cells were washed once with 2ml of Opti-MEM® per well, and finally 1.5 ml of Opti-MEM® were added to each well. 500 µl of the transfectant mixture were then added to each well. The 6-well plates were put back into the incubator (37°C, 5% CO₂) for 4 h. Then, the transfection solution then was replaced by 2 ml of DMEM containing 10% FBS.

2.3.6 Transfection constructs and vector systems

The constructs used for transfection were already available and are listed in Table 2.1.

Table 2.1. Constructs used for transfection. All the constructs were generated with the pcDNA3 vector (see Figure 1.1. for vector map), with the exception of Ero1-L α , which was expressed from the pcDNA3.1/myc-His(-) vector (see Figure 1.2. for vector map). The clones of TMX1, TMX4 and the mutant TMX4s contain a Myc-tag inserted right after the signal peptide (amino acids 1 – 23). PACS-2, which is HA-tagged at the N-terminus, was expressed from pcDNA3 as well. For Ero1-L α the construct containing 3 Myc-Tags, described in Cabibbo et al. (2000) was used. *TMX4mut1: substitution of amino acids 253-255 from EEE to AAA; **TMX4mut2: substitution of amino acids 262-265 from DDEE to AAAA; ***TMXmut3: combination of mut1 and mut2; sequence of Myc-tag: EQKLISEEDLN; sequence of the HA-tag: FYPYDVPDYA.

Vector	Expressed Insert
pcDNA3	Myc-TMX4 
	Myc-TMX1 
	HA-PACS-2
	Myc-TMX4mut1* 
	Myc-TMX4mut2** 
	Myc-TMX4mut3*** 
pcDNA3.1/myc-His(-)	Ero1-L α

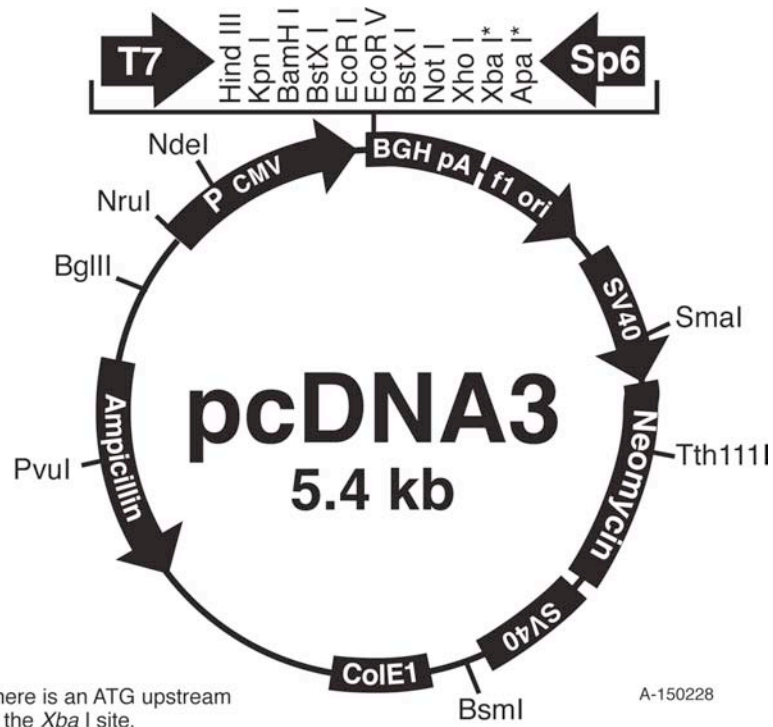


Figure 2.1. Map of the eukaryotic expression plasmid pcDNA3.

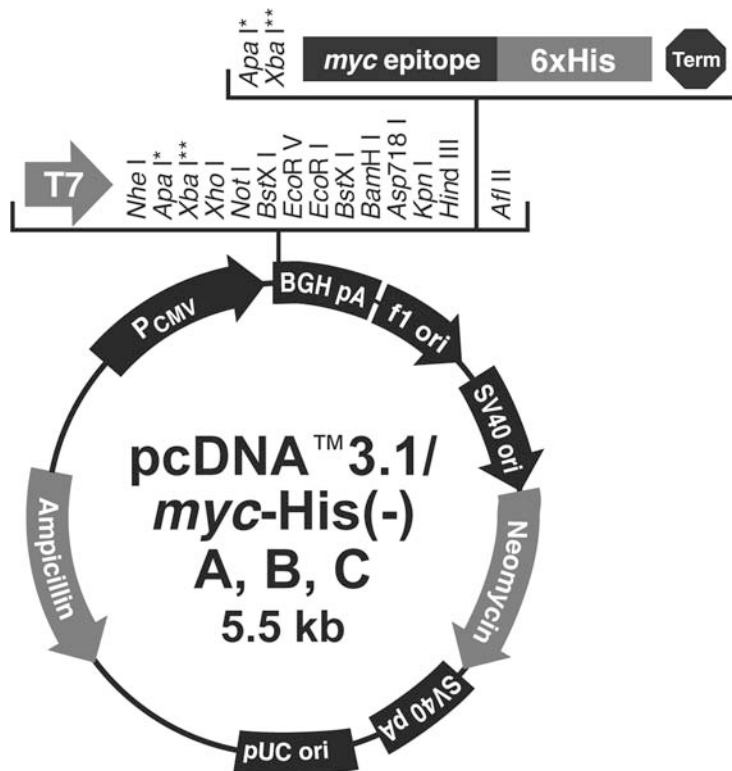


Figure 2.2. Map of the eukaryotic expression plasmid pcDNA™3.1/myc-His(-).

2.3.7 Transfection with Oligofectamine™

For siRNA transfection, 1.5×10^5 to 2×10^5 cells per well were split into 6-well cell culture plates 4 to 6 h prior to transfection.

Per well, 10 μ l siRNA (20 and 25 nM) were added to 175 μ l Opti-MEM® and 4 μ l of Oligofectamine™ were diluted in 11 μ l Opti-MEM® in separate Eppendorf tubes.

The two solutions were set aside for 5 min, then they were combined and incubated for 30 min. Original medium in the wells was removed, the cells were washed twice with 1ml Opti-MEM®, and finally 800 μ l of Opti-MEM® was added to each well. The 200 μ l transfection solution were added to the wells, and the plates were put back into the incubator (37°C, 5% CO₂) for 3 to 4 h. Then, the Opti-MEM® containing the transfectant was exchanged for DMEM w/o FBS.

siRNAs:

siSCR: Ambion Cat#: AM4635 Silencer ® Negative Control siRNA#1 25 nM
Lot#: AS00DZQ5

siTMX1 (TXNDC): TXNDC-HSS129874, 20 nM, Stealth™ RNAi 7128580
(Invitrogen)

siTMX4 (TXNDC13): TXNDC-13-HSS125494, 20 nM, Stealth™ RNAi 098291
(Invitrogen)

siEro1 α : ERO1L-HSS121197, 20nM, Stealth™ RNAi 7147744 (Invitrogen)

siPACS-2: PACS-2-HSS146278, 20 nM, and HSS146280, 20nM, Stealth™ RNAi
097383 (Invitrogen)

2.3.8 Chemical treatment of cells

2.3.8.1 *Treatment with cobaltous chloride (CoCl₂)*

To simulate hypoxic conditions, CoCl₂ (final concentration: 100 μ M) was added to the cells 3-4 hours post transfection.

2.3.8.2 *Treatment with 1,4-dithiothreitol (DTT) and tunicamycin*

To induce ER stress, cells were treated with DTT or tunicamycin to a final concentration of 1 mM or 10 μ M per well, respectively.

2.4 Protein methodology

2.4.1 Cell lysis assay

All steps were carried out on ice. The medium was removed from the wells, and cells were washed twice with 2 ml 1x PBS++; for cell lysis and analysis by non-reducing SDS-PAGE, 1.94 ml 1x PBS++ containing 60 μ l of 0.5 M NEM were used to wash the cells. For cell lysis and subsequent SDS-PAGE under reducing conditions, NEM was omitted. 200 μ l of the respective lysis buffer were then added per well for ~30 seconds. Thereafter, the cells were scraped off with a rubber cell scraper, transferred into an Eppendorf tube and centrifuged at 4°C for 5 min at 0.8 rcf. Supernatants were transferred into a new Eppendorf tubes and used for analysis by SDS-PAGE.

CHAPS buffer (prepared in dH₂O):

- 1% CHAPS
- 10 mM Tris/HCl pH 7.4
- 150 mM NaCl
- 1 mM EDTA

Lysis buffer for subsequent reducing SDS-PAGE:

- 1440 μ l CHAPS buffer
- 60 μ l 25x complete protease inhibitor

Lysis buffer for subsequent non-reducing SDS-PAGE:

- 1410 μ l CHAPS buffer
- 60 μ l 25x complete protease inhibitor
- 40 μ l 0.5 M NEM

2.4.2 EndoH digest

Reaction batch:

- 25 μ l cell lysate
- 1.2 μ l 25x protease inhibitor cocktail from Complete™ tablets (Roche)
- 3 μ l 50 mM sodium citrate buffer pH 5.5
- 0.8 μ l Endo Hf 10⁶ U/ml (#P0703L, New England Biolabs)
- 30 μ l total reaction volume

The reaction batch was incubated at 37°C overnight. 6 μ l of 6x sample buffer were added, the sample was boiled for 7 min at 100°C and analyzed by SDS-PAGE. As a control, undigested lysate was loaded.

2.4.3 Preparation of tissue lysates

Tissue samples from melanomas and breast were obtained frozen from Cross Cancer Institute, Edmonton, Alberta and subsequently stored at -86 °C.

All equipment was being cooled on dry ice for at least 30 min prior to starting work. Pieces of 50 to 150 mg of tissue were cut from the samples with a razor blade, placed in a mortar covered with aluminum foil and ground with a pestle until they had becoming a powder. This tissue powder was transferred into a 2 ml Eppendorf microcentrifuge tube, and 3 times the volume of the powder mRIPA-buffer containing protease inhibitors (Complete™ protease inhibitor cocktail tablets from Roche) was added. The samples were then placed on ice (4°C) for about 5 min so that the detergent in the buffer could take effect. With a T10 basic ULTRA-TURRAX® from IKA®, the samples were then homogenized 3 times for about 30 seconds each. If necessary, homogenization was extended until the homogenization was complete. The homogenates were centrifuged in a cooled centrifuge (4°C) at 16.1 rcf for 10 min. The supernatant was transferred to a fresh Eppendorf tube, and the protein concentration was determined with the Pierce bicinchoninic (BCA) acid assay. As control for the melanoma samples, commercial tissue lysate of normal human skin (Leinco Technologies, Prod. No.: H1427) was used.

<u>mRIPA buffer:</u>	1 mM EDTA (~pH 8)
50 mM Tris/HCl pH 7.5	1% Triton X 100
150 mM NaCl	0.1% SDS
1 mM EGTA (~pH 8)	0.1% NaDOX (sodium deoxycholate)

2.4.4 VEGF secretion assay

If cells were not transfected prior to a hypoxic experiment, 7×10^5 to 9×10^5 cells per well were seeded in 6-well cell culture plates, otherwise respective cell numbers after transfection were used. Plates were incubated for 24 to 72 h in a hypoxic chamber (Ruskin INVIVO2 200 with SI-002 Gas Mixer Q) at 0.1 or 1% O₂ (37°C, 5% CO₂). Control cells were grown in a regular incubator (37°C, 5% CO₂).

Precipitation of cell culture supernatants

Acetone precipitation

Supernatants were aliquoted into different Eppendorf tubes in portions of 300 µl, and 1.2 ml of 90% acetone/10% ddH₂O were added and mixed by shaking. Samples

were put in a -20°C freezer for at least 18 h. The resulting suspensions were centrifuged in a cooled centrifuge (4°C) for 10 min at 16.1 rcf. The obtained protein pellets were resuspended in 30 µl 2x sample buffer, thereby pooling the previously split supernatants. The samples were heated for 7 min at 100°C, and then analyzed by SDS-PAGE.

TCA precipitation

Equal volumes of 50% TCA (trichloroacetic acid) in dH₂O was added to the cell culture supernatants to a final concentration of TCA of 25%. The solution was mixed by flipping the Eppendorf tube, and put on ice (4°C) for 15 min. The samples were spun in a cooled centrifuge (4°C) for 15 min at 16.1 rcf, the supernatant was aspirated, and the protein pellets were washed with 300 µl ice-cold 90% acetone. The samples were centrifuged (4°C) again for 5 min at 16.1 rcf, the supernatant discarded, and the pellets were air-dried. The precipitates were resuspended in 30 µl of 2x sample buffer and boiled for 7 min at 100°C. If the remaining acetone rendered the sample acidic (indicated by bromophenol blue turning yellow), samples were neutralized with small amounts of 1 M Tris/HCl pH 8.8.

2.4.5 SDS Polyacrylamide Gel Electrophoresis (SDS-PAGE)

Protein samples (cell lysates, tissue lysates) were separated by sodium dodecylsulfate polyacrylamide gel electrophoreses (SDS-PAGE), followed by transferring of the separated proteins to a nitrocellulose membrane for immunodetection by Western blotting of proteins of interest.

(1) Reducing SDS-PAGE: 40 µl of 6x reducing sample buffer were added to the protein samples (200 µl). The samples were heated at 100°C for 10 min in a heating block, cooled on ice immediately and then loaded onto SDS-polyacrylamide gels.

(2) Non-reducing SDS-PAGE: 40 µl of 6x non-reducing sample buffer were added to 200 µl of the protein samples. The samples were heated at 100°C for 10 min in a heating block, cooled off on ice immediately and then loaded onto SDS-polyacrylamide gels.

Stacking gels had a concentration of 4% polyacrylamide, whereas separating gels of 8%, 10%, 12% or 15% were used.

Table 2.2. Gel recipes for SDS-PAGE. 30% acrylamide and bis-acrylamide solution from BioRad (CAT# 1610154); APS, ammonium persulfate; TEMED, N,N,N',N'-Tetramethylethylenediamine.

Final % of Acrylamide	3	8	10	12	15
30% Acrylamide/Bis	1	2.7	3.3	4	5
dH ₂ O	6.3	4.8	4.2	3.5	2.5
4x Stacking buffer	2.5	--	--	--	--
4x Separating buffer	--	2.5	2.5	2.5	2.5
10% APS	0.2	0.1	0.1	0.1	0.1
TEMED	0.01	0.005	0.005	0.005	0.005
Total	10.01	10.1	10.1	10.1	10.1

4x Stacking buffer: 1.5 M Tris/HCl pH 6.8

4x Separating buffer: 1.5 M Tris/HCl pH 8.8

The components of the separating gel were mixed and poured into the previously cleaned gel unit and topped with a small quantity of ddH₂O. The gel was allowed to polymerize for about 25 min. Then the components of the stacking gel were combined and poured onto the separating gel after complete removal of the ddH₂O. The combs were inserted and the stacking gel was allowed to polymerize for at least 15 min. The gel unit was placed into the electrophoresis apparatus (SE 250 or SE 260, Amersham Biosciences). The apparatus was filled with running buffer, and the combs were removed. The protein samples were mixed with sample buffer (reducing or non-reducing; as a reducing agent, β-mercaptoethanol was used).

From tissue lysates 50 µg (25 µl) of protein were loaded per slot. Equal volumes (25 µl) of cell lysates were loaded. Precipitated supernatants were resuspended in 30 µl 2x sample buffer (reducing) and loaded, whereas for confirmation and standardization of the VEGF signal, 30 to 60 ng of recombinant VEGF were loaded (VEGF165HumaXpress Cat #: HZ-1013, Humanzyme).

The gels were run at 80-100 V.

1.5 µl Fermentas PageRuler® Plus Prestained Protein Ladder #1811 and 1.5 µl Santa Cruz Biotechnology Broad Range Marker sc-2361 were loaded as markers.

6x sample buffer (reducing):

9% SDS
375 mM Tris/HCl pH 6.8
50% glycerol
9% β -mercaptoethanol
0.03% bromophenol blue

6x sample buffer (non-reducing):

same composition as reducing sample buffer, except w/o β -mercaptoethanol

SDS-PAGE running buffer:

25 mM Tris
250 mM Glycine
0.1% SDS

2.4.6 Western blotting

Subsequent to SDS-PAGE, the proteins were transferred to a nitrocellulose membrane (0.45 μ m, Bio-Rad, Cat.No.: 162-0115) The blotting was performed in a liquid blotting apparatus from APELEX® (mini Gel Trans Blotter, # 430000).

The blot was prepared as follows:

In a blotting cassette, submerged in 1x transfer buffer, the gel and the membrane were sandwiched between one sheet of Whatman paper and two sponges on either side. The cassettes were placed in the blotting apparatus. Blotting was performed at 60V for 180 min or at 15V overnight at 4°C.

Transfer Buffer:

For 1 litre:
0.75 l of dH₂O
200 ml of Methanol
50 ml of 20x "Carbonate Transfer"

"20x Carbonate Transfer Buffer":

For 1 litre:
16.8 g NaHCO₃
6.4 g Na₂CO₃
Add dH₂O to 1 litre

Excess parts of the membrane were cut off, and then it was stained with Ponceau S (Sigma) to check for transfer efficiency and equal loading. For visualization of the proteins, the membrane was destained with ddH₂O.

Ponceau S dye:

5% acetic acid
0.1% Ponceau S
in dH₂O

2.4.7 Detection

The membrane was blocked with Odyssey® blocking buffer from LI-COR® for at least 45 min on a shaker at room temperature. After removal of the blocking buffer,

the membrane was incubated with primary antibody (diluted in 10% skim dry milk in dH₂O) for at least 1 hr at room temperature, or over night at 4°C on a shaker. The membrane was washed twice with 1x TBS-T for 5 min at room temperature on a shaker, and then incubated with IRDye secondary antibody from Invitrogen, diluted 1:5000 in 10% skim dry milk, for 30 to 40 min at room temperature on a shaker. The secondary antibody solution was discarded and the membrane was washed 3x 5 min with 1x TBS-T (RT, shaker) and finally covered with dH₂O. Visualization was performed with the Odyssey® Infrared Imaging System.

TBS-T:

150 mM NaCl

25 mM Tris

3 mM KCl

0.05% Tween-20

in dH₂O, pH adjusted to 7.4

2.5 Immunofluorescence

The day before an immunofluorescence staining was performed, cells were seeded on coverslips previously rinsed with ethanol in 6-well cell culture plates to a final cell count of 5×10^5 to 6×10^5 cells per well.

For visualization of mitochondria, 0.2 µl of Mitotracker® Red CMXRos (Molecular Probes, Invitrogen) in 100 µl OptiMEM® were added to the corresponding wells. The cell culture plate was covered with aluminum foil (to prevent toxic damage of the mitochondria due to the absorption of light) and put in the incubator (37°C, 5% CO₂) for 30 to 45 min. A humid chamber consisting of a 10 by 15 cm plastic blot box lined with Whatman paper soaked in ddH₂O and parafilm on top of it was prepared and placed on ice (4°C).

The 6-well plates were placed on ice as well, the cell culture medium was aspirated, and the coverslips were washed 3 times for 5 min with ice-cold 1x PBS++. After the third washing step, PBS was aspirated and coverslips were covered with a previously prepared solution of 4% PFA in 1x PBS for 20 min. Coverslips were then washed again 3 times for 5 min with ice-cold 1x PBS++. 30 µl of primary antibody dilutions (in PBS++ containing 2% BSA and 0.5% Saponin, or 0.2% Triton X-100, respectively) per coverslip were applied to the parafilm sheet in the humid chamber. The coverslips were transferred from the cell culture plates to the humid chamber and placed face down onto the drops of the primary antibody dilutions. After incubation

for 1 to 3 h at room temperature, coverslips were transferred back into the cell culture plates facing right-side-up and washed twice with ice-cold 1x PBS++. The parafilm sheets in the humid chamber were exchanged for new ones, and 30 μ l drops of secondary antibody dilutions (1:2000 in PBS++ containing 2% BSA and 0.5% Saponin, or 0.2% Triton X-100, respectively) were applied to the parafilm sheets. Coverslips were put face down onto the drops, the humid chamber was covered with aluminum foil to protect the samples from light, and set aside to let incubate for 30 min at room temperature.

Microscope slides with 10 μ l drops of PLAF (Prolong Antifade from Molecular Probes, Invitrogen) were prepared and after dabbing off excess liquid, coverslips were placed face down onto the resin avoiding air bubbles between the coverslip and the microscope slide. The microscope slides were stored at 4°C in the dark.

Microscope setup:

Microscope: Zeiss Observer.Z1 SN: 3834000197

Hg-lamp: X-cite Series 120 by EXFO

Software: Zeiss Axiovision 4.6

2.6 Primary antibodies/antisera

Polyclonal rabbit α -VEGF (Santa Cruz Biotechnology, sc-507)

(Raised against amino acids 1-147 of huVEGF)

Polyclonal rb- α -GAPDH (abcam®, ab37168)

Monoclonal mouse α - β COP (GeneTex, GTX26323)

Ero1 α : ms- α -Ero1 2G4 non-commercial antiserum (Kind gift from Cabibbo, A.)

ERp44: rb- α -TXNDC4 (Sigma-Aldrich®, HPA001318)

TMX4: • rb- α -TMX4 E4504 d72 non-commercial antiserum

• monoclonal ms- α -TMX4 Clone2, non-commercial

Mouse α -Myc Tag clone 4A6 (Upstate, Cat.No.: 05-724, Lot#: JBC1390570)

TMX1: • rb- α -TMX1 R45 non-commercial antiserum 1:1000

• rb- α -TXNDC1 (Sigma-Aldrich®, HPA003085 Batch: R00337)

PACS-2: rb- α -PACS-2 non-commercial antiserum

Polyclonal rb- α -Derlin-1 (MBL MBL Japan, PM018)

Monoclonal ms- α -PDI (Affinity BioReagents®, MA3-019)

Monoclonal ms- α -CNX (BD Biosciences, Cat.No.: 610523)

Monoclonal ms- α -ERGIC-53 (Alexis Biochemicals, ALX-804-602)

2.7 Secondary antibodies

Western blot:

IRDye 680 Goat Anti-Mouse IgG (H + L); Invitrogen (A21057)

IRDye 800CW Goat Anti-Rabbit IgG (H + L); Invitrogen (A21039)

Immunofluorescence: (Molecular Probes®, Invitrogen)

Alexa Fluor 350 donkey anti-mouse IgG (A10035)

Alexa Fluor 488 goat anti-mouse IgG (H+L) (A-11001)

Alexa Fluor 488 chicken anti-mouse IgG (H+L) (A-21200)

Alexa Fluor 488 chicken anti-goat IgG (H+L) (A-21467)

Alexa Fluor 488 goat anti-rabbit IgG (H+L) (A-11008)

Alexa Fluor 594 chicken anti-rabbit IgG (H+L) (A-21442)

Alexa Fluor 594 goat anti-rabbit IgG (H+L) (A-11012)

2.8 Equipment

Hypoxic chamber: Ruskinn INVIVO2 200 and SI-002 Gas Mixer Q

Centrifuge (cooled): eppendorf centrifuge 5415R

VWR digital heatblock

VWR heatplate/stirrer

Shakers: Heidolph DUOMAX 1030

Heidolph POLYMAX 2040

FINEPCR compactROCKER CR 300

Western Blot: MAJOR SCIENCE MP-250N; apparati: APELEX 014977, 010463

Scales: METTLER TOLEDO AB104-S (max 110g min 10mg e 1mg d 0.1mg)

METTLER TOLEDO PB1501-S (max 1510g min 5g e 0.1g d 0.1g)

pH-Meter: METTLER TOLEDO Seven Easy

Microscope: ZEISS Observer.Z1 SN: 3834000197

Hg-lamp: X-cite Series 120 by EXFO

Software: Zeiss Axiovision 4.6

Detection and evaluation of Western blots: Odyssey® Infrared Imaging System

3 RESULTS

3.1 Expression levels of TMX, TMX4, and PACS-2 in melanoma tissue

It was previously published that TMX4 was being overexpressed on average about 10fold at the mRNA level in different melanoma cell lines as compared to normal melanocytes (Hoek et al., 2004; supplementary data, mentioned as the hypothetical protein DJ971N18.2). Hence, it was an aim of this thesis to examine whether the overexpression of TMX4 mentioned in the publication by Hoek et al. (2004) could also be observed at the protein level. To this end we compared melanoma tissue samples with tissue lysates from normal human skin. The melanoma samples were obtained from the Cross Cancer Institute (Edmonton, Alberta, Canada), and the lysates of normal human skin were purchased from Leinco Technologies (St. Louis, Missouri, USA). As Figure 3.1 shows, TMX4 was found to be upregulated in roughly half the randomly chosen melanoma samples (lanes 4-7, 10, 11); however, TMX1 is downregulated in most of the tumor samples (Figure 3.1, bottom panel). PACS-2 was found to be upregulated in most of the samples. Additionally, it could be shown that Ero1 α is upregulated in all melanoma samples.

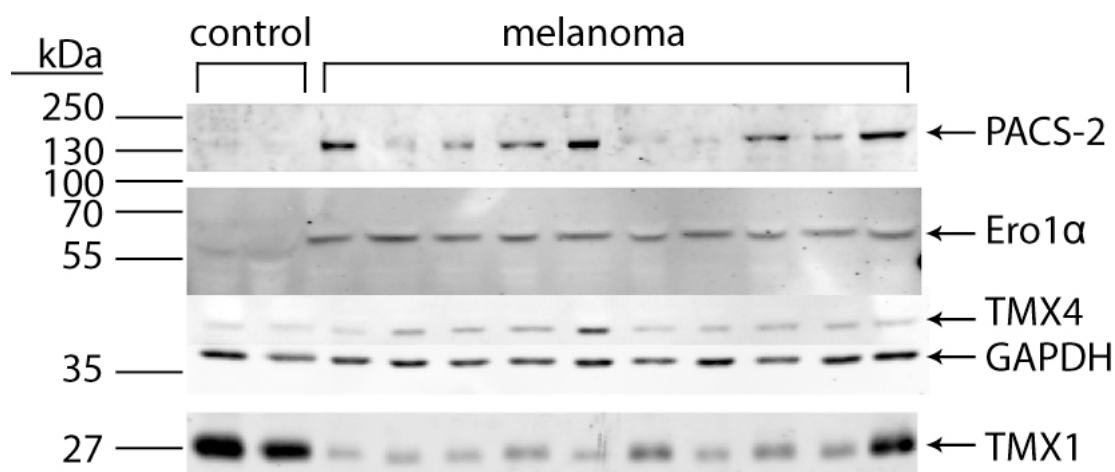


Figure 3.1. Western blot of human skin tissue lysates. As a control, 50 μ g of two commercial normal human skin lysates were loaded in lanes 1 and 2. In the remaining lanes 50 μ g of lysates prepared from different melanoma tissue samples were loaded. The samples were subjected to SDS-PAGE on a 10% gel. Primary antibodies used: rb- α -PACS-2 non-commercial antiserum (1:1250), ms- α -Ero1 α 2G4 non-commercial antiserum (1:2000), rb- α -TMX4 E4504 d72 non-commercial antiserum (1:2000), rb- α -GAPDH from abcam $\text{\textcircled{R}}$ (1:2000), rb- α -TMX1 R45 non-commercial antiserum (1:1000). For detection of proteins of similar size the Western blot was stripped with Western Re-Probe from GBiosciences and then re-probed with another antibody/antiserum.

To determine the possibility that TMX4 was also upregulated in other cancerous tissues, we analyzed samples of breast tumors and normal breast tissue (obtained from the Cross Cancer Institute, as well) for possible differential expression levels. The results are shown in Figure 3.2. In contrary to the melanoma tissue, TMX4 was found to be downregulated in the breast cancer samples compared to the expression levels in normal breast, whereas TMX1 was upregulated in 2 out of 4 breast tumors (lanes 4 and 6). The expression of PACS-2 was increased in 3 out of 4 samples (lanes 3, 4 and 6), of which two also showed less downregulation of TMX4 (lanes 4 and 6). Interestingly, Ero1 α levels seem to be more or less unaffected.

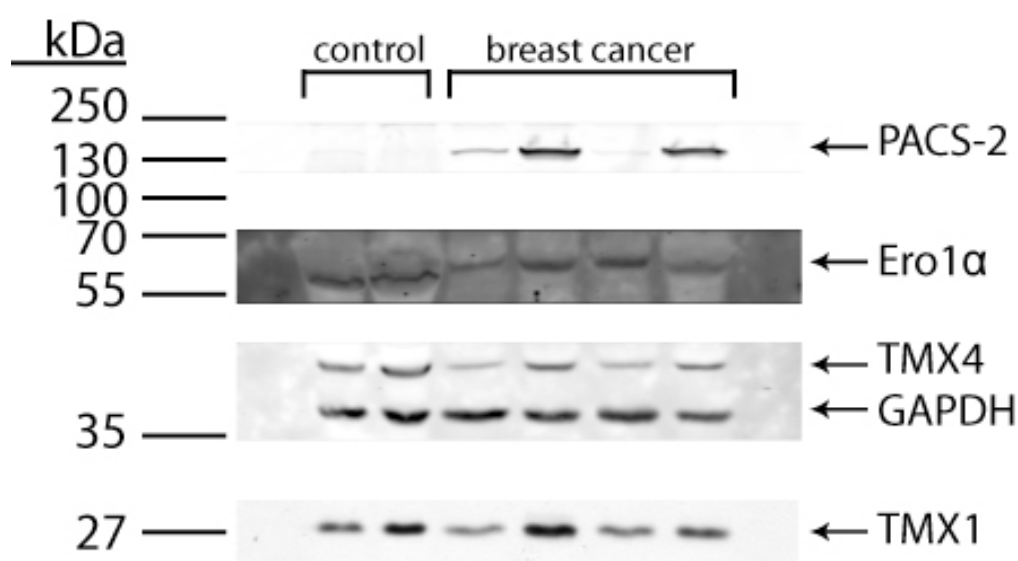


Figure 3.2. Western blot of human breast tissue lysates. As a control, 50 μ g of two human breast tissue lysates diagnosed as normal were loaded in lanes 1 and 2. In the remaining lanes 50 μ g of lysates prepared from different breast cancer tissue samples were loaded. The samples were subjected to SDS-PAGE on a 10% gel. Primary antibodies/antisera used: rb- α -PACS-2 non-commercial antiserum (1:1250), ms- α -Ero1 α 2G4 non-commercial antiserum (1:2000), rb- α -TMX4 E4504 d72 non-commercial antiserum (1:2000), rb- α -GAPDH from abcam® (1:2000), rb- α -TMX1 R45 non-commercial (1:1000). For detection of proteins of similar size the Western blot was stripped with Western Re-Probe from GBiosciences and then reprobated with another antibody.

3.2 Subcellular localization of TMX and TMX4 in A375P cells

For the assessment of the subcellular localization of TMX and TMX4 and their localization within the ER, a series of co-localization experiments using immunofluorescence techniques was performed. The resulting information of possible co-localization with well-studied proteins in the ER was intended to elucidate possible biological roles of TMX and TMX4.

Co-staining of TMX, TMX4, and Ero1 α with mitochondria (Figure 3.3, kindly provided by T. Simmen) show the expected overlap of Ero1 α with mitochondria, corroborating the findings of Simmen et al. (unpublished) that the ER-resident oxidoreductase Ero1 α is localized at the MAM, in close vicinity to mitochondria (Figure 3.3, panel C). However, TMX and TMX4, ER-resident proteins showing distinct reticular staining pattern and co-localization with PDI (Figure 3.6, panel C and F), appear to be localized in different sub-domains of the ER. Whereas TMX, like Ero1 α , is at least partially found in close proximity to mitochondria, TMX4 signals do not overlap with mitochondria (Figure 3.3, panels A and B). Thus, these findings confirm the differential sub-organellar distribution of TMX and TMX4 as assessed by cell lysate fractionation using density gradient centrifugation (Simmen et al., unpublished results).

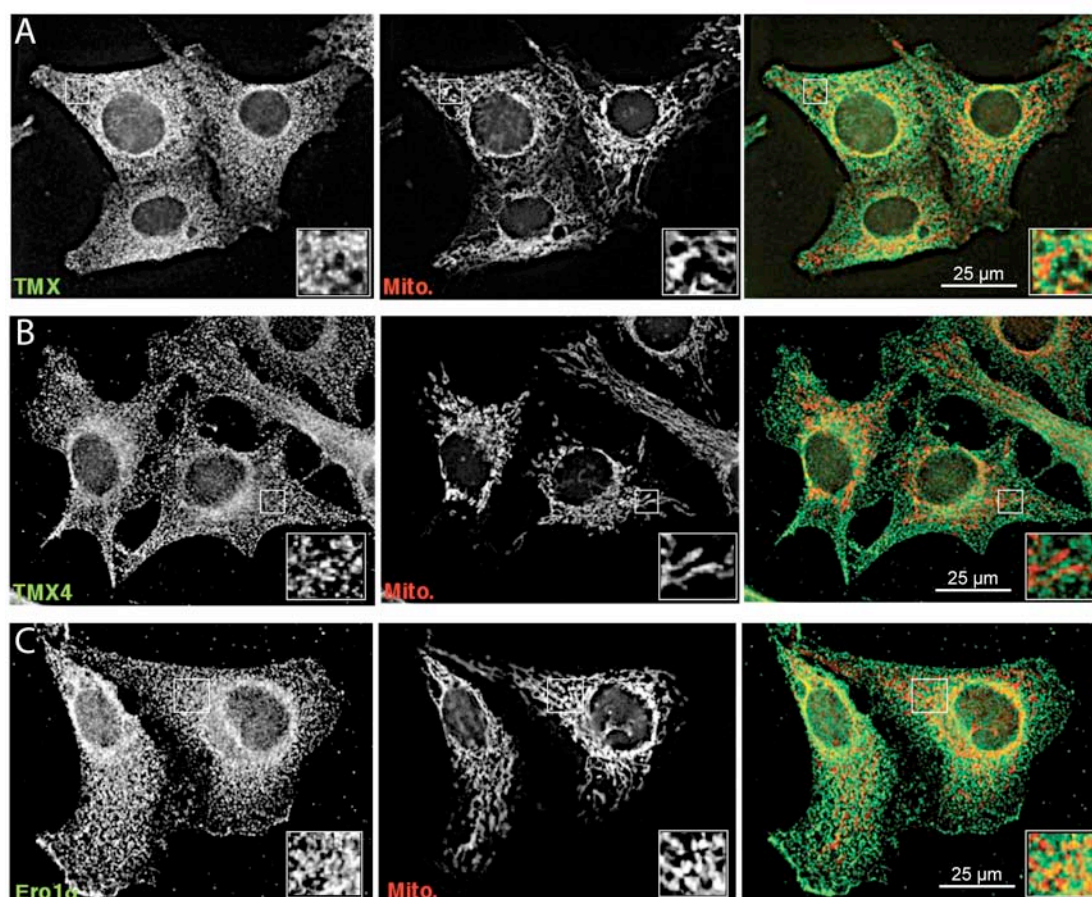


Figure 3.3. Immunofluorescence co-staining of TMX1, TMX4, and Ero1 α with mitochondria. A375P cells were fixed, permeabilized and subsequently stained for the proteins of interest as described in section 2.5. Mitotracker was used to stain mitochondria. rb- α -TMX1 (Atlas) antibody was diluted 1:100, ms- α -TMX4 antibody ~1:67, and ms- α -Ero1 α antiserum 1:100. Corresponding secondary antibodies were diluted 1:5000. (Figure kindly provided by T. Simmen)

To further confirm the different localization patterns of TMX and TMX4, A375P cells were co-stained for the two PDI-family members (Figure 3.4, panel A). As expected TMX and TMX4 signals exhibit only minimal overlap.

To narrow down the localization of TMX4 within the ER, co-staining of TMX4 with several well-studied proteins in the ER and the ER-Golgi intermediate compartment, such as ERp44, CNX, Derlin-1, ERGIC-53, and PACS-2, were performed (Figure 3.4, panel B, and Figure 3.6, panels A, B and D-F). The corresponding staining patterns of these proteins are summarized in Figure 3.5.

The TMX4 signal did not overlap with CNX, or PACS-2; however, it could be observed that TMX4 is, at least partially, co-localized with ERp44, ERGIC-53, and Derlin-1, hence providing information about a possible role of TMX4 within the ER (see Discussion, section 4).

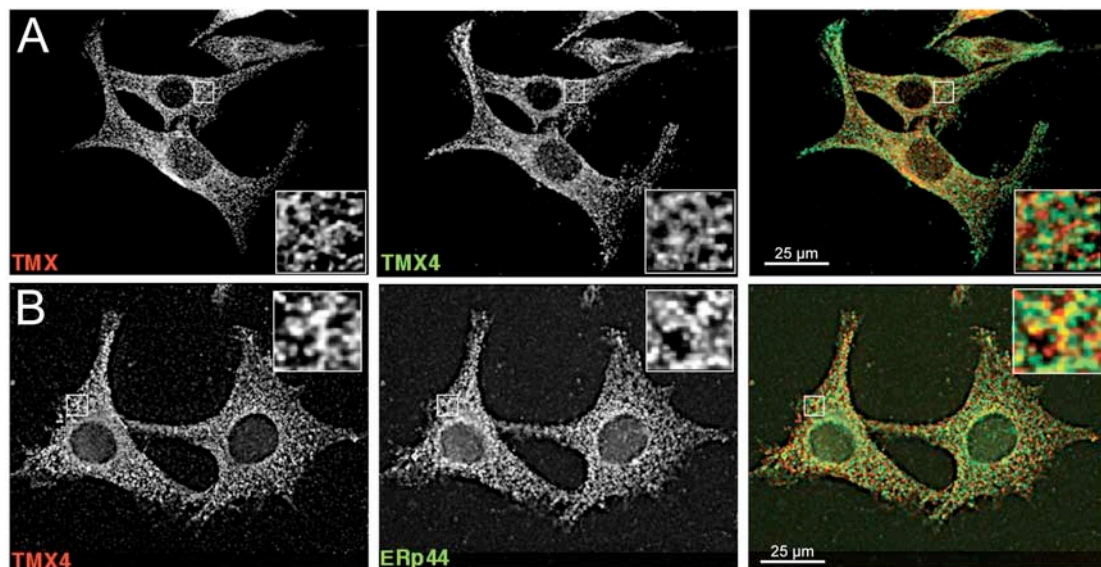


Figure 3.4. Immunofluorescence co-staining of TMX1 with TMX4, and TMX4 ERp44. A375P cells were fixed, permeabilized and subsequently stained for the proteins of interest as described in section 2.5. Rb- α -TMX1 (Atlas) antibody was diluted 1:100, ms- α -TMX4 antibody ~1:67, and rb- α -TXNDC4 (ERp44) antibody from Sigma-Aldrich® 1:100. Corresponding secondary antibodies were diluted 1:5000. (Figure kindly provided by T. Simmen)

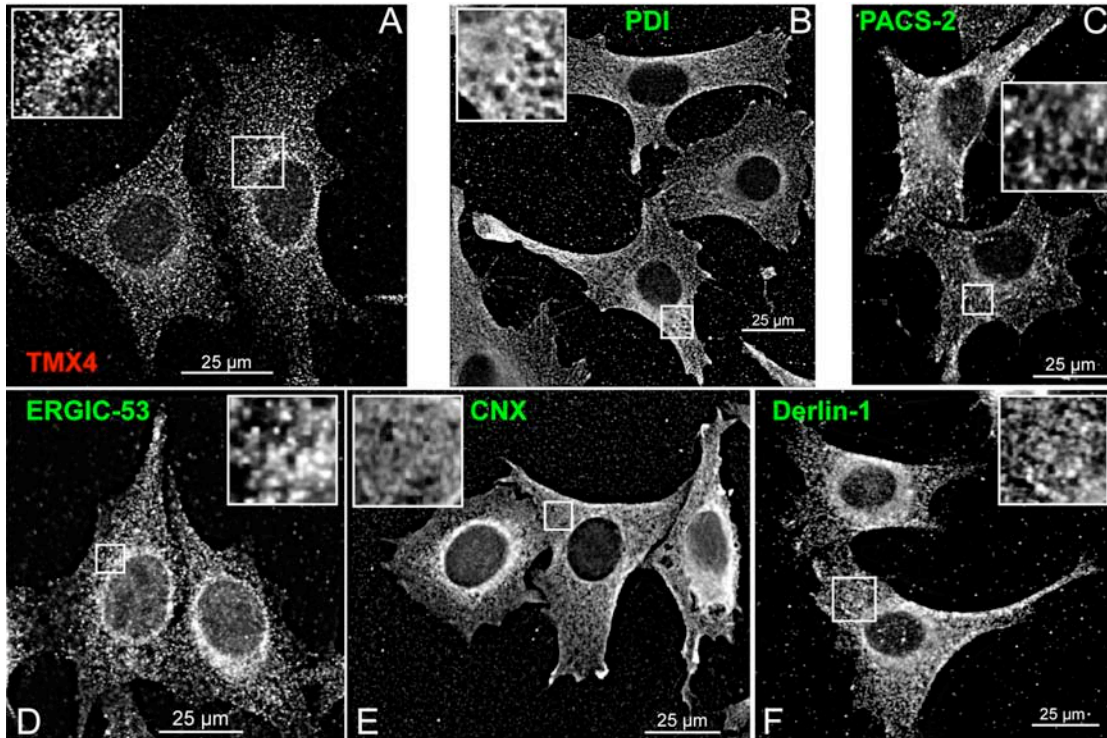


Figure 3.5. Immunofluorescence staining of TMX4 and various marker proteins. A375P cells were fixed, permeabilized and subsequently stained for the proteins of interest as described in section 2.5. Ms- α -TMX4 antibody was diluted \sim 1:67, the other antibodies/antisera, including ms- α -PDI, rb- α -PACS-2, ms- α -ERGIC-53, ms- α -CNX, and ms- α -Derlin-1 were used in a dilution of 1:100. Corresponding secondary antibodies were diluted 1:5000.

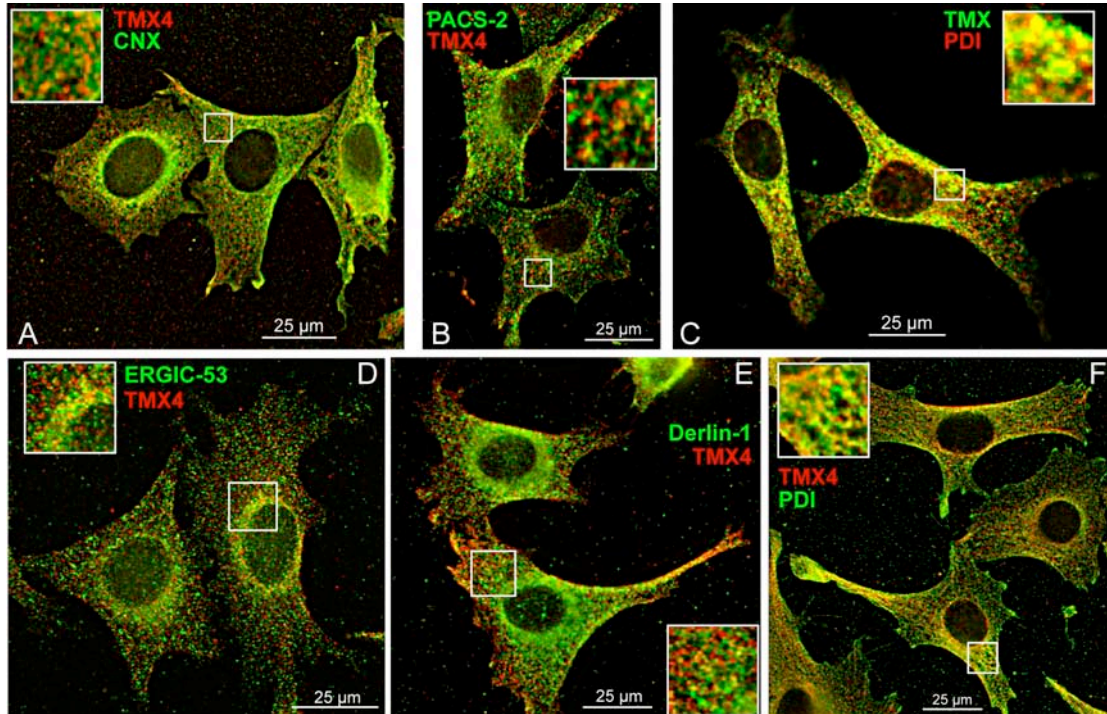


Figure 3.6. Immunofluorescence co-staining of TMX1/TMX4 with various marker proteins. A375P cells were fixed, permeabilized and subsequently stained for the proteins of interest as described in section 2.5. Ms- α -TMX4 antibody was diluted \sim 1:67, the other antibodies/antisera, including rb- α -TMX1, rb- α -TMX4, ms- α -PDI, rb- α -PACS-2, ms- α -ERGIC-53, ms- α -CNX, and ms- α -Derlin-1 were used in a dilution of 1:100. Corresponding secondary antibodies were diluted 1:5000.

3.3 Effects of overexpression of TMX and TMX4 on the oxidation state of Ero1 α in HEK293 cells

HEK293 cells were chosen because of their relatively high expression level of Ero1 α . Ero1 α (also known as Ero1-L α) exists in different oxidation states in the ER. A reduced form and two partially oxidized forms, namely Ox1 and Ox2, have been reported so far. Ox2 is the predominant form and therefore thought of as the active form, and the most stable state of Ero1 α (Benham et al., 2000). To a certain degree, the oxidation state is dependent on the interaction with oxidoreductases like PDI. Most recent findings suggest an intramolecular switch mechanism in the Ox2 form dependent on the availability of reduced PDI (Appenzeller-Herzog et al., 2008). It has also been shown that the oxidation state of Ero1 α can be influenced by reducing agents such as DTT (1,4-diothiothreitol) resulting in a shift to a less oxidized form. Moreover, treatment of cells with oxidizing agents such as diamide has been shown to restore compromised function of Ero1 mutants (Fränd & Kaiser, 1998). As members of the PDI-family, TMX and TMX4 contain single trx-like domains with potential active sites of the sequence CPAC and CPSC, respectively. Thus, overexpression of TMX1 or TMX4 is likely to change the redox environment of the ER.

With this in mind, the first experiment was intended to shed light on the possibility that an overexpression of family members of the thioredoxin-related transmembrane proteins, such as TMX1 and TMX4, could cause a shift in the oxidation state of Ero1 α , a major player in the system of oxidative protein folding. In order to test the rb- α -TMX4 E4504 d72 antiserum, an EndoH digest of A375P (cells expressing TMX4 at high levels) cell lysate was performed. Figure 3.7 shows different migration behaviors of TMX4 with N-glycosylation (46 kDa, as expected) and after removal of the glycan from Asn46 by EndoH, thereby confirming that the antiserum indeed detects TMX4.

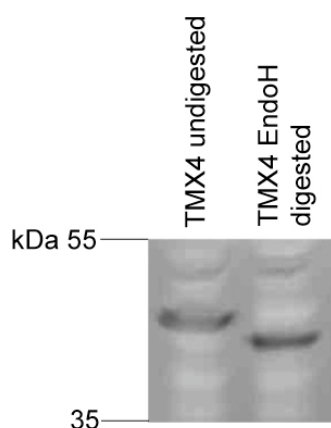


Figure 3.7. Western blot of EndoH digest of TMX4. 7×10^5 cells were cultured in RPMI 1640 supplemented with 10% FBS for 48h (incubator, 37°C, 5% CO₂). 25 μ l of A375P cell lysate were digested with Endo Hf (New England Biolabs), subjected to SDS-PAGE on an 8% gel, and TMX4 was detected with rb- α -TMX4 E4504 d72 non-commercial antiserum (1:2000).

Indeed, upon overexpression of the myc-TMX4 construct, an additional protein band (Ox3) was detectable on non-reducing SDS-PAGE, indicating a possible direct or indirect interaction between TMX4 and Ero1 α . Ox3, a hyperoxidized form of Ero1 α , could reflect oxidation of the regulatory disulfides and the resulting inactivation of Ero1 α (Sevier & Kaiser, 2008; Nardai et al., 2005). No such effect was observed for TMX overexpression (TMX expression not shown).

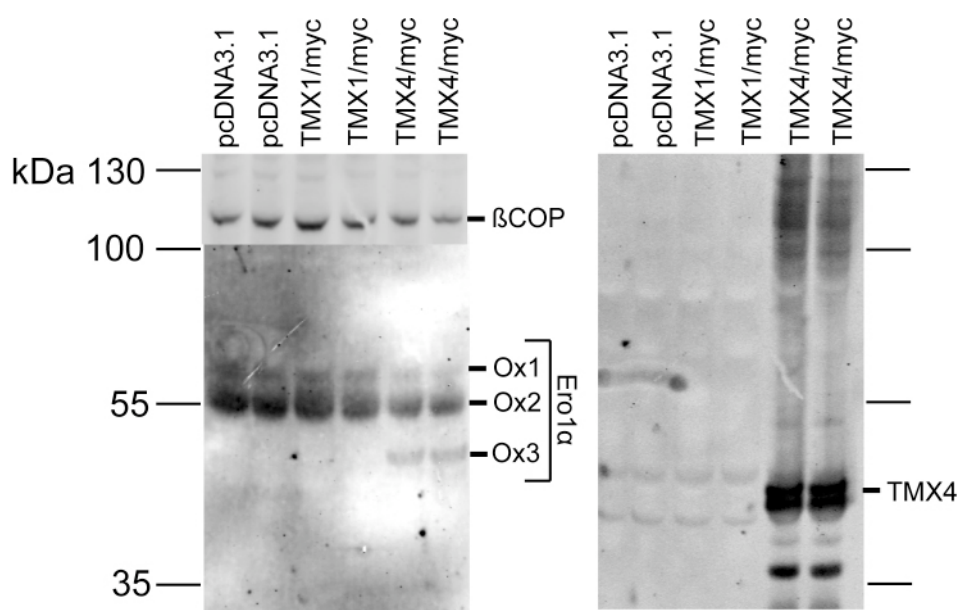


Figure 3.8. Western blot analysis of HEK293 lysates under non-reducing conditions. 8×10^5 cells were cultured in DMEM supplemented with 10% FBS for 48h (incubator, 37°C, 5% CO₂). Twenty-five μ l of lysate from HEK293 cells, transfected as indicated, were subjected to non-reducing SDS-PAGE on an 8% gel and blotted to a nitrocellulose membrane. Ero1 α was detected using the ms- α -Ero1 2G4 non-commercial antiserum (1:2000). For a loading control, β COP was detected with ms- α - β COP from GeneTex (1:1000), and TMX4 was detected with rb- α -TMX4 E4504 d72 non-commercial antiserum (1:4000).

The next experiment was aimed to elucidate the effect of mutations in the acidic clusters in the C-terminal domain of TMX4, which are potential interaction sites with PACS-2. Therefore, HEK293 cells were transfected with empty vector and the myc-wtTMX1 construct as negative controls, the myc-wtTMX4 construct as a positive control, and also with the three myc-TMX4 mutants described in section 2.3.6. The result is shown in Figure 3.9. The observed effect on Ero1 α (see Figure 3.8, and adjoining text) could not be reproduced, however. A hyperoxidized form of Ero1 α (Ox3) could not be detected in any of the transfected cells.

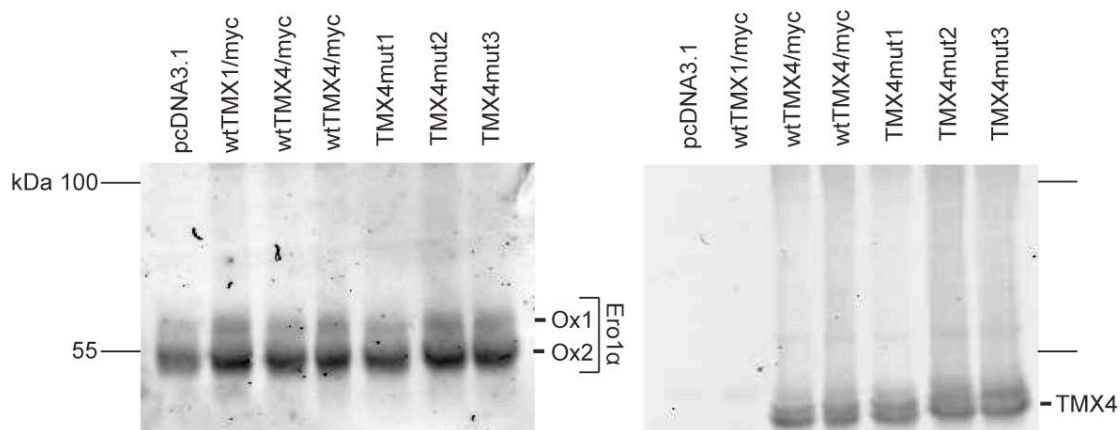


Figure 3.9. Western blot analysis of HEK293 lysates under non-reducing conditions. 8×10^5 cells were cultured in DMEM supplemented with 10% FBS for 48h (incubator, 37°C, 5% CO₂). Twenty-five μ l of lysate from HEK293 cells, transfected as indicated, were subjected to non-reducing SDS-PAGE on an 8% gel and blotted to a nitrocellulose membrane. Ero1 α was detected using the ms- α -Ero1 2G4 non-commercial antiserum (1:2000). TMX4 was detected with rb- α -TMX4 E4504 d72 non-commercial antiserum (1:4000).

3.4 Effects on TMX4 expression in A375P cells

For the investigation of TMX4 expression levels, A375P cells were chosen because of their high expression of TMX4.

Since it could be confirmed that TMX4 is upregulated in skin cancer tissue, and it is, in general, a hallmark of tumors to be undersupplied with oxygen (Semenza, 2009), the next experiment was aimed to investigate if there were any changes in the expression of TMX4 under hypoxic conditions. Interestingly, it was found that cultivation of A375P cells under 1% O₂ led to a significant decrease of TMX4 after 24h and 48h, as compared to A375P cells cultivated in a normal incubator (Figure 3.10).

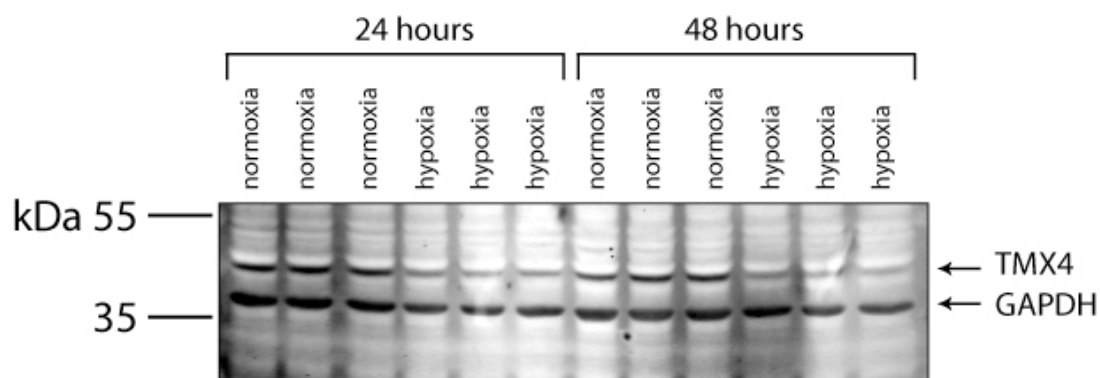


Figure 3.10. Western blot of cell lysates prepared from the melanoma cell line A375P under normoxic and hypoxic conditions. 7×10^5 cells were cultured in RPMI 1640 for 24h and 48h under normoxic (incubator, 37°C, 5% CO₂) and hypoxic (hypoxic chamber, 37°C, 5% CO₂ and 1% O₂) conditions as indicated. Cells were lysed in 200 μ l lysis buffer containing CHAPS, sample buffer was added, samples were heated, and 25 μ l of sample each were loaded and subjected to reducing SDS-PAGE on a 10% gel. TMX4 was detected with rb- α -

TMX4 E4504 d72 non-commercial antiserum (1:2000). GAPDH was used as a loading control and detected with rb- α -GAPDH from abcam® (1:2000).

It can be found in the literature that the effect of hypoxic conditions depends to a certain extent on the particular oxygen tension in the tissue (Koumenis et al., 2006). While 1% O₂ is being considered moderate hypoxia, 0.1% O₂ is in the range referred to as acute hypoxia. It has been shown (Koumenis et al., 2006) that the effects of acute and moderate hypoxia differ. Because of that, also the expression levels of TMX4 under severe hypoxia (0.1% O₂) were investigated. As Figure 3.11 demonstrates the same decrease as with 1% O₂ is observed, starting after 24h and even declining at the 48h timepoint.

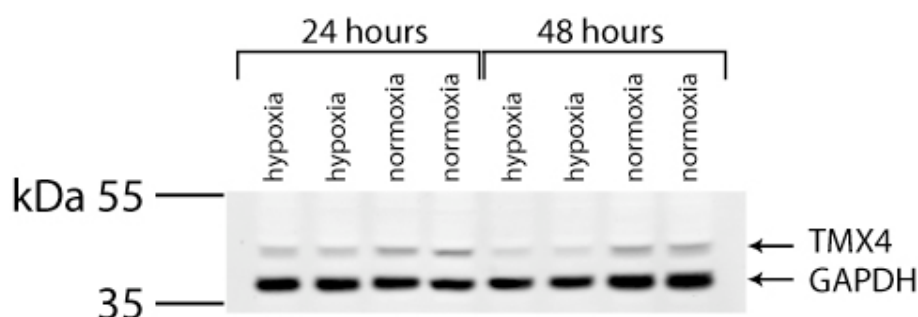


Figure 3.11. Western blot of cell lysates prepared from the melanoma cell line A375P under normoxic and hypoxic conditions. 7 x 10⁵ cells were cultured in RPMI 1640 for 24h and 48h under normoxic (incubator, 37°C, 5% CO₂) and hypoxic (hypoxic chamber, 37°C, 5% CO₂ and 0.1% O₂) conditions as indicated. Cells were lysed in 200 μ l lysis buffer containing CHAPS, sample buffer was added, samples were heated, and 25 μ l of sample each were loaded and subjected to reducing SDS-PAGE on a 10% gel. TMX4 was detected with rb- α -TMX4 E4504 d72 non-commercial antiserum (1:2000). GAPDH was used as a loading control and detected with rb- α -GAPDH from abcam® (1:2000).

ER stress can cause upregulation of ER chaperones and/or ER-resident oxidoreductases (Lee et al., 2003; Harding et al., 2000). Therefore, we used DTT (1,4-dithiothreitol) and tunicamycin, two well-known inducers of ER stress, to assess if treatment leads to any subsequent changes in the expression levels of TMX4 (Arrington et al., 2008 [tunicamycin]; Frand & Kaiser, 1998 [DTT]). DTT generally renders the cellular environment more reducing, thereby decreasing the folding capacity, which the cell tries to compensate through various ER stress pathways (as described in section 1.7). Tunicamycin, a nucleoside antibiotic produced by the bacterium *Streptomyces lysosuperficus*, is a potent inhibitor of N-glycosylation, leading to the accumulation of misfolded proteins.

Figure 3.12 depicts a Western blot with the results of the ER stress experiment. Whereas treatment with DTT did not result in a noticeable alteration in TMX4 expression levels, a decrease in TMX4 protein could be observed upon treatment with tunicamycin. This effect could either arise from global translation attenuation (see UPR, section 1.7), or be caused by increased degradation of TMX4 due to its

inability to fold correctly; however, it has been reported that pretreatment of melanoma cells with tunicamycin results in apoptosis-resistance when treated with microtubule-targeting drugs (Jiang et al., 2009).

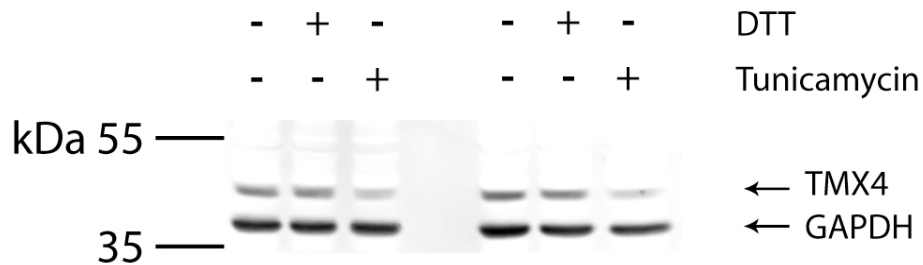


Figure 3.12. Western blot of cell lysates prepared from the melanoma cell line A375P upon ER stress. 7×10^5 cells were cultured in RPMI 1640 until reattachment was confirmed under the microscope. To induce ER stress, cells were treated with final concentrations in the wells of 1 mM DTT or 10 μ M tunicamycin over night. As a control untreated cells were used. Cells were lysed in 200 μ l of lysis buffer containing CHAPS, sample buffer was added, samples were heated, and 25 μ l of sample each were loaded and subjected to reducing SDS-PAGE on a 10% gel. TMX4 was detected with rb- α -TMX4 E4504 d72 non-commercial antiserum (1:2000). GAPDH was used as a loading control and detected with rb- α -GAPDH from abcam® (1:2000).

To examine whether TMX4, lacking its N-glycosylation at Asn46, was degraded by the 26S proteasome, cells treated with tunicamycin were also treated with MG-132, a known proteasome inhibitor. Additionally, since a decrease in TMX4 levels was observed under hypoxic conditions, A375P cells cultivated under hypoxic conditions (1% O₂) were co-treated with MG-132 as well. These experiments were intended to elucidate whether TMX4 levels could be recovered upon inhibition of the 26S proteasome. By comparison of the TMX4 to GAPDH ratio, it was observed that MG-132 might alleviate the decrease in TMX4 levels upon tunicamycin treatment, but not the decrease of TMX4 under hypoxic conditions (Figures 3.13 and 3.14). This indicates that in tunicamycin-treated and hypoxic A375P cells, different mechanisms are involved resulting in declining TMX4 expression levels.

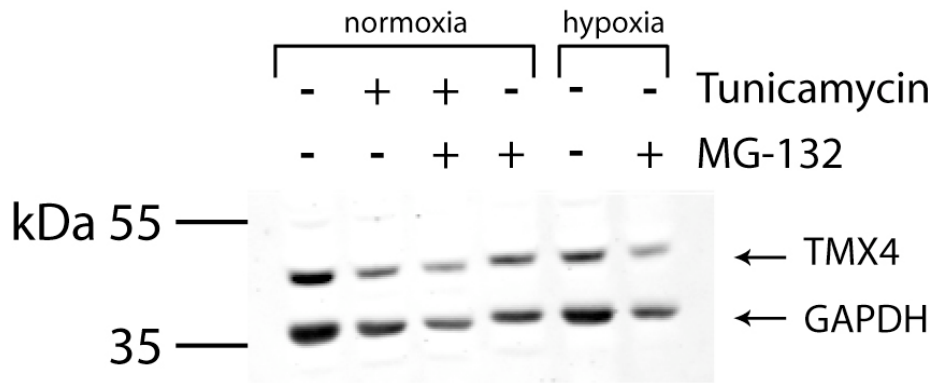


Figure 3.13. Western blot of cell lysates prepared from the melanoma cell line A375P upon ER stress and inhibition of the 26S proteasome with MG-132. 7×10^5 cells were cultured in RPMI 1640 until reattachment was confirmed under the microscope. To induce ER stress, cells were treated with final concentrations in the wells of 10 μ M tunicamycin and/or 20 μ M MG-132 for 18h under normoxic (incubator, 37°C, 5% CO₂) and hypoxic (hypoxic chamber, 37°C, 5% CO₂ and 0.1% O₂) conditions as indicated. As a control untreated cells were used. Cells were lysed in 200 μ l of lysis buffer containing CHAPS, sample buffer was added, samples were heated, and 25 μ l of sample each were loaded and subjected to reducing SDS-PAGE on a 10% gel. TMX4 was detected with rb- α -TMX4 E4504 d72 non-commercial antiserum (1:2000). GAPDH was used as a loading control and detected with rb- α -GAPDH from abcam® (1:2000).

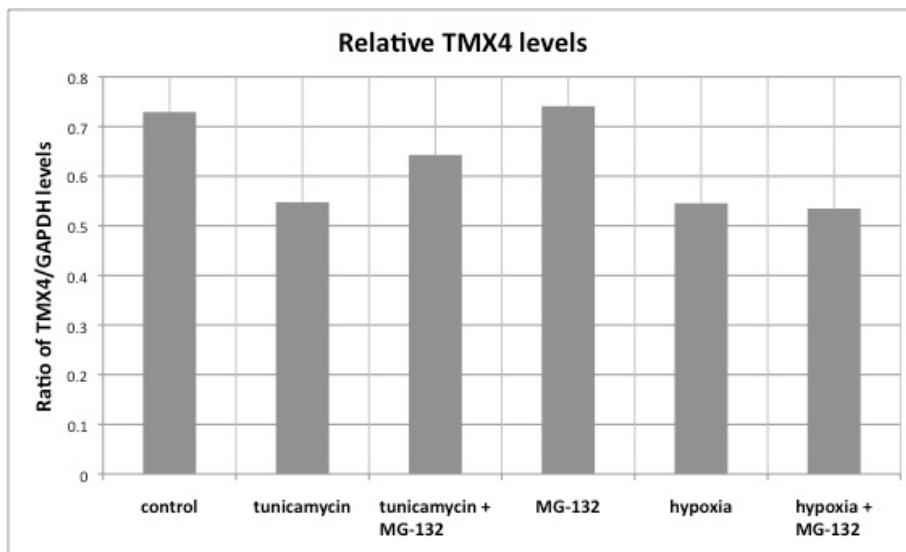


Figure 3.14. Assessment of TMX4 levels relative to GAPDH levels upon ER stress and inhibition of the 26S proteasome with MG-132. Intensities of the signals on the Western blot shown in Figure 3.13 were measured with Odyssey® software from LI-COR® Biosciences and evaluated with Microsoft® Excel 2008.

3.5 Secretion of VEGF by transfected HeLa cells

As described in the Introduction (section 1.13), the undersupply of tissue with oxygen promotes the induction of angiogenic signaling pathways, and amongst those, the secretion of vascular endothelial growth factor (VEGF) (Xie et al., 2004). This and the fact that TMX4 likely is upregulated in skin cancer cell lines, and melanomas themselves, rendered it interesting to look at the secretion of VEGF when TMX4 was being overexpressed. For this purpose HeLa cells, which normally express TMX4 at a level non-detectable by Western blotting, were transfected with several myc-tagged constructs, and treated with CoCl₂, a hypoxia-mimicking reagent acting through the HIF-1 pathway (Wang and Semenza, 1993). Secretion assays were set up for 48h during which cells were incubated in parallel under hypoxic (1% O₂) and normoxic conditions, respectively. The lysates prepared from the HeLa cells were investigated regarding expression of the myc-tagged constructs and GAPDH levels. The Western blot in Figure 3.15 shows that all the constructs (myc-TMX1, myc-TMX4 and Ero1 α -myc) were expressed by the cells, albeit at variable levels. As expected, there are no myc-tagged gene products in lanes 1, 5, 6 and 10. The bands at approximately 55 kDa and 70 kDa appearing in all of the lanes are considered to be background bands due to unspecific binding of the primary antibody (ms- α -myc from Upstate).

Since Ero1 α plays an important role in oxidative protein folding (see Introduction, section 1.4.1; May et al., 2005), the transfection with Ero1 α was used as a positive control. TMX1 served as a comparison on how the difference in the trx-like motif (see introduction, section 1.10) between the two TMX family members would or would not affect the secretion of VEGF. The negative control was performed by transfecting HeLa cells with the empty vector.

To assess the secretion of the particular VEGF isoforms, the conditioned cell culture medium was precipitated as described (see Materials & Methods, section 2.4.4) and analyzed by reducing SDS-PAGE on 15% gels. Due to the complex organization of the VEGF-A gene (reviewed in Xie et al., 2004; Ferrara et al., 2003; Holmes & Zachary, 2005), it was decided to use commercial recombinant human VEGF₁₆₅ (HumanZyme) as size standard to facilitate the interpretation of the results.

Figure 3.16 shows the Western blot of the supernatants corresponding to the cell lysates in Figure 3.15. It is apparent that under normoxic conditions (Figure 3.16, lanes 7 to 11) HeLa cells do not secrete detectable levels of VEGF. Interestingly, this is also the case for the CoCl₂-treated cells (Figure 3.16, lane 11), which would be expected to secrete approximately the same amount of VEGF as the empty vector-transfected negative control under hypoxic conditions. However, as expected, under

hypoxic conditions VEGF is secreted into the cell culture supernatant. Comparing with the recombinant VEGF₁₆₅, there are protein bands representing VEGF₁₆₅ in all of the hypoxia samples (Figure 3.16, lanes 1 to 5). Taking into account the broader bands observed with the control and the CoCl₂-treated cells (Figure 3.16, lanes 1 and 5), it is difficult to make a definitive statement on whether there is less VEGF₁₆₅ present than in the supernatants of HeLa cells transfected with the myc-TMX1, myc-TMX4 and Ero1 α -myc construct. Enhancing the levels in the area around 15 kDa shows an additional band that may represent VEGF₁₂₁, and which is present exclusively after transfection with the myc-TMX1, myc-TMX4, and Ero1 α -myc constructs. (Figure 3.16, lanes 2, 3 and 4).

3.5.1 Overexpression experiments at 1% O₂

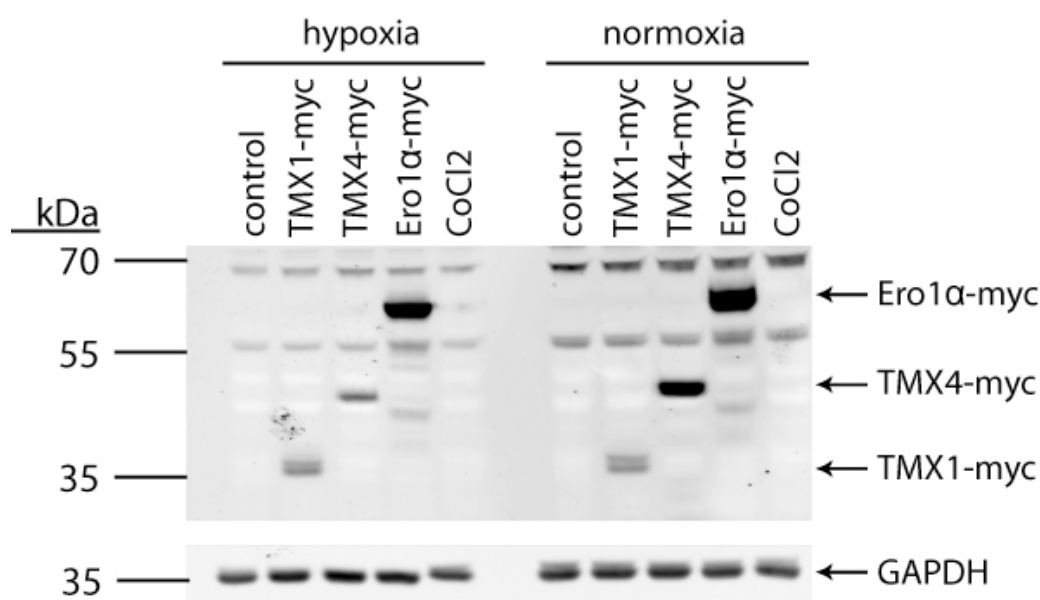


Figure 3.15. Western blot of cell lysates prepared from transfected HeLa cells. 9×10^5 cells per well were cultured under normoxic (incubator, 37°C, 5% CO₂) conditions in high glucose DMEM containing 10% FBS, transfected with Metafectene Pro® in Opti-MEM® as indicated. Lanes 1, 5, 6 and 10 were transfected with empty vector. Additionally lanes 5 and 10 were treated with CoCl₂ at a final concentration of 100 μ M 3 to 4h post transfection. For the secretion assay the medium was changed to high glucose DMEM w/o FBS and cells were cultured under normoxic (incubator, 37°C, 5% CO₂) and hypoxic (hypoxic chamber, 37°C, 5% CO₂ and 1% O₂) conditions as indicated for 48h. Cells were lysed in 200 μ l of lysis buffer containing CHAPS, sample buffer was added, samples were heated, and 25 μ l of sample each were loaded and subjected to reducing SDS-PAGE on a 10% gel. The transfected constructs were detected with ms- α -myc from Upstate (1:1000). GAPDH was used as a loading control and detected with rb- α -GAPDH from abcam® (1:2000).

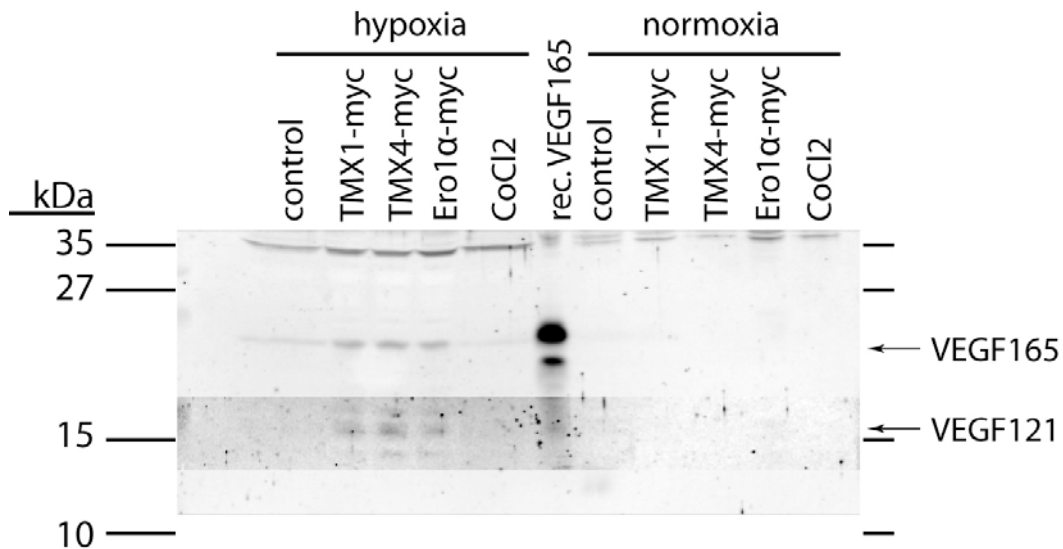


Figure 3.16. Western blot of precipitated supernatants from transfected HeLa cells.

9 x 10⁵ cells per well were cultured under normoxic (incubator, 37°C, 5% CO₂) conditions in high glucose DMEM containing 10% FBS, transfected with Metafectene Pro® in Opti-MEM® as indicated. Lanes 1, 5, 7 and 11 were transfected with empty vector. Additionally lanes 7 and 11 were treated with CoCl₂ at a final concentration of 100 µM 3 to 4h post transfection. In lane 6, 30 ng of recombinant human VEGF165 from HumanZyme were loaded as a size standard. For the secretion assay the medium was changed to high glucose DMEM w/o FBS and cells were cultured under normoxic (incubator, 37°C, 5% CO₂) and hypoxic (hypoxic chamber, 37°C, 5% CO₂ and 1% O₂) conditions as indicated for 48h. Supernatants were precipitated with equal volumes of 50% TCA, resuspended in sample buffer, heated and the resulting 30 µl of sample each were subjected to reducing SDS-PAGE on a 15% gel. VEGF was detected with polyclonal rb-α-VEGF from Santa Cruz Biotechnology (1:400).

To confirm the initial finding that TMX and TMX4 promote the secretion of VEGF, the experiment was repeated several times at the same oxygen level. However, some of the parameters were changed. Because of the lack of a noticeable effect, the use of CoCl₂ was discontinued. Furthermore, it has been suggested that the pathways for VEGF regulation in the presence and absence of CoCl₂ differ, and although upregulation of gene expression is mediated predominantly by HIF-1, it does not account for the full spectrum of the effects of hypoxia on gene expression (Dai et al., 2008; Greijer et al., 2005). Additionally, since PACS-2 possibly interacts with TMX and TMX4 through their C-terminal acidic clusters (T. Simmen, personal communication), HeLa cells were also transfected with the PACS-2-HA construct (e.g. Figure 3.17, lane 5). Transfection efficiency of PACS-2 was proven by blotting with rb-α-PACS-2 antiserum (shown in Figure 3.22). Due to the persistent absence of detectable VEGF protein bands in the normoxia control, this control was omitted.

Figure 3.17 and Figure 3.18 depict the results of Western blotting analysis of the HeLa cell lysates and of the cell culture supernatants, respectively. This time, Ero1α

overexpression resulted in only minimal secretion of VEGF₁₆₅, whereas overexpression of wtTMX1, and wtTMX4 yielded VEGF₁₆₅, VEGF₁₂₁ and additional weak bands at ~27 kDa, which appears to be VEGF₁₈₉. Comparing the expression levels of the transfected constructs in Figure 3.15 with those in Figure 3.17, it is evident that Ero1 α is expressed in smaller amounts relative to TMX1 and TMX4. Transfection with PACS-2-HA did not promote the secretion of VEGF.

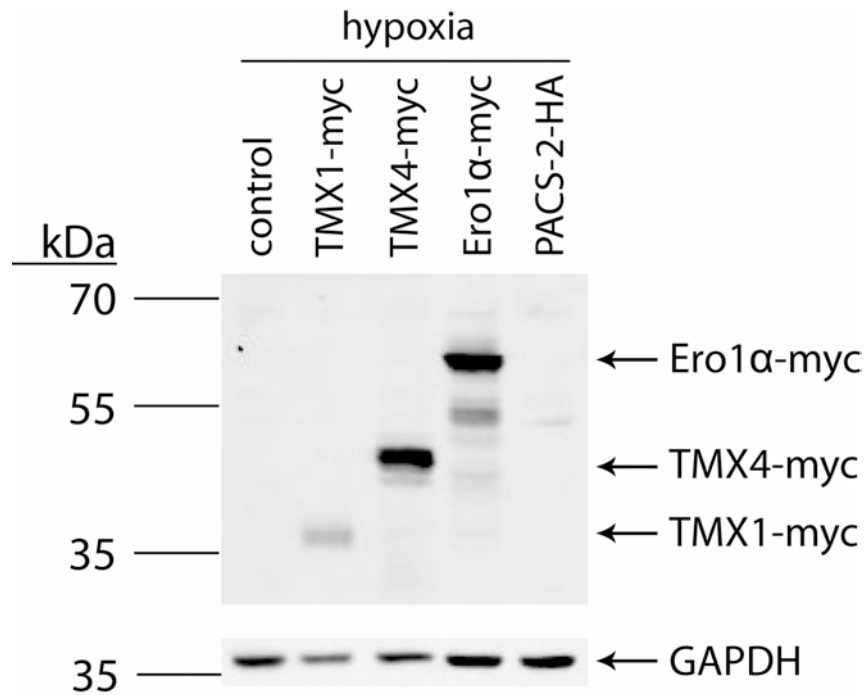


Figure 3.17. Western blot of cell lysates prepared from transfected HeLa cells. 9×10^5 cells per well were cultured under normoxic (incubator, 37°C, 5% CO₂) conditions in high glucose DMEM containing 10% FBS, transfected with Metafectene Pro® in Opti-MEM® as indicated. Lanes 1 and 6 were transfected with empty vector. For the secretion assay the medium was changed to high glucose DMEM w/o FBS and cells were cultured under hypoxic (hypoxic chamber, 37°C, 5% CO₂ and 1% O₂) conditions as indicated for 48h. Cells were lysed in 200 μ l of lysis buffer containing CHAPS, sample buffer was added, samples were heated, and 25 μ l of sample each were loaded and subjected to reducing SDS-PAGE on a 10% gel. The transfected constructs were detected with ms- α -myc from Upstate (1:1000). GAPDH was used as a loading control and detected with rb- α -GAPDH from abcam® (1:2000).

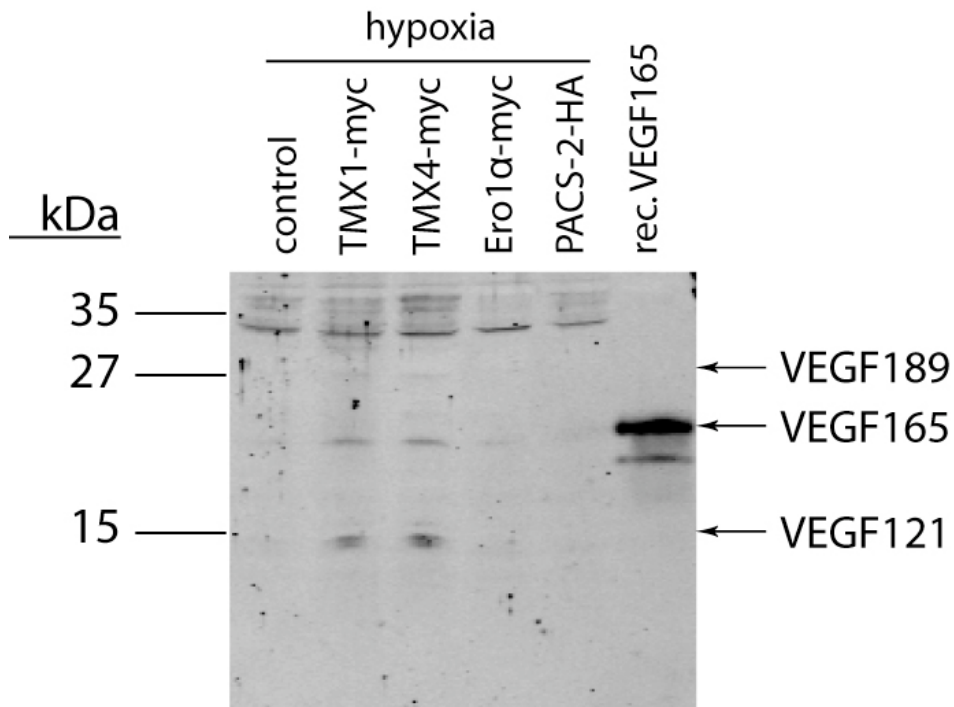


Figure 3.18. Western blot of precipitated supernatants from transfected HeLa cells. 9×10^5 cells per well were cultured under normoxic (incubator, 37°C, 5% CO₂) conditions in high glucose DMEM containing 10% FBS, transfected with Metafectene Pro® in Opti-MEM® as indicated. Lanes 1 and 7 were transfected with empty vector. In lane 6, 30 ng of recombinant human VEGF165 from HumanZyme were loaded as a size standard. For the secretion assay the medium was changed to high glucose DMEM w/o FBS and cells were cultured under hypoxic (hypoxic chamber, 37°C, 5% CO₂ and 1% O₂) conditions as indicated for 48h. Supernatants were precipitated with equal volumes of 50% TCA, resuspended in sample buffer, heated and the resulting 30 μ l of sample each were subjected to reducing SDS-PAGE on a 15% gel. VEGF was detected with polyclonal rb- α -VEGF from Santa Cruz Biotechnology (1:400).

The results of another VEGF secretion experiment are shown in Figure 3.19 and Figure 3.20, representing the HeLa cell lysates and the cell culture supernatants, respectively. In relation to the band intensity of the TMX4 construct, Ero1 α expression is rather low when compared to the expression ratios in e.g., Figure 3.15. Moreover, TMX1 expression has almost reached the detection limit. As Figure 3.20 demonstrates, all cells, regardless of the construct they were transfected with, expressed and secreted VEGF₁₈₉, VEGF₁₆₅, as well as VEGF₁₂₁. However, HeLa cells transfected with TMX1 or TMX4 produced significantly higher amounts of VEGF₁₂₁.

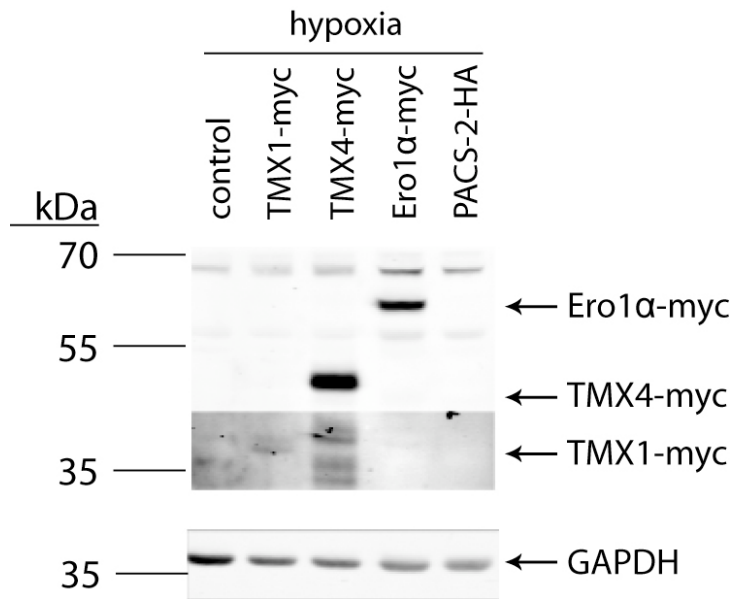


Figure 3.19. Western blot of cell lysates prepared from transfected HeLa cells. 9×10^5 cells per well were cultured under normoxic (incubator, 37°C, 5% CO₂) conditions in high glucose DMEM containing 10% FBS, transfected with Metafectene Pro® in Opti-MEM® as indicated. Lanes 1 and 6 were transfected with empty vector. For the secretion assay the medium was changed to high glucose DMEM w/o FBS and cells were cultured under hypoxic (hypoxic chamber, 37°C, 5% CO₂ and 1% O₂) conditions as indicated for 48h. Cells were lysed in 200 µl of lysis buffer containing CHAPS, sample buffer was added, samples were heated and 25 µl of sample each were loaded and subjected to reducing SDS-PAGE on a 10% gel. The transfected constructs were detected with ms-α-myc from Upstate (1:1000). GAPDH was used as a loading control and detected with rb-α-GAPDH from abcam® (1:2000).

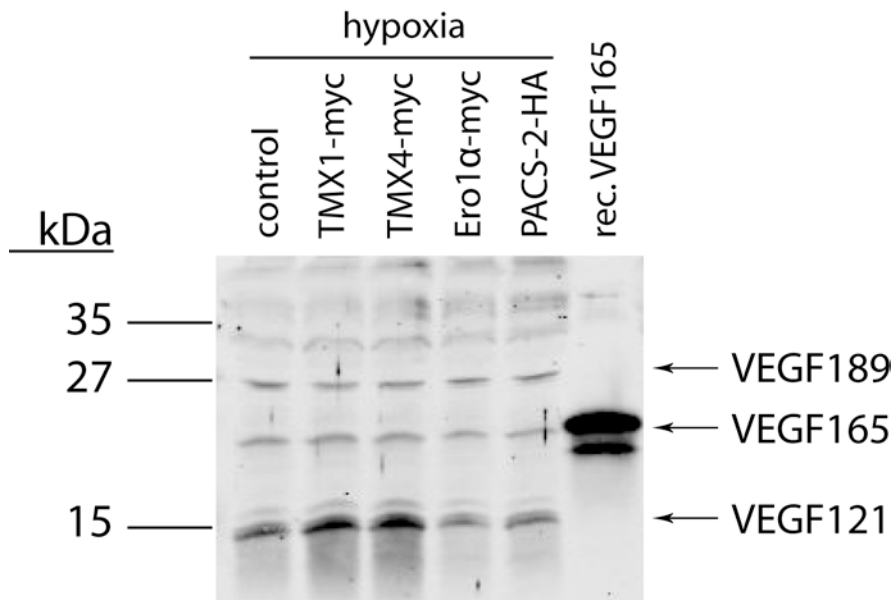


Figure 3.20. Western blot of precipitated supernatants from transfected HeLa cells. 9×10^5 cells per well were cultured under normoxic (incubator, 37°C, 5% CO₂) conditions in high glucose DMEM containing 10% FBS, transfected with Metafectene Pro® in Opti-MEM® as indicated. Lanes 1 and 7 were transfected with empty vector. In lane 6, 30 ng of recombinant human VEGF165 from HumanZyme were loaded as a size standard. For the secretion assay the medium was changed to high glucose DMEM w/o FBS and cells were cultured under hypoxic (hypoxic chamber, 37°C, 5% CO₂ and 1% O₂) conditions as indicated for 48h. Supernatants were precipitated with equal volumes of 50% TCA, resuspended in

sample buffer, heated and the resulting 30 μ l of sample each were subjected to reducing SDS-PAGE on a 15% gel. VEGF was detected with polyclonal rb- α -VEGF from Santa Cruz Biotechnology (1:400).

3.5.2 Overexpression experiment at 0.1% O₂

As addressed above, discrete levels of oxygen saturation determine the mode of reaction of cells subjected to hypoxic conditions. Due to this fact, the VEGF secretion was also performed in an environment of 0.1% O₂. The Western blot of the transfected HeLa cell lysates (Figure 3.21) depicts similar relative transfection efficiency as at 1% O₂ (Figure 3.19). Again, Ero1 α expression is lower than expression levels for TMX4, and the TMX1 construct is hardly detectable. In contrast to moderate hypoxia, the experiment at 0.1% O₂ resulted in differential secretion of VEGF isoforms (Figure 3.23). Whereas VEGF secretion in the control cells, Ero1 α transfected, and PACS-2 transfected cells was limited to VEGF₁₆₅ and VEGF₁₂₁, distinct bands of VEGF₁₈₉ were detectable exclusively in supernatants of TMX1-, and TMX4-transfected cells. Moreover, there was less VEGF₁₂₁ in these supernatants than in those of Ero1 α -, and PACS-2-transfected HeLa cells. Taken together, it appears that Ero1 α overexpression shifts VEGF expression/secretion to the VEGF₁₂₁ isoform, as PACS-2 overexpression does to a lesser extent, while TMX1 and TMX4 overexpression shift VEGF expression/secretion to the larger VEGF₁₈₉.

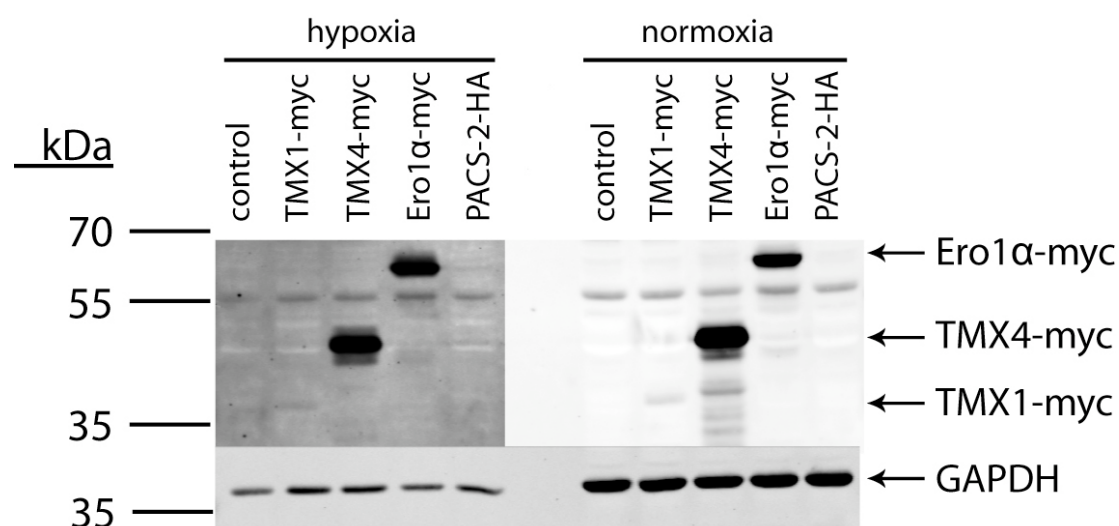


Figure 3.21. Western blot of cell lysates prepared from transfected HeLa cells. 9×10^5 cells per well were cultured under normoxic (incubator, 37°C, 5% CO₂) conditions in high glucose DMEM containing 10% FBS, transfected with Metafectene Pro® in Opti-MEM® as indicated. Lanes 1 and 6 were transfected with empty vector. For the secretion assay the medium was changed to high glucose DMEM w/o FBS and cells were cultured under normoxic (incubator, 37°C, 5% CO₂) and hypoxic (hypoxic chamber, 37°C, 5% CO₂ and 0.1% O₂) conditions as indicated for 48h. Cells were lysed in 200 μ l of lysis buffer containing CHAPS, sample buffer was added, samples were heated, and 25 μ l of sample each were loaded and subjected to reducing SDS-PAGE on a 10% gel. The transfected constructs were

detected with ms- α -myc from Upstate (1:1000). GAPDH was used as a loading control and detected with rb- α -GAPDH from abcam® (1:2000).

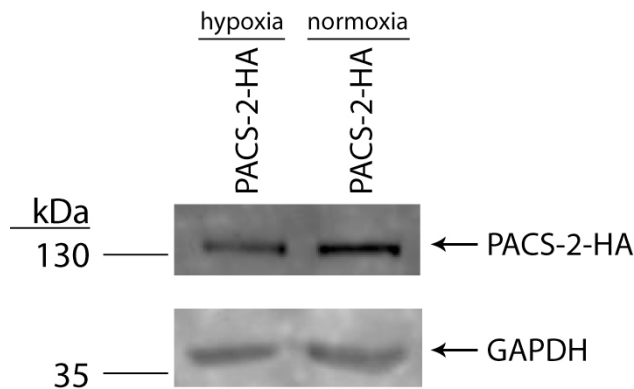


Figure 3.22. Western blot of cell lysates prepared from transfected HeLa cells. 9×10^5 cells per well were cultured under normoxic (incubator, 37°C, 5% CO₂) conditions in high glucose DMEM containing 10% FBS, transfected with Metafectene Pro® in Opti-MEM® as indicated. For the secretion assay the medium was changed to high glucose DMEM w/o FBS and cells were cultured under normoxic (incubator, 37°C, 5% CO₂) and hypoxic (hypoxic chamber, 37°C, 5% CO₂ and 0.1% O₂) conditions as indicated for 48h. Cells were lysed in 200 μ l of lysis buffer containing CHAPS, sample buffer was added, samples were heated, and 25 μ l of sample each were loaded and subjected to reducing SDS-PAGE on a 10% gel. The transfected constructs were detected with rb- α -PACS-2 non-commercial antiserum (1:1250). GAPDH was used as a loading control and detected with rb- α -GAPDH from abcam® (1:2000).

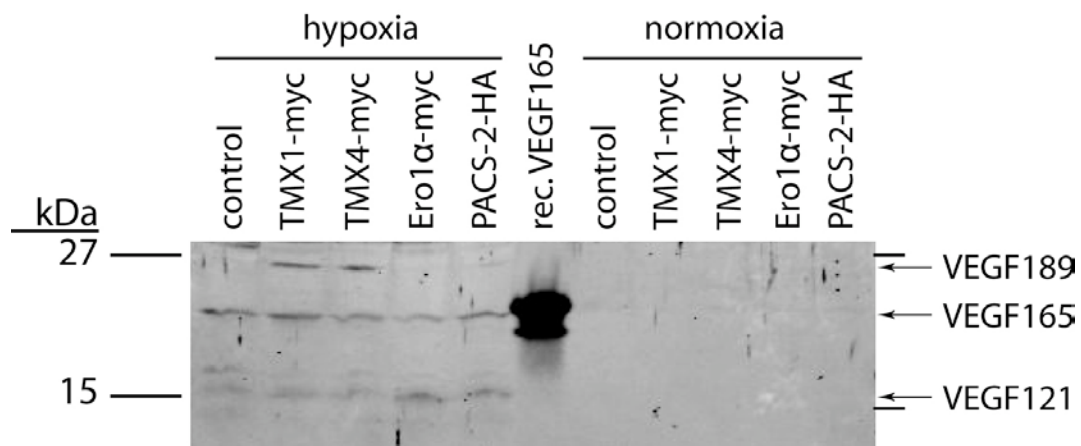


Figure 3.23. Western blot of precipitated supernatants from transfected HeLa cells. 9×10^5 cells per well were cultured under normoxic (incubator, 37°C, 5% CO₂) conditions in high glucose DMEM containing 10% FBS, transfected with Metafectene Pro® in Opti-MEM® as indicated. Lanes 1 and 7 were transfected with empty vector. In lane 6, 30 ng of recombinant human VEGF165 from HumanZyme were loaded as a size standard. For the secretion assay the medium was changed to high glucose DMEM w/o FBS and cells were cultured under normoxic (incubator, 37°C, 5% CO₂) and hypoxic (hypoxic chamber, 37°C, 5% CO₂ and 0.1% O₂) conditions as indicated for 48h. Supernatants were precipitated with equal volumes of 50% TCA, resuspended in sample buffer, heated and the resulting 30 μ l of sample each were subjected to reducing SDS-PAGE on a 15% gel. VEGF was detected with polyclonal rb- α -VEGF from Santa Cruz Biotechnology (1:400).

3.5.3 Silencing experiment at 0.1% O₂

Having investigated the effects of overexpressing the proteins of interest, it remained to be examined whether depletion of TMX1, TMX4, Ero1 α or PACS-2 respectively, had any effects on the secretion levels of VEGF. Figure 3.24 shows a Western blot of HeLa cell lysates upon siRNA transfection. As negative controls, samples in lane 1 were left untransfected, and samples in lane 2 were transfected with Silencer® Negative Control (Ambion). The siRNAs against TMX1, TMX4, and PACS-2 were established by Simmen et al. Thus, only the specificity of the siRNA against Ero1 α had to be demonstrated. It is evident that upon transfection with siEro1 α , the levels of Ero1 α substantially decreased (Figure 3.24, lane 5), as compared to the levels in the remaining samples. The siRNAs used are specified in Materials & Methods, section 2.3.7. In addition, GAPDH levels were used as a loading control. The Western blot of the cell culture supernatants corresponding to the cell lysates is depicted in Figure 3.25. In contrast to the negative controls (Figure 3.25, lanes 1 and 2), siRNA transfected HeLa cells did not secrete VEGF at a detectable level. In lane 1, where the HeLa cells were not transfected with siRNA, a weak band of VEGF₁₈₉ is present (~27 kDa), and in lane 2 (supernatant of Silencer® Negative control transfected cells) a faint VEGF₁₆₅ signal was observed.

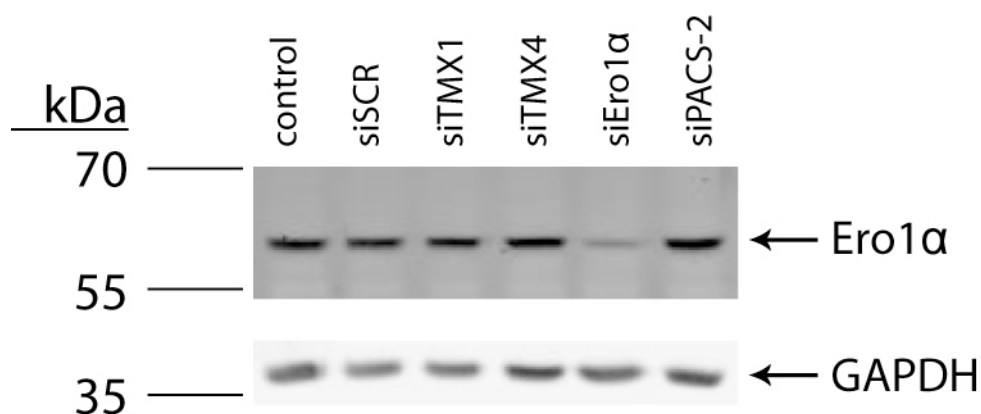


Figure 3.24. Western blot of cell lysates prepared from siRNA transfected HeLa cells.

2×10^5 cells per well were cultured under normoxic (incubator, 37°C, 5% CO₂) conditions in high glucose DMEM containing 10% FBS, transfected with Oligofectamine™ in Opti-MEM® as indicated. For the secretion assay the medium was changed to high glucose DMEM w/o FBS and cells were cultured under hypoxic conditions (hypoxic chamber, 37°C, 5% CO₂ and 0.1% O₂) for 48h. Cells from three wells were pooled and lysed in 200 μ l of lysis buffer containing CHAPS, sample buffer was added, samples were heated, and 25 μ l of sample each were loaded and subjected to reducing SDS-PAGE on a 10% gel. Ero1 α was detected with ms- α -Ero1 α 2G4 non-commercial antiserum (1:2000). GAPDH was used as a loading control and detected with rb- α -GAPDH from abcam® (1:2000).

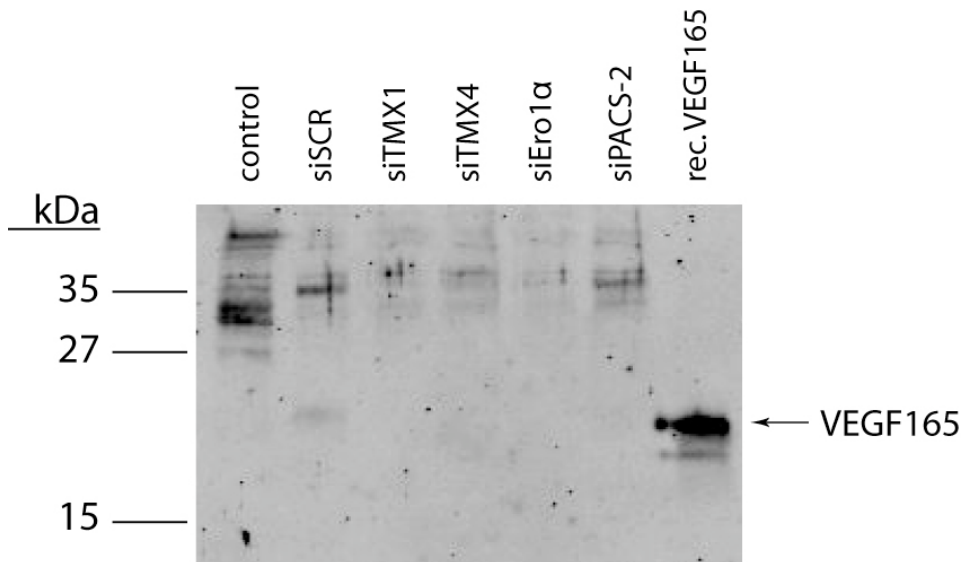


Figure 3.25. Western blot of precipitated supernatants from siRNA transfected HeLa cells. 2×10^5 cells per well were cultured under normoxic (incubator, 37°C, 5% CO₂) conditions in high glucose DMEM containing 10% FBS, transfected with Oligofectamine™ in Opti-MEM® as indicated. For the secretion assay the medium was changed to high glucose DMEM w/o FBS and cells were cultured under hypoxic conditions (hypoxic chamber, 37°C, 5% CO₂ and 0.1% O₂) for 48h. Supernatants from three wells were pooled and precipitated with equal volumes of 50% TCA, resuspended in sample buffer, heated and the resulting 30 µl of sample each were subjected to reducing SDS-PAGE on a 15% gel. VEGF was detected with polyclonal rb-α-VEGF from Santa Cruz Biotechnology (1:400).

4 DISCUSSION

TMX4 expression in human melanoma tissue

Since it was reported by Hoek et al. (2004) that in human melanoma cell lines the transcription of TMX4 mRNA was increased by about 10fold on average, when compared to normal human melanocytes, one of the major aims of this study was to compare TMX4 expression levels in human melanoma tissue with that in normal human skin at the protein level.

It could be shown that in approximately one-half of the investigated melanoma samples, TMX4 protein levels were elevated in comparison to those of commercial tissue lysates of normal human skin (Figure 3.1). This supports the conclusion that an increased level of TMX4 either is beneficial to tumor cells by conferring a growth advantage and/or enhanced resistance to apoptosis, or is a side effect of yet undetermined mechanisms resulting from deregulated or abnormal protein expression patterns. However, the comparative investigation of expression levels of TMX4 protein in normal human breast tissue and cancerous breast tissue revealed no such upregulation, possibly indicating different pathways of tumorigenesis in skin and breast.

Subcellular localization of TMX and TMX4

TMX4 as well as TMX are ER-resident proteins. This is suggested by their typical reticular staining patterns (Figure 3.3, first pictures in panel A and B), and can be shown through co-localization with PDI, which is undoubtedly abundant exclusively in the ER (the co-localization is clearly shown in Figure 3.6, panels C and F). Furthermore, both TMX and TMX4 contain atypical ER-retention signals (Roth et al., unpublished). However, the two proteins are found in different suborganellar domains of the ER. Whereas TMX overlaps at least partially with mitochondria, as does Ero1 α , no overlap between the mitochondria and the TMX4 signal was observed (Figure 3.3, panel B). This might suggest that TMX and Ero1 α , but not TMX4, are at least partially localized to the MAM. Simmen et al. also corroborated this assumption by separation of cell lysates using an optimized density gradient technique (T. Simmen, personal communication). The localization of certain proteins to the MAM, such as calnexin and TMX, appears to be mediated by PACS-2 (Simmen et al., 2005). Consistent with this hypothesis is the lack of a co-localization of TMX4 and PACS-2 when co-stained in A375P cells (Figure 3.6, panel B). Interestingly, the localization of protein chimeras consisting of the TMX4 N-terminus including the transmembrane domain and the cytosolic C-terminal tail of TMX shifts towards the

MAM, which indicates that the MAM-targeting information is contained in the cytosolic tail of TMX (Simmen et al., unpublished).

Co-staining of TMX4 with other ER-localized proteins revealed at least partial overlap with the signals of ERp44, ERGIC-53 and Derlin-1 (Figure 3.4, third picture of panel B; Figure 3.6, panels D and E). Thus, possible roles for TMX4 include (i) involvement in the redox-regulation of IP3 receptors by either interacting with ERp44 or performing a similar function as ERp44, (ii) the assistance of correctly folded proteins to exit the ER and/or (iii) facilitating the protein retro-translocation step of ER-associated degradation. However, assigning any of the mentioned functions to TMX4 remains highly speculative since a reducing and/or oxidative activity of TMX4 is yet to be examined.

Effects of TMX4 overexpression on the redox state of Ero1 α in HEK293 cells

As mentioned in section 3.3, upon transfection of HEK293 cells with the myc-tagged wtTMX4 construct, Ero1 α could be detected in three different oxidation states. Of these, Ox1 and Ox2 represent well-established forms of Ero1 α , and Ox3 is a hyperoxidized form. Since TMX4 lacks the b and b' domains, supposedly mediating protein-protein interaction with proteins containing cysteine residues (see section 1.4.2), it is unlikely that TMX4 directly interacts with Ero1 α to such an effect as to oxidize it. Therefore, if the observed Ox3 form is an actual result of TMX4 overexpression, this is likely achieved through one or more unknown mediator proteins. Another possibility would be that in this experiment, the overexpression of TMX4 resulted in futile oxidation cycles, which rendered the overall ER environment more oxidizing and in turn leading to the formation of a hyperoxidized form of Ero1 α . The fact that the Ox3 form of Ero1 α was observed only twice, and because no such hyperoxidized Ero1 α could be detected in the comparative expression of wtTMX4 and the described mutant TMX4 constructs (Figure 3.9) suggest that TMX4 levels do not influence the Ero1 α oxidation state.

TMX4 expression in A375P cells under hypoxic conditions

Exposure of cells to hypoxic conditions, a hallmark of fast-growing tumor masses, leads to the induction of potent mechanisms of adaptation to cope with the limited availability of molecular oxygen (described in section 1.13), such as attenuation of global translation and/or selective downregulation of gene expression, but also upregulation of specific genes. Hence, it was obvious to examine a possible positive correlation between hypoxia and TMX4 expression. Interestingly, cultivation of

A375P cells, a human melanoma cell line, in a reduced-oxygen atmosphere did not result in increased, but rather substantially decreased TMX4 protein levels (Figure 3.11). No such effect was observed for TMX under hypoxic conditions (data not shown), where TMX expression levels did not change. The decrease of TMX4 in A375P cells, when subjected to hypoxia, is especially puzzling, since the TMX4 gene contains an optimal HRE sequence (5'-ACGTG-3') in the 5' UTR. This leads to the assumption that yet undetermined factors are involved in the regulation of TMX4 expression. Moreover, the decrease in TMX4 could not be reversed by inhibiting the 26S proteasome, which indicates that TMX4 downregulation does not occur at the degradative level (Figure 3.14). It remains to be investigated whether this downregulation takes place at the level of gene expression, through inhibition of translation and/or via mRNA degradation.

TMX4 expression in A375P cells upon induction of ER stress

As mentioned in section 1.7, in order to cope with stress situations resulting from altered redox conditions, perturbed calcium homeostasis and/or accumulation of unfolded proteins in the ER, cells are capable of inducing specific signaling pathways to counteract these ER stresses. The overall defense response is to a certain degree due to the upregulation of specific genes containing ERSE elements upstream of their promoters. Such imperfect ERSE elements are also found in the TMX4 gene.

Therefore we investigated the possibility that TMX4 expression was altered under these circumstances. Induction of ER stress with DTT did not significantly alter TMX4 protein levels relative to GAPDH levels; however, inhibition of N-glycosylation with tunicamycin led to a decrease in TMX4. This decrease can be assumed to result from increased ERAD activity, since TMX4 levels could be partially restored by inhibiting the 26S proteasome (Figure 3.13). These results suggest that non-glycosylated TMX4 is targeted for degradation, due to currently undetermined recognition mechanisms, but possibly mediated by the EDEMs.

Promotion of VEGF secretion through overexpression of TMX and TMX4

Another major aim of this thesis was to examine how the observed upregulation of TMX4 in melanomas, which is apparently independent from hypoxia, could be potentially beneficial to tumors of the skin. The promoting effects of VEGF on tumor development and tumor growth have been addressed extensively in section 1.12. It was therefore of particular interest to examine whether overexpression of TMX4 had any effects on the secretion of VEGF. Indeed, it was observed that transfection of HeLa cells with myc-tagged wtTMX4 constructs, as well as with myc-tagged wtTMX

constructs, altered the secretion patterns of VEGF. However, the results varied, and appeared to correlate with the degree of hypoxia the cells were subjected to. Despite the variation in the results, a trend towards a promoting effect of VEGF secretion upon overexpression of TMX and TMX4 was noticed (see section 3.5). Initial experiments at 1% O₂ suggested that TMX and TMX4 promote the expression and secretion of VEGF₁₆₅ and VEGF₁₂₁, as was observed for the positive control, i.e., Ero1 α -myc transfected HeLa cells (Figure 3.16, lanes 2-4). This hypothesis would have been corroborated by the results shown in Figure 3.18, if it was not for the decreased levels of GAPDH in lanes 2 and 3, the TMX and TMX4 overexpressing samples respectively, of Figure 3.17. Transfection with the PACS-2-HA construct did not appear to have any effect on the secretion of VEGF (Figure 3.18, lane 5). The decrease in GAPDH levels under hypoxic conditions could indicate a growth inhibition of the addressed cells, which in turn would result in increased secretion of VEGF due to elevated stress levels. Furthermore, when comparing relative expression levels of the Ero1 α -construct in Figure 3.15 (lane 4) and Figure 3.17 (lane 4), it appears that Ero1 α is expressed at lower levels in the latter experiment. Correspondingly, the secretion of VEGF in Ero1 α -transfected HeLa cells (Figure 3.18, lane 4) is significantly lower than in lane 4 of Figure 3.16. This suggests that in order to promote secretion of VEGF sufficiently, a certain level of Ero1 α expression is required. In contrast to the experiments addressed so far, in the third experiment at 1% O₂, VEGF levels were elevated in the supernatants of all samples (Figure 3.20), which appeared to be independent of the corresponding GAPDH levels in the cell lysates (Figure 3.19). The use of GAPDH as a loading control is a matter of ongoing discussion. Whereas it has been shown that GAPDH is not regulated by hypoxia in human glioblastoma, human hepatocellular carcinoma cell lines, a human lung adenocarcinoma epithelial cell line as well as two colon cancer cell lines (Said et al., 2007 and 2009), other research groups suggest the use of total protein stains as an alternative to relying on a single gene product (Aldridge et al., 2008). However, it is evident that the levels of VEGF₁₂₁ are again elevated exclusively in the supernatants of TMX- and TMX4-transfected cells (Figure 3.20, lanes 2 and 3). The general increase in secretion of all of the detected VEGF isoforms (VEGF₁₈₉, VEGF₁₆₅, and VEGF₁₂₁) is most likely the result of an infection of the HeLa cells with bacteria of the genus *Mycoplasma*, which was discovered in the course of a routine check for mycoplasma by polymerase chain reaction (PCR) (data not shown). In support of this theory, increased serum levels of VEGF in patients infected with *Mycoplasma*

pneumoniae have been reported by different research groups (Choi, S.H. et al., 2006; Choi, I.S. et al., 2009).

The results of the VEGF secretion experiment performed under conditions of acute hypoxia (0.1% O₂) are particularly interesting. As shown in Figure 3.23, TMX- and TMX4-overexpressing HeLa cells subjected to acute hypoxia appear to shift VEGF expression and/or secretion to the larger VEGF isoform, VEGF₁₈₉. The various VEGF isoforms differ in their effector functions; e.g., VEGF₁₂₁ induces endothelial cell migration and sprouting, VEGF₁₆₅ generally promotes tumor growth and angiogenesis, whereas VEGF₁₈₉ not only plays a role in angiogenesis, but also vasodilation and cell migration (Pan et al., 2007; Ancelin et al., 2004, Hervé et al., 2005 and 2008). Thus, the shift towards VEGF₁₈₉ could represent an adaptation of VEGF secretion influenced by TMX and TMX4. Taken together, TMX- and TMX4-transfected HeLa cells subjected to 1% O₂, and 0.1% O₂ secreted increased amounts of VEGF₁₂₁ and VEGF₁₈₉, respectively. Considering that these two VEGF isoforms not only play a role in the promotion of neovascularization, but also in cell migration, this could point to a possible correlation with the spreading of tumor cells. PACS-2 overexpression seems to have minor effects on the secretion of VEGF, although slightly elevated levels of VEGF₁₂₁ could be detected when compared to the negative control (Figure 3.23, lanes 1 and 5).

Depletion of TMX, TMX4, Ero1 α , and PACS-2

Upon silencing of TMX, TMX4, Ero1 α , and PACS-2, respectively, no VEGF signal could be detected (Figure 3.25). However, this is most likely not a result of the depletion itself, but is rather based on the small number of cells used for siRNA transfections. Even pooling of three samples (~6 x 10⁵ cells) transfected in the same manner did not lead to VEGF concentrations reaching the detection limit. To overcome this limitation, it probably would be necessary to pool at least 5 equally transfected samples, or to use a different protocol for siRNA transfection, allowing for the analysis of more cells.

In conclusion, compared to the healthy tissue, protein levels of TMX and TMX4 were found to be highly aberrant in both melanoma and breast cancer tissue. Furthermore, overexpression of the two homologous proteins TMX and TMX4 in HeLa cells appears not only to promote the secretion of VEGF, a major angiogenic growth factor, but also seems to cause a shift in the VEGF expression pattern under hypoxic conditions. However, distinct biological functions for the two members of the PDI-family remain to be elucidated.

Ongoing studies aim to resolve the targeting mechanisms of TMX and TMX4 through generation of chimeras of TMX and TMX4, in which parts of the proteins are exchanged.

Future studies should determine whether the trx-like domain in TMX4 has a catalytic function, such as that of the trx-like domain of TMX. For this purpose, assays similar to those described by Matsuo et al. (2001 and 2004) could be used, thereby checking for a possible ability of TMX4 to reduce substrate proteins. Additionally, a folding assay, e.g. using the transferrin receptor as a folding template, could be performed to determine whether TMX4 is capable of folding secretory proteins *in vitro*.

To corroborate the hypothesis that TMX and TMX4 are capable of promoting the secretion of VEGF, the transcription levels of VEGF mRNA should be assessed. Moreover, investigation of possible induction of apoptosis in cells subjected to hypoxia could rule out VEGF promoting effects due to imminent cell death. Furthermore, in order to facilitate the analysis of supernatants and to increase throughput, assessment of VEGF protein levels could be achieved by using commercial enzyme-linked immunosorbent assay (ELISA) kits instead of Western blotting technique.

5 REFERENCES

A

- Aldridge, G.M., et al., *The use of total protein stains as loading controls: an alternative to high-abundance single-protein controls in semi-quantitative immunoblotting*. J Neurosci Methods, 2008. **172**(2): p. 250-4.
- Annaert, W.G., et al., *Export of cellubrevin from the endoplasmic reticulum is controlled by BAP31*. J Cell Biol, 1997. **139**(6): p. 1397-410.
- Ancelin, M., et al., *Vascular endothelial growth factor VEGF189 induces human neutrophil chemotaxis in extravascular tissue via an autocrine amplification mechanism*. Lab Invest, 2004. **84**(4): p. 502-12.
- Appenzeller, C., et al., *The lectin ERGIC-53 is a cargo transport receptor for glycoproteins*. Nat Cell Biol, 1999. **1**(6): p. 330-4.
- Appenzeller-Herzog, C. and L. Ellgaard, *The human PDI family: Versatility packed into a single fold*. Biochim Biophys Acta, 2008. **1783**(4): p. 535-48.
- Appenzeller-Herzog, C., et al., *A novel disulphide switch mechanism in Ero1alpha balances ER oxidation in human cells*. Embo J, 2008. **27**(22): p. 2977-87.
- Argon, Y. and B.B. Simen, *GRP94, an ER chaperone with protein and peptide binding properties*. Semin Cell Dev Biol, 1999. **10**(5): p. 495-505.
- Arrington, D.D. and R.G. Schnellmann, *Targeting of the molecular chaperone oxygen-regulated protein 150 (ORP150) to mitochondria and its induction by cellular stress*. Am J Physiol Cell Physiol, 2008. **294**(2): p. C641-50.
- Atkins, K.M., et al., *HIV-1 Nef binds PACS-2 to assemble a multikinase cascade that triggers major histocompatibility complex class I (MHC-I) down-regulation: analysis using short interfering RNA and knock-out mice*. J Biol Chem, 2008. **283**(17): p. 11772-84.

B

- Baltzis, D., et al., *The eIF2alpha kinases PERK and PKR activate glycogen synthase kinase 3 to promote the proteasomal degradation of p53*. J Biol Chem, 2007. **282**(43): p. 31675-87.
- Baryshev, M., E. Sargsyan, and S. Mkrтчian, *ERp29 is an essential endoplasmic reticulum factor regulating secretion of thyroglobulin*. Biochem Biophys Res Commun, 2006. **340**(2): p. 617-24.
- Benham, A.M., et al., *The CXXCXXC motif determines the folding, structure and stability of human Ero1-Lalpha*. Embo J, 2000. **19**(17): p. 4493-502.
- Bertolotti, A., et al., *Dynamic interaction of BiP and ER stress transducers in the unfolded-protein response*. Nat Cell Biol, 2000. **2**(6): p. 326-32.
- Blais, J.D., et al., *Perk-dependent translational regulation promotes tumor cell adaptation and angiogenesis in response to hypoxic stress*. Mol Cell Biol, 2006. **26**(24): p. 9517-32.

- Boelens, J., et al., *Review. The endoplasmic reticulum: a target for new anticancer drugs*. In *Vivo*, 2007. **21**(2): p. 215-26.
- Brahimi-Horn, M.C., J. Chiche, and J. Pouyssegur, *Hypoxia and cancer*. *J Mol Med*, 2007. **85**(12): p. 1301-7.
- Brostrom, M.A. and C.O. Brostrom, *Calcium dynamics and endoplasmic reticular function in the regulation of protein synthesis: implications for cell growth and adaptability*. *Cell Calcium*, 2003. **34**(4-5): p. 345-63.
- Bu, G., *The roles of receptor-associated protein (RAP) as a molecular chaperone for members of the LDL receptor family*. *Int Rev Cytol*, 2001. **209**: p. 79-116.

C

- Cabibbo, A., et al., *ERO1-L, a human protein that favors disulfide bond formation in the endoplasmic reticulum*. *J Biol Chem*, 2000. **275**(7): p. 4827-33.
- Calfon, M., et al., *IRE1 couples endoplasmic reticulum load to secretory capacity by processing the XBP-1 mRNA*. *Nature*, 2002. **415**(6867): p. 92-6.
- Chakravarthi, S. and N.J. Bulleid, *Glutathione is required to regulate the formation of native disulfide bonds within proteins entering the secretory pathway*. *J Biol Chem*, 2004. **279**(38): p. 39872-9.
- Chen, X., J. Shen, and R. Prywes, *The luminal domain of ATF6 senses endoplasmic reticulum (ER) stress and causes translocation of ATF6 from the ER to the Golgi*. *J Biol Chem*, 2002. **277**(15): p. 13045-52.
- Chevet, E., et al., *The endoplasmic reticulum: integration of protein folding, quality control, signaling and degradation*. *Curr Opin Struct Biol*, 2001. **11**(1): p. 120-4.
- Chiu, C.C., et al., *Glucose-regulated protein 78 regulates multiple malignant phenotypes in head and neck cancer and may serve as a molecular target of therapeutic intervention*. *Mol Cancer Ther*, 2008. **7**(9): p. 2788-97.
- Choi, S.H., et al., *Serum vascular endothelial growth factor in pediatric patients with community-acquired pneumonia and pleural effusion*. *J Korean Med Sci*, 2006. **21**(4): p. 608-13.
- Choi, I.S., et al., *Increased serum interleukin-5 and vascular endothelial growth factor in children with acute mycoplasma pneumonia and wheeze*. *Pediatr Pulmonol*, 2009.
- Crump, C.M., et al., *PACS-1 binding to adaptors is required for acidic cluster motif-mediated protein traffic*. *Embo J*, 2001. **20**(9): p. 2191-201.
- Cunnea, P.M., et al., *ERdj5, an endoplasmic reticulum (ER)-resident protein containing DnaJ and thioredoxin domains, is expressed in secretory cells or following ER stress*. *J Biol Chem*, 2003. **278**(2): p. 1059-66.
- Cuozzo, J.W. and C.A. Kaiser, *Competition between glutathione and protein thiols for disulphide-bond formation*. *Nat Cell Biol*, 1999. **1**(3): p. 130-5.

D

Dai, M., et al., *Melatonin modulates the expression of VEGF and HIF-1 alpha induced by CoCl2 in cultured cancer cells*. J Pineal Res, 2008. **44**(2): p. 121-6.

E

Ellgaard, L., M. Molinari, and A. Helenius, *Setting the standards: quality control in the secretory pathway*. Science, 1999. **286**(5446): p. 1882-8.

Ellgaard, L. and A. Helenius, *ER quality control: towards an understanding at the molecular level*. Curr Opin Cell Biol, 2001. **13**(4): p. 431-7.

Ellgaard, L. and A. Helenius, *Quality control in the endoplasmic reticulum*. Nat Rev Mol Cell Biol, 2003. **4**(3): p. 181-91.

Eriksson, S., J. Carlson, and R. Velez, *Risk of cirrhosis and primary liver cancer in alpha 1-antitrypsin deficiency*. N Engl J Med, 1986. **314**(12): p. 736-9.

F

Fagioli, C., A. Mezghrani, and R. Sitia, *Reduction of interchain disulfide bonds precedes the dislocation of Ig-mu chains from the endoplasmic reticulum to the cytosol for proteasomal degradation*. J Biol Chem, 2001. **276**(44): p. 40962-7.

Fels, D.R. and C. Koumenis, *The PERK/eIF2alpha/ATF4 module of the UPR in hypoxia resistance and tumor growth*. Cancer Biol Ther, 2006. **5**(7): p. 723-8.

Ferrara, N., H.P. Gerber, and J. LeCouter, *The biology of VEGF and its receptors*. Nat Med, 2003. **9**(6): p. 669-76.

Forster, M.L., et al., *Protein disulfide isomerase-like proteins play opposing roles during retrotranslocation*. J Cell Biol, 2006. **173**(6): p. 853-9.

Frand, A.R. and C.A. Kaiser, *The ERO1 gene of yeast is required for oxidation of protein dithiols in the endoplasmic reticulum*. Mol Cell, 1998. **1**(2): p. 161-70.

Frickel, E.M., et al., *TROSY-NMR reveals interaction between ERp57 and the tip of the calreticulin P-domain*. Proc Natl Acad Sci U S A, 2002. **99**(4): p. 1954-9.

Frey, S., et al., *The ATPase cycle of the endoplasmic chaperone Grp94*. J Biol Chem, 2007. **282**(49): p. 35612-20.

G

Gess, B., et al., *The cellular oxygen tension regulates expression of the endoplasmic oxidoreductase ERO1-Lalpha*. Eur J Biochem, 2003. **270**(10): p. 2228-35.

Giacomello, M., et al., *Mitochondrial Ca2+ as a key regulator of cell life and death*. Cell Death Differ, 2007. **14**(7): p. 1267-74.

Goplen, D., et al., *Protein disulfide isomerase expression is related to the invasive properties of malignant glioma*. Cancer Res, 2006. **66**(20): p. 9895-902.

Greijer, A.E., et al., *Up-regulation of gene expression by hypoxia is mediated predominantly by hypoxia-inducible factor 1 (HIF-1)*. J Pathol, 2005. **206**(3): p. 291-304.

Gross, E., et al., *Generating disulfides enzymatically: reaction products and electron acceptors of the endoplasmic reticulum thiol oxidase Ero1p*. Proc Natl Acad Sci U S A, 2006. **103**(2): p. 299-304.

H

Harding, H.P., et al., *Regulated translation initiation controls stress-induced gene expression in mammalian cells*. Mol Cell, 2000. **6**(5): p. 1099-108.

Hayashi, T. and T.P. Su, *Sigma-1 receptor chaperones at the ER-mitochondrion interface regulate Ca(2+) signaling and cell survival*. Cell, 2007. **131**(3): p. 596-610.

Hayashi, T., et al., *MAM: more than just a housekeeper*. Trends Cell Biol, 2009. **19**(2): p. 81-8.

Herrmann, J.M., P. Malkus, and R. Schekman, *Out of the ER--outfitters, escorts and guides*. Trends Cell Biol, 1999. **9**(1): p. 5-7.

Herve, M.A., et al., *VEGF189 stimulates endothelial cells proliferation and migration in vitro and up-regulates the expression of Flk-1/KDR mRNA*. Exp Cell Res, 2005. **309**(1): p. 24-31.

Herve, M.A., et al., *Overexpression of vascular endothelial growth factor 189 in breast cancer cells leads to delayed tumor uptake with dilated intratumoral vessels*. Am J Pathol, 2008. **172**(1): p. 167-78.

Hoek, K., et al., *Expression profiling reveals novel pathways in the transformation of melanocytes to melanomas*. Cancer Res, 2004. **64**(15): p. 5270-82.

Hollien, J. and J.S. Weissman, *Decay of endoplasmic reticulum-localized mRNAs during the unfolded protein response*. Science, 2006. **313**(5783): p. 104-7.

Holmes, D.I. and I. Zachary, *The vascular endothelial growth factor (VEGF) family: angiogenic factors in health and disease*. Genome Biol, 2005. **6**(2): p. 209.

Holmgren, A., *Thioredoxin*. Annu Rev Biochem, 1985. **54**: p. 237-71.

Holmgren, A. and C.I. Branden, *Crystal structure of chaperone protein PapD reveals an immunoglobulin fold*. Nature, 1989. **342**(6247): p. 248-51.

Hosoda, A., et al., *JPDI, a novel endoplasmic reticulum-resident protein containing both a BiP-interacting J-domain and thioredoxin-like motifs*. J Biol Chem, 2003. **278**(4): p. 2669-76.

Hwang, C., A.J. Sinskey, and H.F. Lodish, *Oxidized redox state of glutathione in the endoplasmic reticulum*. Science, 1992. **257**(5076): p. 1496-502.

I

- Ireland, B.S., et al., *Lectin-deficient calreticulin retains full functionality as a chaperone for class I histocompatibility molecules*. Mol Biol Cell, 2008. **19**(6): p. 2413-23.
- Iwawaki, T., et al., *Translational control by the ER transmembrane kinase/ribonuclease IRE1 under ER stress*. Nat Cell Biol, 2001. **3**(2): p. 158-64.

J

- Jansens, A., E. van Duijn, and I. Braakman, *Coordinated nonvectorial folding in a newly synthesized multidomain protein*. Science, 2002. **298**(5602): p. 2401-3.
- Jeong, S.Y. and D.W. Seol, *The role of mitochondria in apoptosis*. BMB Rep, 2008. **41**(1): p. 11-22.
- Jessop, C.E., et al., *Oxidative protein folding in the mammalian endoplasmic reticulum*. Biochem Soc Trans, 2004. 32(Pt 5): p. 655-8.
- Jiang, C.C., et al., *Human Melanoma Cells under Endoplasmic Reticulum Stress Acquire Resistance to Microtubule-Targeting Drugs through XBP-1-Mediated Activation of Akt*. Neoplasia, 2009. **11**(5): p. 436-47.

K

- Kaluz, S., M. Kaluzova, and E.J. Stanbridge, *Rational design of minimal hypoxia-inducible enhancers*. Biochem Biophys Res Commun, 2008. **370**(4): p. 613-8.
- Kaul, S.C., et al., *Activation of wild type p53 function by its mortalin-binding, cytoplasmically localizing carboxyl terminus peptides*. J Biol Chem, 2005. **280**(47): p. 39373-9.
- Keck, P.J., et al., *Vascular permeability factor, an endothelial cell mitogen related to PDGF*. Science, 1989. **246**(4935): p. 1309-12.
- Kim, I., W. Xu, and J.C. Reed, *Cell death and endoplasmic reticulum stress: disease relevance and therapeutic opportunities*. Nat Rev Drug Discov, 2008. **7**(12): p. 1013-30.
- Kottgen, M., et al., *Trafficking of TRPP2 by PACS proteins represents a novel mechanism of ion channel regulation*. Embo J, 2005. **24**(4): p. 705-16.
- Koumenis, C. and B.G. Wouters, *"Translating" tumor hypoxia: unfolded protein response (UPR)-dependent and UPR-independent pathways*. Mol Cancer Res, 2006. **4**(7): p. 423-36.
- Kozlov, G., et al., *Crystal structure of the bb' domains of the protein disulfide isomerase ERp57*. Structure, 2006. **14**(8): p. 1331-9.
- Kuznetsov, G., K.T. Bush, P.L. Zhang, and S.K. Nigam, *Perturbations in maturation of secretory proteins and their association with endoplasmic reticulum chaperones in a cell culture model for epithelial ischemia*. Proc Natl Acad Sci U S A, 1996. **93**(16): p. 8584-9.

L

- Lai, E., T. Teodoro, and A. Volchuk, *Endoplasmic reticulum stress: signaling the unfolded protein response*. Physiology (Bethesda), 2007. **22**: p. 193-201.
- Lee, A.H., N.N. Iwakoshi, and L.H. Glimcher, *XBP-1 regulates a subset of endoplasmic reticulum resident chaperone genes in the unfolded protein response*. Mol Cell Biol, 2003. **23**(21): p. 7448-59.
- Lee, A.S. and L.M. Hendershot, *ER stress and cancer*. Cancer Biol Ther, 2006. **5**(7): p. 721-2.
- Leung, D.W., et al., *Vascular endothelial growth factor is a secreted angiogenic mitogen*. Science, 1989. **246**(4935): p. 1306-9.
- Li, J. and A.S. Lee, *Stress induction of GRP78/BiP and its role in cancer*. Curr Mol Med, 2006. **6**(1): p. 45-54.
- Liu, C.Y., M. Schroder, and R.J. Kaufman, *Ligand-independent dimerization activates the stress response kinases IRE1 and PERK in the lumen of the endoplasmic reticulum*. J Biol Chem, 2000. **275**(32): p. 24881-5.
- Liu, Q., et al., *A Fenton reaction at the endoplasmic reticulum is involved in the redox control of hypoxia-inducible gene expression*. Proc Natl Acad Sci U S A, 2004. **101**(12): p. 4302-7.
- Lu, P.D., H.P. Harding, and D. Ron, *Translation reinitiation at alternative open reading frames regulates gene expression in an integrated stress response*. J Cell Biol, 2004. **167**(1): p. 27-33.

M

- Maattanen, P., et al., *ERp57 and PDI: multifunctional protein disulfide isomerases with similar domain architectures but differing substrate-partner associations*. Biochem Cell Biol, 2006. **84**(6): p. 881-9.
- Matsuo, Y., et al., *Identification of a novel thioredoxin-related transmembrane protein*. J Biol Chem, 2001. **276**(13): p. 10032-8.
- Matsuo, Y., et al., *TMX, a human transmembrane oxidoreductase of the thioredoxin family: the possible role in disulfide-linked protein folding in the endoplasmic reticulum*. Arch Biochem Biophys, 2004. **423**(1): p. 81-7.
- May, D., et al., *Ero1-L alpha plays a key role in a HIF-1-mediated pathway to improve disulfide bond formation and VEGF secretion under hypoxia: implication for cancer*. Oncogene, 2005. **24**(6): p. 1011-20.
- McCullough, K.D., et al., *Gadd153 sensitizes cells to endoplasmic reticulum stress by down-regulating Bcl2 and perturbing the cellular redox state*. Mol Cell Biol, 2001. **21**(4): p. 1249-59.
- Molteni, S.N., et al., *Glutathione limits Ero1-dependent oxidation in the endoplasmic reticulum*. J Biol Chem, 2004. **279**(31): p. 32667-73.

Myhill, N., et al., *The Subcellular Distribution of Calnexin is Mediated by PACS-2*. Mol Biol Cell, 2008.

N

Nadanaka, S., et al., *Role of disulfide bridges formed in the luminal domain of ATF6 in sensing endoplasmic reticulum stress*. Mol Cell Biol, 2007. **27**(3): p. 1027-43.

Nakamura, H., K. Nakamura, and J. Yodoi, *Redox regulation of cellular activation*. Annu Rev Immunol, 1997. **15**: p. 351-69.

Nardai, G., et al., *Diabetic changes in the redox status of the microsomal protein folding machinery*. Biochem Biophys Res Commun, 2005. **334**(3): p. 787-95.

Ni, M. and A.S. Lee, *ER chaperones in mammalian development and human diseases*. FEBS Lett, 2007. **581**(19): p. 3641-51.

Nichols, W.C., et al., *Mutations in the ER-Golgi intermediate compartment protein ERGIC-53 cause combined deficiency of coagulation factors V and VIII*. Cell, 1998. **93**(1): p. 61-70.

Novoa, I., et al., *Feedback inhibition of the unfolded protein response by GADD34-mediated dephosphorylation of eIF2alpha*. J Cell Biol, 2001. **153**(5): p. 1011-22.

O

Okada, T., et al., *Distinct roles of activating transcription factor 6 (ATF6) and double-stranded RNA-activated protein kinase-like endoplasmic reticulum kinase (PERK) in transcription during the mammalian unfolded protein response*. Biochem J, 2002. **366**(Pt 2): p. 585-94.

Osibow, K., S. Frank, R. Malli, R. Zechner, and W.F. Graier, *Mitochondria maintain maturation and secretion of lipoprotein lipase in the endoplasmic reticulum*. Biochem J, 2006. **396**(1): p. 173-82.

Oyadomari, S., et al., *Cotranslocational degradation protects the stressed endoplasmic reticulum from protein overload*. Cell, 2006. **126**(4): p. 727-39.

Ozawa, K., et al., *Regulation of tumor angiogenesis by oxygen-regulated protein 150, an inducible endoplasmic reticulum chaperone*. Cancer Res, 2001. **61**(10): p. 4206-13.

P

Pagani, M., et al., *Endoplasmic reticulum oxidoreductin 1-beta (ERO1-Lbeta), a human gene induced in the course of the unfolded protein response*. J Biol Chem, 2000. **275**(31): p. 23685-92.

Pan, Q., et al., *Neuropilin-1 binds to VEGF121 and regulates endothelial cell migration and sprouting*. J Biol Chem, 2007. **282**(33): p. 24049-56.

Park, H.R., et al., *Effect on tumor cells of blocking survival response to glucose deprivation*. J Natl Cancer Inst, 2004. **96**(17): p. 1300-10.

Plempner, R.K. and D.H. Wolf, *Retrograde protein translocation: ERADication of secretory proteins in health and disease*. Trends Biochem Sci, 1999. **24**(7): p. 266-70.

Pollard, M.G., K.J. Travers, and J.S. Weissman, *Ero1p: a novel and ubiquitous protein with an essential role in oxidative protein folding in the endoplasmic reticulum*. Mol Cell, 1998. **1**(2): p. 171-82.

Pollard, P.J. and P.J. Ratcliffe, *Cancer. Puzzling patterns of predisposition*. Science, 2009. **324**(5924): p. 192-4.

R

Rapoport, T.A., *Protein translocation across the eukaryotic endoplasmic reticulum and bacterial plasma membranes*. Nature, 2007. **450**(7170): p. 663-9.

Raven, J.F. and A.E. Koromilas, *PERK and PKR: old kinases learn new tricks*. Cell Cycle, 2008. **7**(9): p. 1146-50.

Ron, D., *Translational control in the endoplasmic reticulum stress response*. J Clin Invest, 2002. **110**(10): p. 1383-8.

Roth, D., E. Lynes, N. Althaus, T. Simmen, and L. Ellgaard, *A non-classical localization signal targets the novel ER oxidoreductase TMX4 to the endoplasmic reticulum*. Journal of Biological Chemistry, 2008. **in revision**.

Ruddock, L.W. and M. Molinari, *N-glycan processing in ER quality control*. J Cell Sci, 2006. **119**(Pt 21): p. 4373-80.

Russell, S.J., et al., *The primary substrate binding site in the b' domain of ERp57 is adapted for endoplasmic reticulum lectin association*. J Biol Chem, 2004. **279**(18): p. 18861-9.

Rutishauser, J. and M. Spiess, *Endoplasmic reticulum storage diseases*. Swiss Med Wkly, 2002. **132**(17-18): p. 211-22.

Ruvinsky, I. and O. Meyuhas, *Ribosomal protein S6 phosphorylation: from protein synthesis to cell size*. Trends Biochem Sci, 2006. **31**(6): p. 342-8.

S

Said, H.M., et al., *GAPDH is not regulated in human glioblastoma under hypoxic conditions*. BMC Mol Biol, 2007. **8**: p. 55.

Said, H.M., et al., *Absence of GAPDH regulation in tumor-cells of different origin under hypoxic conditions in - vitro*. BMC Res Notes, 2009. **2**: p. 8.

Schubert, U., et al., *Rapid degradation of a large fraction of newly synthesized proteins by proteasomes*. Nature, 2000. **404**(6779): p. 770-4.

Scott, G.K., et al., *A PACS-1, GGA3 and CK2 complex regulates CI-MPR trafficking*. Embo J, 2006. **25**(19): p. 4423-35.

Senger, D.R., et al., *Tumor cells secrete a vascular permeability factor that promotes accumulation of ascites fluid*. Science, 1983. **219**(4587): p. 983-5.

- Semenza, G.L., *HIF-1 and mechanisms of hypoxia sensing*. Curr Opin Cell Biol, 2001. **13**(2): p. 167-71.
- Semenza, G.L., *Regulation of cancer cell metabolism by hypoxia-inducible factor 1*. Semin Cancer Biol, 2009. **19**(1): p. 12-6.
- Sevier, C.S. and C.A. Kaiser, *Disulfide transfer between two conserved cysteine pairs imparts selectivity to protein oxidation by Ero1*. Mol Biol Cell, 2006. **17**(5): p. 2256-66.
- Sevier, C.S., et al., *Modulation of cellular disulfide-bond formation and the ER redox environment by feedback regulation of Ero1*. Cell, 2007. **129**(2): p. 333-44.
- Sevier, C.S. and C.A. Kaiser, *Ero1 and redox homeostasis in the endoplasmic reticulum*. Biochim Biophys Acta, 2008. **1783**(4): p. 549-56.
- Shen, J., et al., *ER stress regulation of ATF6 localization by dissociation of BiP/GRP78 binding and unmasking of Golgi localization signals*. Dev Cell, 2002. **3**(1): p. 99-111.
- Shi, Y., et al., *Identification and characterization of pancreatic eukaryotic initiation factor 2 alpha-subunit kinase, PEK, involved in translational control*. Mol Cell Biol, 1998. **18**(12): p. 7499-509.
- Shin-Ya, K., *Novel antitumor and neuroprotective substances discovered by characteristic screenings based on specific molecular targets*. Biosci Biotechnol Biochem, 2005. **69**(5): p. 867-72.
- Simmen, T., J.E. Aslan, A.D. Blagoveshchenskaya, L. Thomas, L. Wan, Y. Xiang, S.F. Feliciangeli, C.H. Hung, C.M. Crump, and G. Thomas, *PACS-2 controls endoplasmic reticulum-mitochondria communication and Bid-mediated apoptosis*. Embo J, 2005. **24**(4): p. 717-29.
- Stamnes, M.A., et al., *The cyclophilin homolog ninaA is a tissue-specific integral membrane protein required for the proper synthesis of a subset of Drosophila rhodopsins*. Cell, 1991. **65**(2): p. 219-27.
- Stevens, F.J. and Y. Argon, *Protein folding in the ER*. Semin Cell Dev Biol, 1999. **10**(5): p. 443-54.
- Sullivan, D.C., et al., *EndoPDI, a novel protein-disulfide isomerase-like protein that is preferentially expressed in endothelial cells acts as a stress survival factor*. J Biol Chem, 2003. **278**(47): p. 47079-88.

T

- Tagaya, Y., et al., *ATL-derived factor (ADF), an IL-2 receptor/Tac inducer homologous to thioredoxin; possible involvement of dithiol-reduction in the IL-2 receptor induction*. Embo J, 1989. **8**(3): p. 757-64.
- Tang, B.L., et al., *COPII and exit from the endoplasmic reticulum*. Biochim Biophys Acta, 2005. **1744**(3): p. 293-303.

- Tortorella, D., et al., *Dislocation of type I membrane proteins from the ER to the cytosol is sensitive to changes in redox potential*. J Cell Biol, 1998. **142**(2): p. 365-76.
- Tsai, B., et al., *Protein disulfide isomerase acts as a redox-dependent chaperone to unfold cholera toxin*. Cell, 2001. **104**(6): p. 937-48.
- Tsai, B., Y. Ye, and T.A. Rapoport, *Retro-translocation of proteins from the endoplasmic reticulum into the cytosol*. Nat Rev Mol Cell Biol, 2002. **3**(4): p. 246-55.
- Tu, B.P., et al., *Biochemical basis of oxidative protein folding in the endoplasmic reticulum*. Science, 2000. **290**(5496): p. 1571-4.

V

- van Anken, E. and I. Braakman, *Versatility of the endoplasmic reticulum protein folding factory*. Crit Rev Biochem Mol Biol, 2005. **40**(4): p. 191-228.
- van den Beucken, T., M. Koritzinsky, and B.G. Wouters, *Translational control of gene expression during hypoxia*. Cancer Biol Ther, 2006. **5**(7): p. 749-55.
- Vance, J.E., *Phospholipid synthesis in a membrane fraction associated with mitochondria*. J Biol Chem, 1990. **265**(13): p. 7248-56.
- Varga, K., et al., *Efficient intracellular processing of the endogenous cystic fibrosis transmembrane conductance regulator in epithelial cell lines*. J Biol Chem, 2004. **279**(21): p. 22578-84.
- Vembar, S.S. and J.L. Brodsky, *One step at a time: endoplasmic reticulum-associated degradation*. Nat Rev Mol Cell Biol, 2008. **9**(12): p. 944-57.
- Verkhatsky, A. and O.H. Petersen, *The endoplasmic reticulum as an integrating signaling organelle: from neuronal signaling to neuronal death*. Eur J Pharmacol, 2002. **447**(2-3): p. 141-54.

W

- Wadhwa, R., et al., *Upregulation of mortalin/mthsp70/Grp75 contributes to human carcinogenesis*. Int J Cancer, 2006. **118**(12): p. 2973-80.
- Wakana, Y., et al., *Bap31 Is an Itinerant Protein That Moves between the Peripheral Endoplasmic Reticulum (ER) and a Juxtannuclear Compartment Related to ER-associated Degradation*. Mol Biol Cell, 2008. **19**(5): p. 1825-1836.
- Wang, C.C. and C.L. Tsou, *Protein disulfide isomerase is both an enzyme and a chaperone*. FASEB J, 1993. **7**(15): p. 1515-7.
- Wang, G.L. and G.L. Semenza, *Characterization of hypoxia-inducible factor 1 and regulation of DNA binding activity by hypoxia*. J Biol Chem, 1993. **268**(29): p. 21513-8.
- Wilkinson, B. and H.F. Gilbert, *Protein disulfide isomerase*. Biochim Biophys Acta, 2004. **1699**(1-2): p. 35-44.

Wu, J. and R.J. Kaufman, *From acute ER stress to physiological roles of the Unfolded Protein Response*. Cell Death Differ, 2006. **13**(3): p. 374-84.

Wu, Y., et al., *A lag in intracellular degradation of mutant alpha 1-antitrypsin correlates with the liver disease phenotype in homozygous PiZZ alpha 1-antitrypsin deficiency*. Proc Natl Acad Sci U S A, 1994. **91**(19): p. 9014-8.

X

Xie, K., et al., *Constitutive and inducible expression and regulation of vascular endothelial growth factor*. Cytokine Growth Factor Rev, 2004. **15**(5): p. 297-324.

Y

Yao, Y., Y. Zhou, and C. Wang, *Both the isomerase and chaperone activities of protein disulfide isomerase are required for the reactivation of reduced and denatured acidic phospholipase A2*. Embo J, 1997. **16**(3): p. 651-8.

Yoshida, H., et al., *Identification of the cis-acting endoplasmic reticulum stress response element responsible for transcriptional induction of mammalian glucose-regulated proteins. Involvement of basic leucine zipper transcription factors*. J Biol Chem, 1998. **273**(50): p. 33741-9.

Z

Zheng, H.C., et al., *Overexpression of GRP78 and GRP94 are markers for aggressive behavior and poor prognosis in gastric carcinomas*. Hum Pathol, 2008. **39**(7): p. 1042-9.

ACKNOWLEDGEMENTS

I han mi dazua entschlossa, dass I mine Danksagung in minam Dialekt schrieb, sodass des Ganze a kle authentischer isch.

Es gibt a paar Lütt bi deanna I mi herzlich bedanka möcht und I nimm oh glei vorweg, dass die Reihenfolge koa Ussag über da Stellawert, dens für mi hat, trifft.

I bin dankbar für dHilfe und dUnterstützung, dia I vu minra Freundin, da Jeannine, über dia ganza letschta Johr gnüßa han dürfa. Des hat ma Vieles leichter gmacht und oft hätt I oh ned gwisst, was I ohne sie toa hätt.

Danke Mama, Oma und Opa, dass ar mi zu deam Mensch gmacht hond, der I bin. Durch euch han I glernt, dassma Sacha hinterfroga muass und ned immer Alles gleich ufan erschta Blick erkennbar isch. I bin froh, dassar für mi do sind/gsi sind. I han euch lieb!

Danke Lilo und Wolfgang für eure Unterstützung in vielna Lebenssituationa und danke Wolfgang für die mit bereitwilligam Korrekturleasa verbrochta Stunda.

Bei mina Freunde möcht I mi bedanka für da Spaß, den ma gemeinsam gha hond und hoffentlich oh wieterhin ha wörrand. Danke Richard, Lukas, Jo, Luki, Andi & Eva, Alex & Saskia und Flo.

Da Katharina und ihra Familie möcht I danke säga, dass se mi ufgnoh hond und ma durch a schwere Zit gholfa hond.

Bei da Bella möcht I mi einerseits dafür bedanka, dass se so a tolle Chefin war und, dass se mar ermöglicht hat mine Diplomarbeit in Kanada zum macha.

Danke Thomas dafür, dass I mine Diplomarbeit bei dir im Labor macha han dürfa und dass Alles so unkompliziert abglaufa isch. Und oh danke an die ganze Arbeitsgruppa, dia mi so freundlich ufgnoh hat (special thanks to Mike!).

Danke Giovanni, dass du di bereit erklärt hasch min Betreuer uf da BOKU zum si und immer Zit gha hasch.

DANKE